

Tribological Properties of Lubricin Mutant Mouse Knee Joints

By

Elizabeth I. Drewniak

Sc.B., Brown University, May 2004

Sc.M., Brown University, May 2005

Submitted in partial fulfillment of the requirements for the degree of Doctor of
Philosophy in the Program in Biomedical Engineering at Brown University

Providence, Rhode Island

May 2011

© Copyright 2011 by Elizabeth I. Drewniak

This dissertation by Elizabeth I. Drewniak, Sc.M. is accepted in its present form
by the Department of Biomedical Engineering as satisfying the
dissertation requirement for the degree of Doctor of Philosophy.

Date _____

Joseph J. Crisco, Ph.D., Advisor

Date _____

Gregory D. Jay, M.D., Ph.D., Reader

Date _____

Braden C. Fleming, Ph.D., Reader

Date _____

Eric M. Darling, Ph.D., Reader

Date _____

Farshid Guilak, Ph.D., External Reader

Approved by the Graduate Council

Date _____

Peter M. Weber, Dean of the Graduate School

Curriculum Vitae

Elizabeth (Liz) I. Drewniak was born on April 30, 1983 in South Weymouth, MA to Stephen and Elizabeth Drewniak. Liz was raised in Hanson, MA with her two brothers, John and Michael. She graduated from Whitman-Hanson Regional High School as the Class of 2000's valedictorian. She went on to matriculate at Brown University in the Fall of 2000 where she pursued Biomedical Engineering. She received her Bachelor's of Science degree in June of 2004. Following completion of her Bachelor's degree, Liz chose to stay at Brown University and enroll in the 5th Year Integrated Master's Program, a joint degree program between the Division of Engineering and the Division of Biology and Medicine. During this time, she joined the Bioengineering Laboratory within the Department of Orthopaedics at the Alpert Medical School of Brown University/Rhode Island Hospital. Under the direction of Joseph J. (Trey) Crisco III, Ph.D., Liz completed a Master's Thesis entitled: An Investigation of the Use of Mechanical Testing to Predict the Efficacy of Chest Protectors in Reducing Sudden Cardiac Death (Commotio Cordis) from Blunt Impact. Upon completion of her Master's Degree in 2005, she enrolled in the Biomedical Engineering Ph.D. program at Brown University. Continuing her work with Dr. Crisco as her dissertation advisor, she has been involved in a multitude of studies focusing on osteoarthritis and has been an author on several peer-reviewed publications.

CURRICULUM VITAE

ELIZABETH IRENE DREWNIAK

Bioengineering Laboratory
Coro West, Suite 404
1 Hoppin Street
Providence, RI 02903

(781) 710-1588 phone
(401) 444-4418 fax
Liz_Drewniak@brown.edu
LizDrewniak@gmail.com

Education

Brown University, Providence, RI, USA

Ph.D. Biomedical Engineering, expected May 2011

Brown University, Providence, RI, USA

Sc.M., Biomedical Engineering, May 2005

Brown University, Providence, RI, USA

Sc.B., Biomedical Engineering, May 2004

Theses/Dissertations

Drewniak EI (2005). An Investigation of the Use of Mechanical Testing to Predict the Efficacy of Chest Protectors in Reducing Sudden Cardiac Death (Commotio Cordis) from Blunt Impact (Master's thesis).

Original Peer Reviewed Publications

1. **Drewniak EI**, Jay GD, Fleming BC, Crisco JJ. "Comparison of two methods for calculating the frictional properties of articular cartilage using a simple pendulum and intact mouse knee joints." *Journal of Biomechanics*, 2009, 42 (12): 1996-9. (PMID: 19632680)
2. **Drewniak EI**, Spenciner DB, Crisco JJ. "Mechanical properties of chest protectors and the likelihood of ventricular fibrillation due to commotio cordis," *Journal of Applied Biomechanics*, 2007, 23 (4): 282-288. (PMID: 18089926)
3. **Drewniak EI**, Crisco JJ, Spenciner DB, Fleming BC. "Accuracy of contact area measurements with thin-film pressure sensors," *Journal of Biomechanics*, 2007, 40: 2569-2572. (PMID: 17270193)
4. Crisco JJ, **Drewniak EI**, Alvarez MP, Spenciner DB. "Physical and mechanical properties of various field lacrosse balls," *Journal of Applied Biomechanics*, 2005, 21: 383-393. (PMID: 16498183)

Research Experience

Brown University, Providence, RI, USA (2004 – Present)

- PhD Student – Department of Orthopaedics, Alpert Medical School

Brown University, Providence, RI, USA (2003)

- Research Assistant – Division of Engineering

Brigham and Women's Hospital/Faulkner Hospital, Boston, MA, USA (2001)

- Research Assistant – Department of Gastroenterology

Teaching Experience

Division of Engineering, Brown University - *Teaching Assistant* (2003 – 2006)

- Appropriate Technology (Brown University Course EN93)
 - Mentored students through the stages of design projects
 - Evaluated and graded student homework assignments
- BioInstrumentation Design (Brown University Course EN123)
 - Provided guidance to students on weekly laboratory design projects
 - Administered laboratory assignment evaluations
- Entrepreneurship and Good Work (Brown University Course EN193)
 - Lead weekly discussion sections with 10-15 students
 - Developed and organized class website

Honors and Awards

American Society of Biomechanics 2009 *Grant-in-Aid* Award recipient (\$2000)

Professional Memberships

American Society of Biomechanics (ASB): 2005 – present.

Biomedical Engineering Society (BMES): 2004 – present.

Orthopaedic Research Society (ORS): 2008 – present.

Osteoarthritis Research Society International (OARSI): 2008 – present.

Society of Women Engineers (SWE): 2004 – present.

Volunteer Positions

Campus Life Subcommittee on Athletics and Physical Education. Brown University, Providence, RI, USA (2007 – Present)

- Graduate Student Representative

Dorcas Place Adult & Family Learning Center, Inc., Providence, RI, USA (2005 – 2008)

- Tutor

Angkor Hospital for Children, Siem Reap, Cambodia (June 2005, August 2007)

- Biomedical Engineer

Podium Presentations

1. **Drewniak EI**, Jay GD, Fleming BC, Zhang L, Warman ML, Crisco JJ: “*Prg4*+/- Mouse Knee Joints Show the Largest Response to Cyclic Loading when Compared to *Prg4*+/+ and *Prg4*-/- Joints.” Transactions of the 57th Annual Meeting of the Orthopaedic Research Society, Long Beach, CA; January 13-16, 2011.
2. **Drewniak EI**, Jay GD, Fleming BC, Zhang L, Warman ML, Crisco JJ: “Cyclic Loading Increases Friction and Articular Cartilage Damage in Lubricin Deficient Mice.” Transactions of the 56th Annual Meeting of the Orthopaedic Research Society, New Orleans, LA; March 6-9, 2010.

3. **Drewniak EI**, Jay GD, Fleming BC, Crisco JJ: “The Effect of Cyclic Loading on the Coefficient of Friction Differs by Gender In the Articular Cartilage of Murine Knee Joints.” Annual Meeting of the American Society of Biomechanics, State College, PA; August 26-29, 2009.
4. **Drewniak EI**, Rainbow M, Jay G, Fleming B, Crisco J: “Frictional Properties of Intact Mutant PRG4 Mouse Knee Articular Cartilage.” North American Congress on Biomechanics, Ann Arbor, MI; August 5-9, 2008.
5. **Drewniak EI**, Jay GD, Fleming BC, Cha CJ, Crisco JJ: “Cartilage Wear Testing of Intact Mutant PRG4 Mouse Knees with a Pendulum System.” 34th Annual Northeast Bioengineering Conference, Providence, RI; April 4-6, 2008.
6. **Drewniak, EI**: “Bioengineering and Orthopaedic Research at Brown/RIH.” Regional Bioengineering and Biotechnology Conference, University of Massachusetts – Dartmouth, Dartmouth, MA; February 9, 2007.

Abstracts

1. **Drewniak EI**, Jay GD, Cha CJ, Warman ML, Fleming BC, Crisco JJ: “Coefficient of Friction of Articular Cartilage of Intact *Prg4* Mutant Mouse Knees Increases with Cyclic Loading,” Transactions of the 55th Annual Meeting, Orthopaedic Research Society, Las Vegas, NV; February 22-25, 2009.
2. Henn CM, Brunner AM, **Drewniak EI**, Lesieur-Brooks AM, Crisco JJ, Ehrlich MG: “At What Point Can We Save Cartilage?,” Transactions of the 55th Annual Meeting, Orthopaedic Research Society, Las Vegas, NV; February 22-25, 2009.
3. **Drewniak EI**, Crisco JJ: “Cartilage Wear Testing of Intact Mutant PRG4 Mouse Knees with a Pendulum System,” 16th Annual Research Celebration, Rhode Island Hospital, Providence, RI November 20, 2008.
4. Henn CM, Brunner AM, **Drewniak EI**, Lesieur-Brooks AM, Crisco JJ, Ehrlich MG: “*In Vivo* Joint Forces and Early Biomechanical Evidence of Osteoarthritis During Progressive Bowing in the Rabbit Knee,” 2008 Pediatric Orthopaedic Society of North America, Albuquerque, NM; May 1-3, 2008.
5. **Drewniak EI**, Crisco JJ: “Cartilage Wear Testing of Intact Mutant PRG4 Mouse Knees with a Pendulum System,” Transactions of the 54th Annual Meeting, Orthopaedic Research Society, San Francisco, CA; March 2-5 2008.
6. **Drewniak EI**, Crisco JJ, “Wear Testing of Articular Joints with an Unconstrained Driven Pendulum System,” 15th Annual Research Celebration, Rhode Island Hospital, Providence, RI; November 9, 2007.

7. **Drewniak EI**, Crisco JJ: “Wear Testing of Articular Joints with an Unconstrained Driven Pendulum System,” Transactions of the 53rd Annual Meeting, Orthopaedic Research Society, San Diego, CA; February 11-14, 2007.
8. **Drewniak EI**, Crisco JJ, Spenciner DB, Fleming BC: “Accuracy of Contact Area Measurements with Thin-Film Pressure Sensors,” 14th Annual Research Celebration, Rhode Island Hospital, Providence, RI; November 9, 2006.
9. **Drewniak EI**, Crisco JJ, Spenciner DB, Fleming BC: “Accuracy of Contact Area Measurements with Thin-Film Pressure Sensors,” Proceedings of the ASB 30th Annual Meeting, Blacksburg, VA; September 6-9, 2006.
10. **Drewniak E**, Spenciner DB, Crisco JJ: “Do Mechanical Properties of Chest Protectors Correlate with the Incidence of Ventricular Fibrillation in a Sudden Death (Comotio Cordis) Swine Model?” 13th Annual Research Celebration, Rhode Island Hospital, Providence, RI; September 29, 2005.
11. **Drewniak E**, Spenciner DB, Crisco JJ: “Do Mechanical Properties of Chest Protectors Correlate with the Incidence of Ventricular Fibrillation in a Sudden Death (Comotio Cordis) Swine Model?” Proceedings of the ISB XXth Congress - ASB 29th Annual Meeting, Cleveland, OH; August 1-5, 2005.

Skills

Computer: MatLab, Tekscan, VICON, Qualisys, Visual3D, Solid Works, Scion/NIH Image, Adobe Illustrator, Adobe Photoshop

Microscopy: Bright Field, Differential Interference Contrast, Fluorescence, Confocal, Scanning Electron Microscopy, Transmission Electron Microscopy

Animal Surgery: Mouse, Rat, Rabbit, Pig

Preface and Acknowledgements

I find it apropos to be writing my acknowledgements just days before Thanksgiving. When touring Brown's campus with a smile plastered across my face in April of 1999, I knew I had found *the* school for me; however, I did not realize that I'd spend more than a decade pursuing an education in Providence, enjoying every step along the way.

First, I must acknowledge my PhD advisor, Trey Crisco, Ph.D. My graduate experience had been truly wonderful. Thank you for taking a chance on an undergrad in need of a research experience, and thank you for giving me the opportunity to continue on as a graduate student (twice). It's nearly impossible for me to list all of the lessons you've taught me over the past 6.5+ years. You've set an amazing example, demonstrating how to be a highly accomplished and successful researcher, while maintaining a life outside of the lab, which I will strive to emulate. A "thank you" doesn't begin to convey my gratitude.

I'd also like to thank my committee members, Drs. Fleming, Jay, Darling, and Guilak. I'm extremely fortunate to have had such extraordinary mentors guiding me through my graduate experience. Thank you for all of the time you have devoted to my growth and development as a biomedical engineer. I must also acknowledge and thank Doug Moore for his guidance over the past several years; your advice and support have meant a great deal to me.

My graduate research experience would not have been the same without the Bioengineering Lab, and it would not have been possible without the support of Dr. Michael Ehrlich and the Department of Orthopaedics. Thank you to the faculty, staff, and

students (both past and present) of the Bioengineering Lab, and of course our adopted lab members from the Jay, Ehrlich, and Blaine Labs. You've helped to make this a truly enjoyable experience, from conferences, to lab celebrations, to lunch at the conference table – I'll look back my time as a member of the lab with fondness.

While the lab has played such a large role in my life for the past 6.5 years, I must thank my friends outside of the lab. The older I get, the more I realize how blessed I am to have such amazing friends. Thank you for all the support, laughs, and love.

Next, I must thank my amazing fiancé, Mike, for providing so much support and encouragement over the past few years. Your drive to succeed inspires me to constantly set higher goals. I'm so lucky to have you in my life, and I couldn't imagine it without you. I look forward to becoming Dr. Watts on 10/01/11.

Finally, to my family ... I must start by acknowledging John H. Corcoran (Grampy) for exposing me to the field of engineering at a very young age, encouraging all of my educational endeavors, and for teaching me that “nothing succeeds like success.” To my Godmother, Patricia Drewniak: thank you for always taking such a great interest in my work (even though my mouse knees aren't nearly as big as your goat heads). Should I pursue a career in teaching, I can only hope to be half as good of a professor as you. To my big brother, John: #5400 is (and always will be) my hero! To my “little” brother, Mike: I'd like to take this opportunity to formally apologize for wishing that I had a younger sister for the majority of our childhood; and, in all seriousness, thank you for always being ready and willing to provide answers (to my endless questions) and comic relief – Not too shabby for a Harvard man. To my parents: I'm struggling to find the words to express my gratitude for all of your unending support, constant sacrifices,

and unconditional love. It should go without saying that I would not be the person I am today without you both. I just wish that all children could be so blessed to have parents as loving, kind, and generous as the two of you. I love you, Mom and Dad and thank you.

Table of Contents

Signature Page	iii
Curriculum Vitae	iv
Preface and Acknowledgements	ix
Table of Contents	xii
List of Tables	xv
List of Figures	xvi
Chapter 1 – Introduction	1
1.1 Overview	1
1.2 Background	3
1.2.1 Osteoarthritis	3
1.2.2 Articular Cartilage	4
1.2.3 Tribology	5
1.2.3.1 Friction	6
1.2.3.2 Joint Lubrication	7
1.2.3.13 Wear	8
1.2.4 Lubricin	10
1.2.5 Biomechanical Testing/Cyclic Loading	11
1.3 Significance	13
1.4 Specific Aims	14
1.4.1 Aim 1: Design two pendulum systems for testing intact mouse knee joints – a passive system to measure the coefficient of friction and an active system to perform cyclic loading	14
1.4.2 Aim 2: Investigate the effects of cyclic loading on the coefficient of friction of intact lubricin mutant mouse knee joints	14
1.4.3 Aim 3: Characterize the effects of cyclic loading on the surface integrity of lubricin mutant mouse knee cartilage	15
1.5 References	16
Chapter 2 – Comparison of Two Methods for Calculating the Frictional Properties of Articular Cartilage Using a Simple Pendulum and Intact Mouse Knee Joints	29
2.1 Abstract	29
2.2 Introduction	31

2.3	Methods.....	33
2.4	Results.....	35
2.5	Discussion.....	36
2.6	Acknowledgements.....	38
2.7	References.....	39

Chapter 3 – Cyclic Loading Increases the Coefficient of Friction of Frozen *Prg4*^{+/+} and *Prg4*^{+/-} Mouse Knee Joints but Not Fresh Knee Joints 46

3.1	Abstract.....	46
3.2	Introduction.....	48
3.3	Methods.....	49
3.4	Results.....	51
3.5	Discussion.....	52
3.6	Acknowledgements.....	55
3.7	References.....	56

Chapter 4 – Cyclic Loading Increases Friction and Changes Cartilage Surface Integrity in Lubricin Mutant Mouse Knees 60

4.1	Abstract.....	60
4.1.1	Objective.....	60
4.1.2	Methods.....	61
4.1.3	Results.....	61
4.1.4	Conclusion.....	61
4.2	Introduction.....	62
4.3	Materials and Methods.....	64
4.3.1	Specimens.....	64
4.3.2	Pendulum Systems.....	64
4.3.3	Cyclic Loading Protocol.....	66
4.3.4	Histological Processing and Analysis.....	66
4.3.5	Chondrocyte Viability.....	67
4.3.6	Statistical Analysis.....	68
4.4	Results.....	69
4.5	Discussion.....	71
4.6	Acknowledgements.....	77
4.7	References.....	78

Chapter 5 – Discussion and Conclusions 90

5.1	Discussion.....	90
5.1.1	Friction Modeling: Linear versus Exponential.....	90

5.1.2	Effect of Gender and Cyclic Loading on CoF	93
5.1.3	Imaging of Murine Articular Cartilage	95
5.1.3.1	Scanning Electron Microscopy (SEM)	95
5.1.3.2	White Light Interferometry (WLI).....	99
5.1.3.3	Atomic Force Microscopy (AFM).....	102
5.1.4	Future Applications of the Pendulum Systems.....	105
5.2	Conclusions.....	109
5.2.1	Aim 1: Design two pendulum systems for testing intact mouse knee joints – a passive system to measure the coefficient of friction and an active system to perform cyclic loading.....	109
5.2.2	Aim 2: Investigate the effects of cyclic loading on the coefficient of friction of intact lubricin mutant mouse knee joints	110
5.2.3	Aim 3: Characterize the effects of cyclic loading on the surface integrity of lubricin mutant mouse knee cartilage	112
5.3	Summary	114
5.4	References.....	115

List of Tables

Chapter 1

Table 1.1: Experimental coefficient of friction (CoF) values of intact joints obtained with pendulum systems or custom-built apparatus.....	25
Table 1.2: Coefficient of friction values collected from pin-on-disc cartilage plug systems with a variety of opposing surfaces and lubricants	26

Chapter 4

Table 4.1: Means and standard deviations of histological scores for all categories and overall totals for cyclically loaded (Exp) and unloaded (Ctl) <i>Prg4</i> mouse knee cartilage. * denotes significantly higher AC Surface Structure and Surface Layer Morphology scores compared to <i>Prg4</i> ^{+/+} and +/- (p<0.001). + denotes significantly higher Surface Layer Morphology score compared to unloaded <i>Prg4</i> ^{-/-} scores	84
---	----

Chapter 5

Table 5.1: Mean (\pm SD) coefficient of friction (CoF) values for articular cartilage of both males and females prior to cyclic loading (Initial) and immediately following all testing (Final). * denotes that final female CoF values were significantly higher than initial female CoF values (p<0.009).....	118
Table 5.2: Mean and standard deviation values (n=5 scans per specimen; n=2 pairs per <i>Prg4</i> genotype) for <i>Prg4</i> ^{+/+} , <i>Prg4</i> ^{+/-} , and <i>Prg4</i> ^{-/-} femoral chondyle articular cartilage surface roughness parameters measured with atomic force microscopy. As anticipated, <i>Prg4</i> ^{-/-} RMS values were higher than <i>Prg4</i> ^{+/+} and <i>Prg4</i> ^{+/-} RMS values.....	119
Table 5.3: Surface roughness data obtained with atomic force microscopy comparing cyclically loaded (experimental; n=5 scans per specimen; n=2 specimens per <i>Prg4</i> genotype) and unloaded (contra-lateral control; n=5 scans per specimen; n=2 specimens per <i>Prg4</i> genotype) joints from <i>Prg4</i> ^{+/+} , <i>Prg4</i> ^{+/-} , and <i>Prg4</i> ^{-/-} femoral chondyle articular cartilage. We expected that cyclically loaded surfaces would have increased RMS values compared to their unloaded control joints. However, unloaded joints had higher RMS values for each genotype.....	120
Table 5.4: Mean CoF values, standard deviations, and root mean square error calculations for intact rat knee joints and the same measures for the joints following transection of the anterior cruciate ligament (ACLT). CoF values determined with the Stanton linear decay model and the exponential model that accounts for viscous damping..	121

List of Figures

Chapter 1

- Figure 1.1: A schematic representation of the chondrocyte arrangement of articular cartilage. The inhomogenous distribution of chondrocytes and collagen result in a noticeable zonal arrangement. Zones have been named based upon their orientation within the tissues. The chondrocytes that comprise the superficial zone are oblong and align parallel to the articulating surface. The middle zone contains randomly-dispersed, round chondrocytes. The chondrocytes that comprise the deep zone are arranged in columns that run perpendicular to the tidemark, which separates the calcified and noncalcified cartilage. 27
- Figure 1.2: A schematic representation of lubricin (Prg4). This full-length protein contains twelve coding exons and includes: two somatomedin B-like domains, a heparin binding domain, chondroitin sulfate attachment sites, two O-linked glycosylated mucin-like domains, and a hemopexin-like domain. Adapted from [37]. 28

Chapter 2

- Figure 2.1: Schematic of simple pendulum system used for amplitude decay data collection (A). The pendulum arm was fixed to the proximal end of the femur and the tibia was rigidly mounted to a base platform. Four reflective markers were attached to both the pendulum arm and to the base (not all markers shown) for 3-D motion tracking. The arm was set to an initial angle of $\sim 12^\circ$, released, and allowed to oscillate freely until damping out completely. Close-up schematic of the knee joint mounting system (B). Both limbs were embedded in square 6.25 mm tubing with a urethane-potting compound and secured into the apparatus at a resting angle of 70° . The tibia was fixed to the base with four set screws (two on each side of the limb). The proximal end of the tube-fitted femur fit into a square notch cut into the pendulum arm. 43
- Figure 2.2: Representative plot of pendulum oscillation decay starting with initial release of the pendulum arm through damping out of the system. Points denote the maximum amplitude of each cycle. 44
- Figure 2.3: Representative plot of the Lin μ (dashed line) and Exp μ (solid line), which accounts for viscous damping fit to the maximum amplitudes points for each cycle. The Exp μ model provided a much closer fit to the experimental data with a RMSE of 0.078° and an ASE of 0.033° , versus the Lin μ RMSE of 0.55° and ASE of 0.185° 45

Chapter 3

- Figure 3.1: A custom-built, active pendulum was used to perform unconstrained cyclic loading with intact *Prg4*^{+/+} and *Prg4*^{+/-} mouse knee joints serving as the fulcrum of the system. The DC motor drives the specimen through $\pm 15^\circ$ of flexion-extension via a series of linkages, rotary bearings, and a linear bearing. A well containing cell culture medium hydrates the joint and helps to maintain viability.....58
- Figure 3.2: Mean values of experimental and contra-lateral control CoF values of Fresh and Frozen joints from *Prg4*^{+/+} and *Prg4*^{+/-} mice (n=12 fresh pairs per genotype; n=6 frozen pairs per genotype) over the course of testing. Standard deviation error bars provided for cyclically loaded groups. CoF values of unloaded joints remained constant between their initial and final CoF measurements. Experimental Frozen and Fresh CoF values started approximately equal; however, the Frozen CoF values of both *Prg4* genotypes significantly (* denotes $p < 0.001$; ** denotes $p = 0.015$) increased following 120 minutes of cyclic loading, as compared to their initial (t=0min) CoF measurements.59

Chapter 4

- Figure 4.1: Two pendulum systems were used to complete the experiments. A passive pendulum system was used to measure the CoF (A). Experimental joints were loaded into an active pendulum system for cyclic loading (B). Specimens were loaded into the mounting block (C).....85
- Figure 4.2: A flowchart of the experimental protocol starting with a pair of *Prg4* mouse hind limbs. Each experimental limb underwent 26 cumulative hours of cyclic loading, twelve hours of unloading in cell culture medium, and oscillation data collection at sixteen time points while control limbs remained in an unloaded state in culture medium for the duration of testing.86
- Figure 4.3: A.) Mean values of experimental and contra-lateral control CoF data over the course of testing with the coefficient of friction values on the y-axis and time (hr) on the x-axis. The shaded bars at the bottom represent the time during which the experimental joint is cyclically loaded and unloaded. All control CoF values remained constant; however, the *Prg4*^{-/-} control CoF values were significantly higher than the CoF values of the other two genotypes ($p < 0.0001$). Experimental *Prg4*^{-/-} CoF values started significantly higher and rose steadily during the twenty-six hours of cyclic loading. Experimental *Prg4*^{+/+} and *Prg4*^{+/-} CoF values started approximately equal; however, by the final time point, *Prg4*^{+/-} CoF values were closer to those of *Prg4*^{-/-} joints than to *Prg4*^{+/+} joints. B.) Mean CoF values for each genotype at t = 0, 16, 18, 38hrs. At t = 0, 16 and 18 hrs, *Prg4*^{-/-} CoF values were significantly higher than the wild type and heterozygous values, as denoted with * ($p < 0.0001$). However, at t = 38hrs, both *Prg4*^{-/-} and *Prg4*^{+/-} CoF values were significantly higher than *Prg4*^{+/+} values. ** denotes $p = 0.0028$, while *** denotes $p < 0.0001$87
- Figure 4.4: The images displayed within this figure represent the median total histological score for each *Prg4* genotype and treatment group. Cyclically loaded

Prg4 +/+ with a score of 1.0 (A), unloaded *Prg4* +/+ with a score of 1.0 (D), cyclically loaded *Prg4* +/- with a score of 2.5 (B), unloaded *Prg4* +/- with a score of 2.0 (E), cyclically loaded *Prg4* -/- with a score of 5.0 (C), unloaded *Prg4* -/- with a score of 5.0 (F) specimens captured at 10x magnification. Scale bar denotes 100 μm .

.....88
 Figure 4.5: Representative FDA/PI viability images of femoral chondylar cartilage from cyclically loaded *Prg4* +/+ (A), unloaded *Prg4* +/+ (D), cyclically loaded *Prg4* +/- (B), unloaded *Prg4* +/- (E), cyclically loaded *Prg4* -/- (C), unloaded *Prg4* -/- (F) specimens which were loaded or unloaded for 38 hours. Images were captured at 20x magnification with the scale bar denoting 50 μm 89

Chapter 5

Figure 5.1: An example of a trial of oscillation decay with a rapid decrease in oscillation amplitude followed by a smooth, gradual decay (a), which most likely resulted from soft tissue within the capsule impeding upon the movement at the larger oscillation angles. By excluding the first few oscillation maximums, both models were able to more closely fit the data (b). Doing so reduced the Stanton CoF from 0.0337 ± 0.002 (mean \pm SD) to 0.0302 ± 0.0012 , and allowed the exponential model to fit to the data and calculate a CoF value of 0.0193 ± 0.0017122

Figure 5.2: An example of a highly complex oscillation decay pattern. Neither model could obtain a close fit to the experimental data (a), even resulting in the failure of the exponential model (CoF value of ~ 0 for this trial). In this example, the highly complex pattern was affected by the extreme varus-valus motion of the joint (b). .123

Figure 5.3: SEM image of the tibial plateau of a 12-week-old *Prg4*+/+ mouse. The majority of the articular cartilage appeared smooth and featureless. The visual surface damage was most likely artifact from the specimen dissection and preparation.....124

Figure 5.4: SEM image of the medial femoral chondyle of a 12-week-old *Prg4*+/- mouse. The surface was smooth and featureless. The magnified image (scale bar = 16.7 μm) of the articulating surface was displayed a small degree of roughness.....125

Figure 5.5: SEM image of the lateral femoral chondyle of a 12-week-old *Prg4*-/- mouse. In comparison to SEM images of *Prg4*+/+ and *Prg4*+/- AC, *Prg4*-/- AC (**Figures 5.3 and 5.4**) shows a greater degree of damage126

Figure 5.6: WLI output of a 10-week-old *Prg4*+/- femoral chondyle imaged with a 20x mirau objective. Image output includes a surface profile (top left), intensity map (top right), and oblique plot (bottom). Ideally, the surface profile would include no black space, which represents missing data.....127

Figure 5.7: Image of a 10 week old *Prg4*+/+ femoral chondyle captured with atomic force microscopy. This image demonstrates what we would expect; the surface is clear, and the image does not contain blurred lines denoting the slipping of the tip across the sample.....128

Figure 5.8: Examples of 10-week-old *Prg4*+/+ (a) and *Prg4*-/- (b) femoral chondyles imaged with atomic force microscopy in which the surfaces were covered with large pillow-like particles. While surface asperities would be expected on *Prg4*-/- specimens, *Prg4*+/+ should be featureless like the **Figure 5.7**. However, most of the

collected images displayed irregular surfaces. More work is required to optimize the preparation and data collecting settings in order to obtain better results, but this task will be hindered by the curvature of the tibial plateaus and femoral chondyles.....129

Figure 5.9: There was a correlation between RMSE of the CoF models and Max_y (Maximum Difference in Amplitude). Increases in RMSE correlated with larger Max_y values. The CoF models base their calculations upon flexion-extension; so, in the case that the knee joint has an abnormally large amount of varus-valgus motion (Max_y), the models will not fit as closely to the data, resulting in larger RMSE values.....130

Chapter 1

Introduction

1.1 Overview

The human body contains three types of joints: fibrous, cartilaginous, and synovial (also referred to as diarthrodial). Synovial joints, such as knees, are responsible for a majority of the movement of the human body. Articular cartilage (AC) is the smooth, white, featureless connective tissue that lines the ends of long bones within synovial joints. In a healthy state, AC functions to (1) distribute loads across the articulating surface in order to decrease the stresses experienced by the joint and (2) allows for the motion between two opposing cartilaginous surfaces while minimizing both friction and wear. While AC has the potential to remain healthy and smooth for decades, there are a variety of risk factors that lead to a degenerative joint disorder called osteoarthritis (OA), which is characterized by the erosion of AC within diarthrodial joints. In attempts to gain a better understanding of AC and OA, many researchers have turned to tribology, the engineering science that studies friction, lubrication, and wear.

Over the past several decades, numerous studies have investigated the frictional properties (coefficient of friction; CoF) of AC. These studies have examined the CoF values of AC from an assortment of joints using a wide range of testing schemes. Additionally, a variety of lubrication theories have been investigated in an attempt to determine how AC allows for such low friction upon its bearing surfaces. Experimental testing has proven that lubricants, such as synovial fluid, help reduce the CoF within joints, while also minimizing wear. Lubricin, the critical lubricating component within synovial fluid and on the articulating surface of AC, reduces friction and provides chondroprotection within diarthrodial joints. In addition to quantifying the CoF values of AC and synovial joints, a great deal of information can be gained by subjecting joints to biomechanical testing, such as cyclic loading, and assessing the effects.

The long-term goal of this line of research would ultimately be the development of a tribological supplement for synovial joints at-risk for the onset and development of OA. However, the work presented within this dissertation serves to address the more immediate goals of developing a whole joint testing system capable of investigating the tribological properties of lubricin mutant mouse knee joints. This goal was accomplished with two pendulum systems designed to provide repeatable and reliable *ex vivo* biomechanical studies of intact mouse knee joints.

1.2 Background

1.2.1 Osteoarthritis

Osteoarthritis (OA) is a degenerative disease affecting the synovial joints of nearly 27 million Americans [1]. Characterized by varying degrees of pain and deterioration, OA is the most common joint disease and the leading cause of disability in the United States [2-3]. Marked by radiographic bony changes such as osteophyte formation, cysts, subchondral sclerosis, and joint space narrowing, OA manifests clinically with a variety of symptoms. These symptoms include joint pain, swelling, stiffness, restriction of motion, crepitus with motion, joint effusions, and deformity [4]. While these symptoms most commonly present in the knee, hip, and hand, OA can manifest in any synovial joint.

At this point in time, the etiology of OA is not well understood; however, several risk factors have been attributed to this disease. Age, ethnicity, gender, genetics, obesity, and traumatic joint injury, among other factors, all put individuals at a heightened risk for developing OA [2]. Given the fact that life expectancy has increased in the US and obesity has reach epidemic proportions, the need for a better understanding of OA is crucial [2-3].

The pathophysiology of OA involves a combination of morphological, structural, biochemical, and biomechanical factors. An imbalance of articular cartilage (AC) biosynthesis and degradation contribute to the development of OA [3]. This disease results in degeneration of all tissues within the joint, including: AC, subchondral and metaphyseal bone, synovium, intra-articular ligaments (anterior cruciate (ACL); posterior

cruciate (PCL)), joint capsule, and muscles. The onset and progression of this multifaceted disease can be separated into three stages: proteolytic breakdown of the cartilage matrix, fibrillation and erosion of the AC, and, lastly, synovial inflammation [5]. The deterioration of AC can be more specifically characterized with softening, fibrillation, and ulceration, and finally cartilage loss [5]. Diarthrodial joints depend upon healthy AC to maintain proper joint function.

1.2.2 Articular Cartilage

Articular cartilage is the smooth, translucent, featureless connective tissue that lines the ends of bones within synovial joints. While healthy AC allows for decades-worth of painless joint motion, its lack of a blood supply, lymphatic channels, and neurological innervation impairs its ability to self-repair [6-7]. In addition to providing relative motion within synovial joints while minimizing friction and wear, AC also serves to disperse loads throughout the entire joint. By distributing loads across the articulating surfaces, AC decreases the stresses experienced within the joint tissues.

From a biomechanical standpoint, AC is a multiphasic tissue comprised of water, collagen, and cells, called chondrocytes. While the percentages of these components vary across joints and species, water accounts for up to 85% of AC. Collagen is distributed throughout articular cartilage in an inhomogeneous manner. However, chondrocytes can be divided into specific zones based upon their orientation, as depicted in **Figure 1.1**. The superficial zone accounts for approximately 10-20% of the total thickness of AC, and the chondrocytes within this zone are oblong in shape and oriented along the axis parallel to the articulating surface. The middle zone comprises 40-60% of the total thickness of the

tissue. The chondrocytes within this zone are round and randomly assorted. Lastly, the deep zone, located between the middle zone and the tidemark, which separates the calcified and uncalcified cartilage, contains chondrocytes with columnar orientation [8]. This multiphasic composition is essential to its function by directly contributing to the biomechanical properties of articular cartilage. These properties help to provide interstitial fluid pressurization, which in turn affects the load bearing and lubricating abilities of the tissue [4, 8-9].

1.2.3 Tribology

Tribology is the study of friction, lubrication, and wear. For the past several decades, the classical engineering principles of tribology have been used in attempts to better understand AC. Researchers have employed a variety of lubrication theories to describe the low friction and wear environments of synovial joints. At this point in time, no single theory has been capable of accounting for the lubricating abilities of AC under all physiologic loading conditions; hence, many believe that more than one lubrication mechanism occurs at one time [9]. However, when lubrication mechanisms fail, friction within the joint increases and wear has the potential to develop on the articulating surfaces. While tribological studies are difficult, if not impossible to conduct *in vivo*, there are a variety of ways in which friction, lubrication, and wear can be investigated with *ex vivo* or *in vitro* methods. Tribological studies have investigated the properties of articular cartilage through the use of intact synovial joints, as well as cartilage plugs alone [6].

1.2.3.1 Friction

Friction can be described as the resistance of motion between two surfaces in contact with each other [9], and it is quantified with the coefficient of friction (CoF). Surface friction results from the adhesions of one surface impeding another surface due to roughness or the viscosity of a lubricant situated between two surfaces. CoF can be defined by laws postulated by Amonton and Coulomb several centuries ago [9]:

$$CoF = W / F \quad (1)$$

where F is the frictional force independent of the area of contact and W is the applied load. Bulk friction arises when internal energy within a bulk material dissipates. In terms of AC, bulk friction occurs when interstitial fluid flows through the extracellular matrix of the tissue. However, theoretical calculations have determined that this measure of AC friction is negligible. Lastly, plowing friction is found within synovial joints as a load moves across the articulating surface, resulting in interstitial fluid flow [9].

Historically, like the study of tribology, friction is generally a principle applied to materials and mechanical engineering. As will be discussed, a wide range of CoF values have been obtained for AC; however, most measured values are still lower than those reported for manmade materials. UHMWPE on cobalt chrome is used in artificial joints and yields CoF values ranging from 0.01 to 0.05. Also, Teflon has a reported CoF of 0.04. Additionally, ice on ice at 0°C and graphite on steel have measured CoF values of 0.1 [9].

Despite the severe loading conditions imposed upon AC during activities of daily living, it is able to provide an almost-frictionless bearing surface within synovial joints. Over the past several decades, many groups have measured the CoF of AC. These

investigations have examined a variety of species and joints across a range of methods. While most early studies utilized methods to study the frictional properties of intact synovial joints, more recent work has employed techniques and equipment to look more closely at AC alone. Methods include whole joint friction pendulum systems and custom-made friction simulators [10-12], and the sliding of excised cartilage plugs against various surfaces [13-18]. There are advantages and disadvantages related to both the use of intact joints and the use of cartilage plug samples.

Tribological studies that investigate the frictional properties of intact joints allow for the preservation of physiological conditions. These studies require custom-built systems, such as pendulums or arthrotripsometers, in which the joint serves as a fulcrum that the apparatus pivots around. Reported frictional coefficients of articular cartilage measured from intact joints range from as low as 0.0009 to as high as 0.35 (**Table 1.1**). Additional work has demonstrated that the use of cartilage samples against flat, manmade surfaces allows for the direct measurement of the CoF. Frictional coefficients measured with cartilage plugs (Table 2) utilizing lubricants such as synovial fluid and saline with cartilage against glass, metal, and cartilage range from 0.0014 to 0.9 (**Table 1.2**).

1.2.3.2 Joint Lubrication

There are several proposed theories of joint lubrication, which should be able to account for the reduction of friction and minimization of wear of AC under a variety of loading conditions and assorted motions [8-9]. A fluid-film theory has been applied to explain synovial joint lubrication. In general, fluid-film lubrication occurs when a thin fluid-film layer allows for an increased separation of two surfaces. This situation is most

likely to arise in joints that are subjected to high speeds and low loads. More specific fluid-film theories include: hydrodynamic lubrication, a self-generating lubrication mechanism, and squeeze-film lubrication. In addition to fluid-film, others have proposed theories of self-pressurized hydrostatic lubrication, boosted lubrication, interstitial fluid pressurization and diarthrodial joint lubrication, as well as boundary lubrication [6, 8-9].

Boundary lubrication has been described by several research groups. Charnley, one of the first investigators of joint friction and lubrication, proposed that a monolayer of lubricant was responsible for the separation of the two articulating surfaces during normal joint function [10]. Davis *et al.* proposed that a thin layer of “structured water” was responsible for absorbing into the articulating surface, and hence, providing the necessary boundary lubrication [19]. Swann and Radin *et al.* focused their attention on lubricin as a primary mode of boundary lubrication. They proposed that this glycoprotein complex could be adsorbed to each articulating surface within the knee joint, hence providing layers of lubricant [9, 20-25]. To date there are many studies demonstrating that lubricin acts as a boundary lubricant within synovial joints [6, 11, 26-33]. However, experimental data has also shown that boundary lubrication must act in conjunction with another form of lubrication. While some of the more recent work in this field suggests that interstitial fluid pressurization is the most probable theory, more work is needed to further expose the underlying mechanisms of joint lubrication [9, 16-17, 26, 34].

1.2.3.3 Wear

When lubrication mechanisms fail and the friction within a joint rises, AC has the potential to develop signs of wear. In engineering terms, wear can be described as the

loss or removal of material from a solid surface resulting from mechanical action. It can be categorized into fatigue wear or interfacial wear. Interfacial wear can more accurately be described in terms of abrasive wear and adhesive wear. While the former arises when a soft material is scraped or rubbed away by a harder surface, the latter occurs when two surfaces come in contact with one another causing surface fragments to come in contact with, adhere to, and subsequently tear away from one another during movement. By definition, fatigue wear is independent of any lubrication phenomena. Instead, it arises as a result the cyclic stresses and strains associated with repetitive loading produced by joint motion. Fatigue wear may occur within the bulk of the tissue and increase in size through the accumulation of microscopic damage. While there is more than one mode of wear, a variety of factors have been shown to intensify the loss of cartilage within a synovial joint. Such factors include joint trauma, irregular loading patterns, altered biochemical degradation, and lack of lubricating mechanisms, among others [9].

To date, the study of AC wear has been empirical science. A majority of the work investigating AC wear relies upon surface topography evaluations and imaging techniques. As discussed in Chapter 5, potential imaging procedures and surface topography techniques include: scanning electron microscopy, atomic force microscopy, laser profilometry, and interferometry. However, very few of these methods are capable of generating accurate quantitative results [9, 16, 35].

It is difficult to conduct wear studies *in vivo* due to the fact that wear must be quantified as the mass of a material removed from interacting surfaces per unit of time or as the lost volume. Both of these measures would require high-powered imaging tools and constant monitoring. Hence, minimal information exists regarding the quantification

of wear mechanisms and rates of biological tissues such as AC. Despite the complexity surrounding the quantification of wear within synovial joints, some general conclusions have been drawn. Wear rates decrease until they reach a constant value, which is contingent upon the roughness of the surfaces and applied pressures. Additionally, wear rates rise as joint motion increases. Lastly, lubricants, such as synovial fluid, help to reduce wear rates [9].

1.2.4 Lubricin

Lubricants such as synovial fluid act to reduce friction and wear, and, hence, are vital to maintaining proper function within knee joints. Originally discovered by Swann *et al.* [24-25], in the early 1980s, lubricin's lubricating properties were further characterized by Jay through a series of bench top investigations [20-23]. Lubricin is a mucinous glycoprotein encoded by the gene *Prg4* [36] containing twelve coding exons which include: two somatomedin B-like domains, a heparin binding domain, chondroitin sulfate attachment sites, two O-linked glycosylated mucin-like domains, and a hemopexin-like domain (**Figure 1.2**) [37]. In addition to being a major component of synovial fluid, it is also produced by superficial zone chondrocytes and hence found on the articulating surface of AC.

In order to better understand the *in vivo* function of lubricin, lubricin-null mice (*Prg4*^{-/-}) were generated [36]. The generation of these mice has been previously described and they have been backcrossed onto a C57BL6/J background resulting in *Prg4*^{+/+} (wild type) and *Prg4*^{+/-} (heterozygous) mice [36]. While *Prg4*^{-/-} mice appear normal at birth, they gradually develop precocious clinical, radiological, and histological

signs of joint disease as they age [38]. These features recapitulate findings in patients with the camptodactyly-arthropathy-coxa vara-pericarditis syndrome (CACP), due to an inherited lack of lubricin. Based upon studies conducted with *Prg4*^{-/-} mice, lubricin was postulated to provide chondroprotection by acting as a boundary lubricant, a cell adhesion inhibitor, and a synoviocyte growth regulator [38-39]. While the precocious cartilage failure observed in patients with CACP and in *Prg4*^{-/-} mice indicate lubricin is essential for chondroprotection, it is not known whether lubricin levels that are below *Prg4*^{+/+} levels, but not completely missing, such as the levels present in *Prg4*^{+/-} mice, would also negatively affect chondroprotection. *In vitro* studies that measured boundary lubrication at varying concentrations of lubricin, and clinical studies showing that lubricin levels fall in humans and other mammals following traumatic joint injury, suggest that a correlation may exist between lubricin concentration and chondroprotection [11, 20, 22-23, 33, 39-48].

1.2.5 Biomechanical Testing/Cyclic Loading

While there has been decades of research investigating the tribological properties of articular cartilage and synovial joints, additional work is needed to examine the response of friction, lubrication and wear to biomechanical testing, such as cyclic loading [6]. Exposing test specimens to biomechanical testing leads to greater insight and allows for a simulation of *in vivo* joint conditions. Using the medial compartment of bovine knee joints, McCann *et al.* demonstrated that cyclic loading with a pendulum system resulted in CoF increases [49]. Forster and Fisher also showed that cyclic loading of bovine cartilage plugs with a custom-made apparatus yields an increase in CoF [16]. Nugent-

Derfus *et al.* determined that cyclic loading of bovine stifle joints has beneficial effects upon lubrication; they were able to demonstrate that continuous passive motion upregulated the production of lubricin [46]. Clearly, a great deal of knowledge can be gained from simulating physiologic conditions. The work presented in the following chapters examines the effects of long-term cyclic loading on the tribological properties of lubricin mutant mouse knee joints.

1.3 Significance

In a healthy state, synovial joints such as the knee allow for decades of pain-free motion; however, there is a multitude of factors that can disrupt proper joint function. The studies described within this dissertation focus on the characterization of the tribological properties of lubricin mutant mouse knee joints. This work further demonstrates lubricin's ability to provide chondroprotection within synovial joints by assessing the effects of cyclic loading on the frictional properties and surface integrity. The findings presented in the following chapters provide the justification and groundwork for a variety of future studies. The design and development of the pendulum systems will allow for biomechanical studies of intact synovial joints. Additionally, the results regarding the lubricin-dose response warrant further investigations of patients who are carriers of CACP. Lastly, this work supports the development of tribological supplementation for patients at-risk for the onset and progression of OA.

1.4 Specific Aims

Specific Aim 1: Design two pendulum systems for testing intact mouse knee joints – a passive system to measure the coefficient of friction and an active system to perform cyclic loading.

The objectives of the first aim were to design and build two pendulum systems capable of performing biomechanical testing on intact mouse knees. In both pendulums, the mouse knee joint served as the fulcrum of the system. One pendulum was designed to investigate the whole joint frictional properties (CoF) of intact mouse knee joints. Using this simple pendulum system in conjunction with a 3-D motion tracking system, oscillation data was recorded and used to calculate the CoF values. The second pendulum apparatus was a driven system that could cyclically load intact mouse knee joints through unconstrained flexion and extension. We hypothesized that we could develop reliable and reproducible *ex vivo* methods for the quantification of the effects of cyclic loading on the frictional properties intact lubricin mutant mouse knee joints.

Specific Aim 2: Investigate the effects of cyclic loading on the coefficient of friction of intact lubricin mutant mouse knee joints.

The objective of the second aim was to examine the effects of cyclic loading on the CoF of mouse knees with two alleles of lubricin (*Prg4*^{+/+}), one allele of lubricin (*Prg4*^{+/-}), and no alleles of lubricin (*Prg4*^{-/-}). This was accomplished by cyclically

loading knee joints from each *Prg4* genotype for a specified length of time with brief pauses to measure the CoF. The contra-lateral joint from each mouse served as the control for each cyclically loaded joint. Our primary hypothesis was that cyclically loaded joints would have increased CoF values when compared to their contra-lateral control joints. Additionally, we hypothesized that joints from *Prg4*^{-/-} mice would have higher CoF values compared to joints from *Prg4*^{+/+} and *Prg4*^{+/-} mice.

Specific Aim 3: Characterize the effects of cyclic loading on the surface integrity of lubricin mutant mouse knee cartilage.

The objective of the third aim was to characterize the effects of cyclic loading on the surface integrity of lubricin mutant mouse knee cartilage. While a number of imaging techniques were investigated, ultimately, the effects of cyclic loading on the articular cartilage were assessed with histological scoring methods and chondrocyte viability staining. We hypothesized that the articular cartilage of cyclically loaded specimens would show increased surface damage compared to their unloaded contra-lateral controls. Additionally, we hypothesized that articular cartilage from knee joints from *Prg4*^{-/-} mice would have increased surface damage compared to joints from *Prg4*^{+/+} and *Prg4*^{+/-} mice.

1.5 References

1. Lawrence, R.C., D.T. Felson, C.G. Helmick, L.M. Arnold, H. Choi, R.A. Deyo, S. Gabriel, R. Hirsch, M.C. Hochberg, G.G. Hunder, J.M. Jordan, J.N. Katz, H.M. Kremers, and F. Wolfe, *Estimates of the prevalence of arthritis and other rheumatic conditions in the United States. Part II*. *Arthritis & Rheumatism*, 2008. **58**(1): p. 26-35.
2. Felson, D.T., R.C. Lawrence, P.A. Dieppe, R. Hirsch, C.G. Helmick, J.M. Jordan, R.S. Kington, N.E. Lane, M.C. Nevitt, Y. Zhang, M. Sowers, T. McAlindon, T.D. Spector, A.R. Poole, S.Z. Yanovski, G. Ateshian, L. Sharma, J.A. Buckwalter, K.D. Brandt, and J.F. Fries, *Osteoarthritis: new insights. Part 1: the disease and its risk factors*. *Ann Intern Med*, 2000. **133**(8): p. 635-46.
3. Griffin, T.M. and F. Guilak, *The role of mechanical loading in the onset and progression of osteoarthritis*. *Exerc Sport Sci Rev*, 2005. **33**(4): p. 195-200.
4. Buckwalter, J.A., H.J. Mankin, and A.J. Grodzinsky. *Articular Cartilage and Osteoarthritis*. in *AAOS Instructional Course Lectures*. 2005.
5. Knecht, S., B. Vanwanseele, and E. Stussi, *A review on the mechanical quality of articular cartilage - implications for the diagnosis of osteoarthritis*. *Clin Biomech* (Bristol, Avon), 2006. **21**(10): p. 999-1012.
6. Katta, J., Z. Jin, E. Ingham, and J. Fisher, *Biotribology of articular cartilage--a review of the recent advances*. *Med Eng Phys*, 2008. **30**(10): p. 1349-63.
7. Mankin, H.J., *The response of articular cartilage to mechanical injury*. *Journal of Bone and Joint Surgery Am*, 1982. **64**: p. 460-466.

8. Nordin, M. and V. Frankel, *Basic Biomechanics of the Musculoskeletal System*. 3rd ed. 2001, Philadelphia: Lippincott Williams & Wilkins.
9. Mow, V.C., Huiskes, R., ed. *Basic Orthopaedic Biomechanics & Mechano-Biology*. Third ed. 2005, Lippincott, Williams & Wilkins: Philadelphia. 720.
10. Charnley, J. *The lubrication of animal joints*. in *Symposium on Biomechanics. Institution of mechanical engineers*. 1959.
11. Jay, G.D., J.R. Torres, D.K. Rhee, H.J. Helminen, M.M. Hytinen, C.J. Cha, K. Elsaid, K.S. Kim, Y. Cui, and M.L. Warman, *Association between friction and wear in diarthrodial joints lacking lubricin*. *Arthritis Rheum*, 2007. **56**(11): p. 3662-9.
12. Radin, E.L. and I.L. Paul, *Response of joints to impact loading. I. In vitro wear*. *Arthritis & Rheumatism*, 1971. **14**(3): p. 356-62.
13. Chappuis, J., I.A. Sherman, and A.W. Nwemann, *Surface tension of animal cartilage as it relates to friction in joints*. *Ann. Biomed. Engng.*, 1983. **11**: p. 435-449.
14. Clift, S.E., B. Harris, P.A. Dieppe, and A. Hayes, *Frictional response of articular cartilage containing crystals*. *Biomaterials*, 1989. **10**: p. 329-334.
15. Forster, H. and J. Fisher, *The influence of loading time and lubricant on the friction of articular cartilage*. *Proceedings of the Institution of Mechanical Engineers, Part H*, 1996. **210**(2): p. 109-19.
16. Forster, H. and J. Fisher, *The influence of continuous sliding and subsequent surface wear on the friction of articular cartilage*. *Proceedings of the Institution of Mechanical Engineers, Part H*, 1999. **213**(4): p. 329-45.

17. Forster, H., J. Fisher, D. Dowson, and V. Wright. *The effect of stationary loading on the friction and boundary lubrication of articular cartilage in the mixed lubrication regime.* in *21st Leeds/Lyon Symposium on Tribology, Lubrication and lubricants.* 1995: Elsevier Science.
18. Stachowiak, G.W., A.W. Batchelor, and L.J. Griffiths, *Friction and wear changes in synovial joints.* *Wear*, 1994. **171**: p. 135-142.
19. Davis, W., S. Lee, and L. Sokoloff, *A proposed model of boundary lubrication by synovial fluid: structuring of boundary water.* *Journal of Biomechanical Engineering*, 1979. **101**: p. 185-192.
20. Jay, G.D., *Characterization of a bovine synovial fluid lubricating factor. I. Chemical, surface activity and lubricating properties.* *Connect Tissue Res*, 1992. **28**(1-2): p. 71-88.
21. Jay, G.D., E. Drummond, and B. Lane, *Altered surface character of stretched condom latex.* *Contraception*, 1992. **45**(2): p. 105-10.
22. Jay, G.D. and B.S. Hong, *Characterization of a bovine synovial fluid lubricating factor. II. Comparison with purified ocular and salivary mucin.* *Connect Tissue Res*, 1992. **28**(1-2): p. 89-98.
23. Jay, G.D., B.P. Lane, and L. Sokoloff, *Characterization of a bovine synovial fluid lubricating factor. III. The interaction with hyaluronic acid.* *Connect Tissue Res*, 1992. **28**(4): p. 245-55.
24. Swann, D.A., F.H. Silver, H.S. Slayter, W. Stafford, and E. Shore, *The molecular structure and lubricating activity of lubricin isolated from bovine and human synovial fluids.* *Biochem J*, 1985. **225**(1): p. 195-201.

25. Swann, D.A., S. Sotman, M. Dixon, and C. Brooks, *The isolation and partial characterization of the major glycoprotein (LGP-I) from the articular lubricating fraction from bovine synovial fluid*. *Biochem J*, 1977. **161**(3): p. 473-85.
26. Caligaris, M. and G.A. Ateshian, *Effects of sustained interstitial fluid pressurization under migrating contact area, and boundary lubrication by synovial fluid, on cartilage friction*. *Osteoarthritis Cartilage*, 2008. **16**(10): p. 1220-7.
27. Gleghorn, J.P., A.R. Jones, C.R. Flannery, and L.J. Bonassar, *Boundary mode frictional properties of engineered cartilaginous tissues*. *Eur Cell Mater*, 2007. **14**: p. 20-8; discussion 28-9.
28. Jay, G.D., K. Haberstroh, and C.J. Cha, *Comparison of the boundary-lubricating ability of bovine synovial fluid, lubricin, and Healon*. *J Biomed Mater Res*, 1998. **40**(3): p. 414-8.
29. Jay, G.D., D.A. Harris, and C.J. Cha, *Boundary lubrication by lubricin is mediated by O-linked beta(1-3)Gal-GalNAc oligosaccharides*. *Glycoconj J*, 2001. **18**(10): p. 807-15.
30. Jay, G.D., J.R. Torres, M.L. Warman, M.C. Laderer, and K.S. Breuer, *The role of lubricin in the mechanical behavior of synovial fluid*. *Proc Natl Acad Sci U S A*, 2007. **104**(15): p. 6194-9.
31. Katta, J., Z. Jin, E. Ingham, and J. Fisher, *Effect of nominal stress on the long term friction, deformation and wear of native and glycosaminoglycan deficient articular cartilage*. *Osteoarthritis and Cartilage*, 2009. **17**(5): p. 662-8.

32. Zappone, B., G.W. Greene, E. Oroudjev, G.D. Jay, and J.N. Israelachvili, *Molecular aspects of boundary lubrication by human lubricin: effect of disulfide bonds and enzymatic digestion*. Langmuir, 2008. **24**(4): p. 1495-508.
33. Zappone, B., M. Ruths, G.W. Greene, G.D. Jay, and J.N. Israelachvili, *Adsorption, lubrication, and wear of lubricin on model surfaces: polymer brush-like behavior of a glycoprotein*. Biophys J, 2007. **92**(5): p. 1693-708.
34. Ateshian, G.A., *The role of interstitial fluid pressurization in articular cartilage lubrication*. Journal of Biomechanics, 2009. **42**(9): p. 1163-76.
35. Graindorge, S. and G. Stachowiak, *Changes occurring in the surface morphology of articular cartilage during wear*. Wear, 2000. **241**: p. 143-150.
36. Rhee, D.K., J. Marcelino, M. Baker, Y. Gong, P. Smits, V. Lefebvre, G.D. Jay, M. Stewart, H. Wang, M.L. Warman, and J.D. Carpten, *The secreted glycoprotein lubricin protects cartilage surfaces and inhibits synovial cell overgrowth*. J Clin Invest, 2005. **115**(3): p. 622-31.
37. Marcelino, J., J.D. Carpten, W.M. Suwairi, O.M. Gutierrez, S. Schwartz, C. Robbins, R. Sood, I. Makalowska, A. Baxevanis, B. Johnstone, R.M. Laxer, L. Zemel, C.A. Kim, J.K. Herd, J. Ihle, C. Williams, M. Johnson, V. Raman, L.G. Alonso, D. Brunoni, A. Gerstein, N. Papadopoulos, S.A. Bahabri, J.M. Trent, and M.L. Warman, *CACP, encoding a secreted proteoglycan, is mutated in camptodactyly-arthritis-coxa vara-pericarditis syndrome*. Nat Genet, 1999. **23**(3): p. 319-22.
38. Bao, J.P., W.P. Chen, and L.D. Wu, *Lubricin: a novel potential biotherapeutic approaches for the treatment of osteoarthritis*. Mol Biol Rep, 2010.

39. Coles, J.M., L. Zhang, J.J. Blum, M.L. Warman, G.D. Jay, F. Guilak, and S. Zauscher, *Loss of cartilage structure, stiffness, and frictional properties in mice lacking PRG4*. *Arthritis Rheum*, 2010. **62**(6): p. 1666-74.
40. Elsaid, K.A., B.C. Fleming, H.L. Oksendahl, J.T. Machan, P.D. Fadale, M.J. Hulstyn, R. Shalvoy, and G.D. Jay, *Decreased lubricin concentrations and markers of joint inflammation in the synovial fluid of patients with anterior cruciate ligament injury*. *Arthritis & Rheumatism*, 2008. **58**(6): p. 1707-15.
41. Elsaid, K.A., G.D. Jay, M.L. Warman, D.K. Rhee, and C.O. Chichester, *Association of articular cartilage degradation and loss of boundary-lubricating ability of synovial fluid following injury and inflammatory arthritis*. *Arthritis & Rheumatism*, 2005. **52**(6): p. 1746-55.
42. Elsaid, K.A., J.T. Machan, K. Waller, B.C. Fleming, and G.D. Jay, *The impact of anterior cruciate ligament injury on lubricin metabolism and the effect of inhibiting tumor necrosis factor alpha on chondroprotection in an animal model*. *Arthritis & Rheumatism*, 2009. **60**(10): p. 2997-3006.
43. Graindorge, S., W. Ferrandez, E. Ingham, Z. Jin, P. Twigg, and J. Fisher, *The role of the surface amorphous layer of articular cartilage in joint lubrication*. *Proceedings of the Institution of Mechanical Engineers, Part H*, 2006. **220**(5): p. 597-607.
44. Jay, G.D., D.E. Britt, and C.J. Cha, *Lubricin is a product of megakaryocyte stimulating factor gene expression by human synovial fibroblasts*. *Journal of Rheumatology*, 2000. **27**(3): p. 594-600.

45. Jay, G.D., B.C. Fleming, B.A. Watkins, K.A. McHugh, S.C. Anderson, L.X. Zhang, E. Teeple, K.A. Waller, and K.A. Elsaid, *Prevention of cartilage degeneration and restoration of chondroprotection by lubricin tribosupplementation in the rat following anterior cruciate ligament transection*. *Arthritis & Rheumatism*, 2010. **62**(8): p. 2382-91.
46. Nugent-Derfus, G.E., T. Takara, K. O'Neill J, S.B. Cahill, S. Gortz, T. Pong, H. Inoue, N.M. Aneloski, W.W. Wang, K.I. Vega, T.J. Klein, N.D. Hsieh-Bonassera, W.C. Bae, J.D. Burke, W.D. Bugbee, and R.L. Sah, *Continuous passive motion applied to whole joints stimulates chondrocyte biosynthesis of PRG4*. *Osteoarthritis and Cartilage*, 2007. **15**(5): p. 566-74.
47. Taguchi, M., Y.L. Sun, C. Zhao, M.E. Zobitz, C.J. Cha, G.D. Jay, K.N. An, and P.C. Amadio, *Lubricin surface modification improves extrasynovial tendon gliding in a canine model in vitro*. *Journal of Bone and Joint Surgery Am*, 2008. **90**(1): p. 129-35.
48. Zhao, C., Y.L. Sun, R.L. Kirk, A.R. Thoreson, G.D. Jay, S.L. Moran, K.N. An, and P.C. Amadio, *Effects of a lubricin-containing compound on the results of flexor tendon repair in a canine model in vivo*. *Journal of Bone and Joint Surgery Am*, 2010. **92**(6): p. 1453-61.
49. McCann, L., E. Ingham, Z. Jin, and J. Fisher, *Influence of the meniscus on friction and degradation of cartilage in the natural knee joint*. *Osteoarthritis and Cartilage*, 2009. **17**(8): p. 995-1000.
50. Jones, E.S., *Joint Lubrication*. *The Lancet*, 1936. **230**: p. 1043-1044.

51. Barnett, C.H. and A.F. Cobbold, *Lubrication within living joints*. The Journal of Bone and Joint Surgery, 1962. **44B**(3): p. 662-674.
52. Unsworth, A., D. Dowson, and V. Wright, *Some new evidence on human joint lubrication*. Ann Rheum Dis, 1975. **34**(4): p. 277-85.
53. Unsworth, A., D. Dowson, and V. Wright, *The Frictional Behavior of Synovial Joints – Part 1: Natural Joints*. Journal of Lubrication Technology, 1975: p. 369-376.
54. Roberts, B.J., A. Unsworth, and N. Mian, *Modes of lubrication in human hip joints*. Ann Rheum Dis, 1982. **41**(3): p. 217-24.
55. Mabuchi, K., Y. Tsukamoto, T. Ohara, and T. Yamaguchi, *The effect of additive hyaluronic acid on animal joints with experimentally reduced lubricating ability*. Journal of Biomedical Material Research, 1994. **28**: p. 865-870.
56. Clarke, I.C., R. Contini, and R.M. Kenedi, *Friction and wear studies of articular cartilage: a scanning microscope study*. Journal of Lubrication Technology, 1975. **97**: p. 358-368.
57. O'Kelly, J., A. Unsworth, D. Dowson, D.A. Hall, and V. Wright, *A study of the role of synovial fluid and its constituents in the friction and lubrication of human hip joints*. Engng in Medicine, 1978. **7**: p. 73-83.
58. Charnley, J., *The lubrication of animal joints in relation to surgical reconstruction by arthroplasty*. Ann Rheum Dis, 1960. **19**: p. 10-9.
59. McCutchen, C.W., *The frictional properties of animal joints*. Wear, 1962. **5**: p. 1.
60. Linn, F.C., *Lubrication of animal joints. I. The arthrotripsometer*. Journal of Bone and Joint Surgery Am, 1967. **49**(6): p. 1079-98.

61. Linn, F.C., *Lubrication of animal joints. II. The mechanism.* Journal of Biomechanics, 1968. **1**(1968): p. 193-205.
62. Teeple, E., K.A. Elsaid, B.C. Fleming, G.D. Jay, K. Aslani, J.J. Crisco, and A.P. Mechrefe, *Coefficients of friction, lubricin, and cartilage damage in the anterior cruciate ligament-deficient guinea pig knee.* Journal of Orthopaedic Research, 2008. **26**(2): p. 231-7.
63. Teeple, E., B.C. Fleming, A.P. Mechrefe, J.J. Crisco, M.F. Brady, and G.D. Jay, *Frictional properties of Hartley guinea pig knees with and without proteolytic disruption of the articular surfaces.* Osteoarthritis and Cartilage, 2007. **15**(3): p. 309-15.
64. Dowson, D., M.D. Longfield, P.S. Walker, and V. Wright, *An investigation of the frictional and lubrication in human joints.* Proc Inst Mech Eng [H], 1967/1968. **182**: p. 68-76.
65. Walker, P.S., A. Unsworth, D. Dowson, J. Sikorski, and V. Wright, *Mode of aggregation of hyaluronic acid protein complex on the surface of articular cartilage.* Ann. Rheum. Dis., 1970. **29**: p. 591-602.
66. Ikeuchi, K., M. Oka, and S. Kubo. *The relation between friction and creep deformation in articular cartilage.* in *20th Leeds/Lyon Symposium on Tribology, Dissipative processes in tribology.* 1994.

Table 1.1: Experimental coefficient of friction (CoF) values of intact joints obtained with pendulum systems or custom-built apparatus.

Intact Joints		
Coefficient of Friction	Joint	Reference
0.02	Horse stifle	[50]
0.014-0.024	Human ankle	[10]
0.018-0.03	Canine ankle	[51]
0.02-0.042	Human hip	[52-53]
0.04	Human hip	[54]
0.007 (± 0.004)	Canine hip	[55]
0.001-0.003	Human hip	[56]
0.01-0.08	Human hip	[57]
0.005-0.02	Human knee	[58]
0.02-0.35	Porcine shoulder	[59]
0.005-0.01	Canine ankle	[60-61]
0.01-0.04	Human hip	[52]
0.075-0.13	Guinea pig knee	[62-63]
0.0009-0.0029	Murine knee	[11]
0.01-0.07	Bovine knee	[49]

Table 1.2: Coefficient of friction values collected from pin-on-disc cartilage plug systems with a variety of opposing surfaces and lubricants.

Cartilage Plugs			
Coefficient of Friction	Contact	Lubricant	Reference
0.003-0.1	Glass	Synovial Fluid	[59]
0.1-0.9	Glass	Synovial Fluid	[64]
0.0014-0.07	Glass	Synovial Fluid	[65]
0.01-0.1	Glass	Synovial Fluid	[13]
0.1-0.2	Glass	None	[14]
~0-0.28	PMMA	Saline	[66]
0.016-0.028	Cartilage	Saline	[66]
0.02-0.2	Metal	Synovial Fluid	[18]
0.003-0.35	Metal	Synovial Fluid	[15-17]

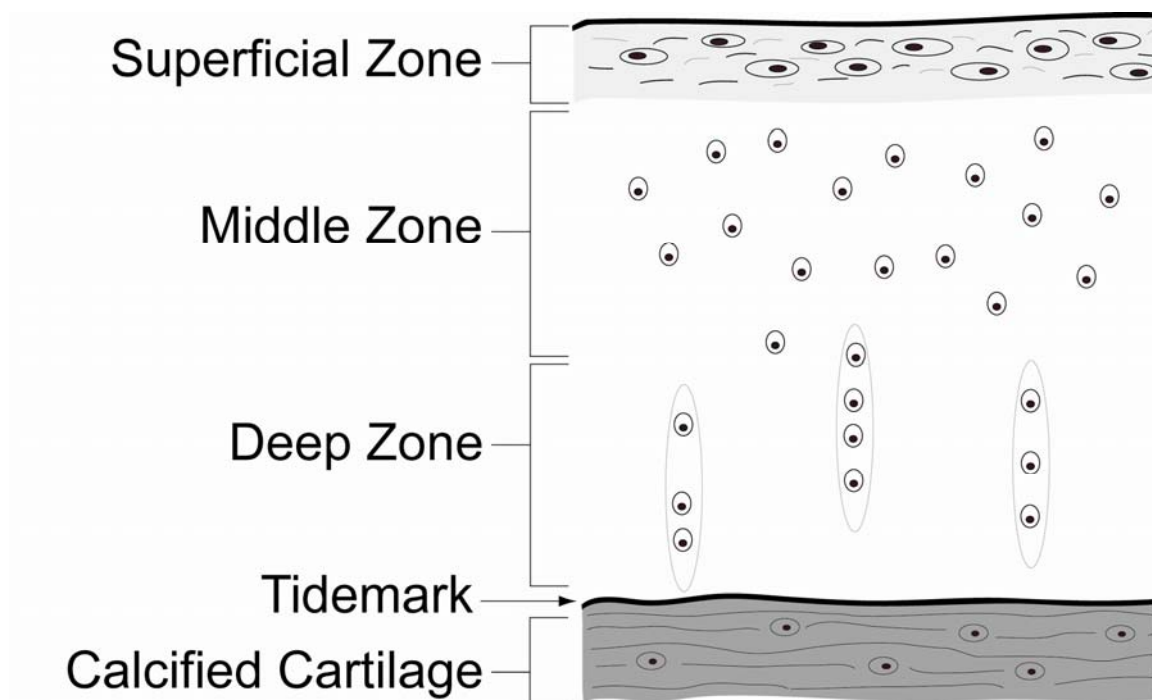


Figure 1.1: A schematic representation of the chondrocyte arrangement of articular cartilage. The inhomogenous distribution of chondrocytes and collagen result in a noticeable zonal arrangement. Zones have been named based upon their orientation within the tissues. The chondrocytes that comprise the superficial zone are oblong and align parallel to the articulating surface. The middle zone contains randomly-dispersed, round chondrocytes. The chondrocytes that comprise the deep zone are arranged in columns that run perpendicular to the tidemark, which separates the calcified and noncalcified cartilage.

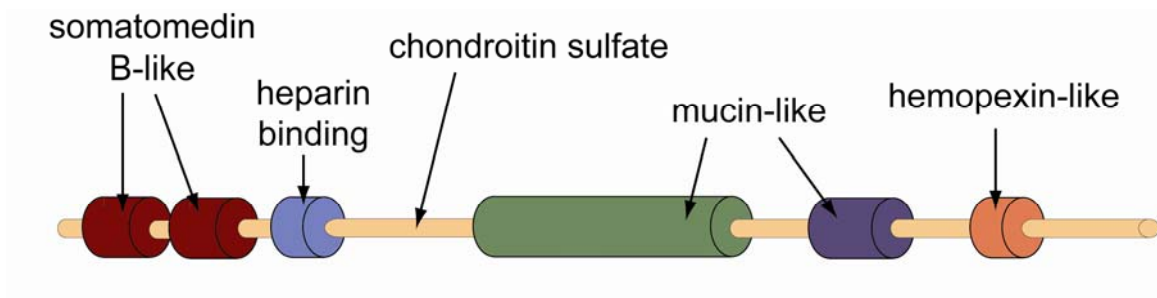


Figure 1.2: A schematic representation lubricin (Prg4). This full-length protein contains twelve coding exons and includes: two somatomedin B-like domains, a heparin binding domain, chondroitin sulfate attachment sites, two O-linked glycosylated mucin-like domains, and a hemopexin-like domain. Adapted from [37].

Chapter 2

Comparison of Two Methods for Calculating the Frictional Properties of Articular Cartilage Using a Simple Pendulum and Intact Mouse Knee Joints

Elizabeth I. Drewniak, Gregory D. Jay, Braden C. Fleming, Joseph J. Crisco,

The following chapter was published in *Journal of Biomechanics*, 42 (12): 1996-1999 (2009). (PMID: 19632680)

2.1 Abstract

In attempts to better understand the etiology of osteoarthritis (OA), a debilitating joint disease that results in the degeneration of articular cartilage in synovial joints, researchers have focused on joint tribology, the study of joint friction, lubrication, and

wear. Several different approaches have been used to investigate the frictional properties of articular cartilage. In this study, we examined two analysis methods for calculating the coefficient of friction (CoF) using a simple pendulum system and BL6 murine knee joints (n=10) as the fulcrum. A Stanton linear decay model (Lin μ) and an exponential model that accounts for viscous damping (Exp μ) were fit to the decaying pendulum oscillations. Root mean square error (RMSE), asymptotic standard error (ASE), and coefficient of variation (CV) were calculated to evaluate the fit and measurement precision of each model. This investigation demonstrated that while Lin μ was more repeatable, based on CV (5.0% for Lin μ ; 18% for Exp μ), Exp μ provided a better fitting model, based on RMSE (0.165° for Exp μ ; 0.391° for Lin μ) and ASE (0.033 for Exp μ ; 0.185 for Lin μ), and had a significantly lower CoF value (0.022±0.007 for Exp μ ; 0.042±0.016 for Lin μ) (p=0.001). This study describes the use of a simple pendulum for examining cartilage properties *in situ* that will have applications investigating cartilage mechanics in a variety of species. The Exp μ model provided a more accurate fit to the experimental data for predicting the frictional properties of intact joints in pendulum systems.

2.2 Introduction

Osteoarthritis is a common degenerative joint disease that can be characterized by the gradual loss of articular cartilage (AC) within synovial joints such as the knee. In a healthy state, AC is a relatively smooth tissue that covers articulating surfaces, distributes loads, decreases stresses on contact areas, and allows for motion of two surfaces while minimizing friction and wear. In attempts to better understand how and why cartilage becomes osteoarthritic, many researchers have investigated the coefficient of friction (CoF) of AC using a variety of methods, including whole joints in pendulums [1-6], cartilage plugs with custom-built apparatuses [6-13], and atomic force microscopy (AFM) [14-15].

Cartilage plugs are extremely useful in the study of the mechanical properties of AC; however, they pose challenges when using small animal models, including mice. Despite their small size, murine models have many benefits, including transgenic capabilities related to the development and homeostasis of AC. A study by Jay *et al.* [16] investigated the frictional properties of *Prg4* mutant mice using a simple pendulum system. Like Jay *et al.*'s study, the present study examines the frictional properties of mouse knee cartilage using a pendulum, but there were some differences between the two studies, including pendulum weight, resting angle, range of motion, and data analysis. Of note, the method described herein allows for collection of three-dimensional (3-D) joint motion and automated data processing.

A recent study examined two mathematical models for calculating CoF: a Stanton linear decay model (Lin μ) and an exponential decay model (Exp μ) that accounts for

viscous damping caused by extra-articular structures [1] The objective of the present study was to compare these two models for calculating CoF using experimental data collected and processed with an automated approach. This objective was accomplished using a simple pendulum system and BL6 mouse knees.

2.3 Methods

Using procedures approved by the RIH Animal Welfare Committee, hind limbs from 10-week-old BL6 mice ($n = 10$) were excised and flash frozen with liquid nitrogen post-euthanasia. Specimens were stored at -80°C for 1-7 weeks. Pilot data showed no differences between CoF of AC from fresh and frozen knee joints. On the day of testing, specimens were thawed and the skin, musculature, and supporting connective tissue were dissected away, leaving the joint capsule intact. The proximal femur and distal tibia were rigidly embedded in square, 6.25 mm-wide brass tubes with a urethane-potting compound (Smooth-ON, Easton, PA). The pendulum arm, weighing approximately 50 grams ($\sim 2x$'s body weight) was fit to the tube encasing the femur. The tube encasing the tibia was rigidly fixed with four set screws to a platform designed to place the resting angle of the knee at $\sim 70^{\circ}$ when the pendulum was in equilibrium. This resting angle was chosen following analysis of small rodent kinematic studies [17-18]. Four reflective markers were attached to both the pendulum arm and to the base of apparatus (**Figure 2.1**). The pendulum was rotated to place the knee joint at an initial offset angle of $\sim 12^{\circ}$, released, and allowed to oscillate freely. Five trials were collected for each knee. Pendulum motion was tracked in 3-D at 100 Hz (VICON, Centennial, CO.) with rotational accuracy of better than 0.05° and translational accuracy of better than 0.06 mm. Oscillation data was then processed with Visual3D software (C-Motion, Inc., Germantown, MD) and custom MATLAB (MathWorks, Inc., Natick, MA) code to determine the peak amplitude of each cycle of oscillation.

Two models for computing CoF were fit to the experimental peak amplitude data using custom MATLAB code. The Stanton model provided a linear fit (Lin μ), while the second model fit the experimental data with an exponential curve (Exp μ) that included a calculation for viscous damping (c) [1]. The goodness of fit of each model was described using the root mean square error (RMSE). The asymptotic standard error (ASE) was calculated to determine the uncertainty of the curve-fitted parameters relative to each model. The Lin μ , Exp μ , and c values were determined for each specimen by averaging over the five trials. Mean (\pm SD) CoF values for each model were then calculated across all specimens. The measurement precision of each model in estimating CoF was quantified using coefficient of variation analysis (CV). The reliability of each model was quantified with an intra-class correlation coefficient (ICC). The RMSE, ASE, CV, Lin μ and Exp μ values were evaluated for statistical differences with a Mann-Whitney Rank Sum Test (SigmaStat3.5, Systat Software, Inc., San Jose, CA). A significant value of $p < 0.05$ was set *a priori*.

2.4 Results

With an initial offset angle of $12 \pm 1^\circ$, the BL6 knees oscillated for 78 ± 25 cycles before damping brought the pendulum to equilibrium (**Figure 2.2**). In all trials, the decay in peak amplitude was curvilinear when plotted as a function of cycle number. The frequency of the pendulum motion was approximately 1Hz.

Exp μ provided a significantly ($p < 0.001$) closer fit to the experimental data (**Figure 2.3**) than Lin μ with overall average RMSE values of $0.17^\circ \pm 0.062$ and $0.40^\circ \pm 0.14$, respectively. The ASE for Exp μ was significantly lower ($p < 0.001$) than that of Lin μ , 0.033 and 0.185, respectively. The CoF values predicted by Exp μ (0.022 ± 0.007) were significantly less than the CoF values predicted by Lin μ (0.042 ± 0.016). The range of Exp μ values was 0.016-0.037, while the range of Lin μ was 0.031-0.080. CV of CoF for Exp μ was 18% and 5.0% for Lin μ . The ICC for Lin μ was 0.975, while the ICC for Exp μ was 0.708. The value of viscous damping predicted by Exp μ was $2.969 \times 10^{-5} \pm 3.409 \times 10^{-5}$ kg*m²/s.

2.5 Discussion

We modeled the decay of oscillations of a simple pendulum with intact BL6 mouse knees as the fulcrum using two models, Lin μ and Exp μ . The use of a pendulum provides a simple, cost-effective method for measuring the CoF of the AC of intact murine knee joints, while allowing for unconstrained motion with compressive loads that emulate *in vivo* conditions. While there are benefits with a pendulum system, there are also limitations. The calculated values represent the entire articular surface and joint, including capsular ligaments and synovium. Both models neglect aerodynamic drag created by the pendulum apparatus. Like this study, Jay *et al.* [16] used a pendulum with a mouse knee joint serving as the fulcrum of the system and each specimen consisted of a mouse hind limb with an intact knee capsule. While Jay *et al.* calculate CoF within the midpoint of joint oscillation, our models compute CoF using the entire oscillation data. This difference in data processing method may account for the differences in calculated CoF values we observed, which were higher than that of Jay *et al.* [16].

Cartilage plugs are useful for studying the frictional properties of AC without the influence of intra-capsular ligaments and surrounding tissues. However, transgenic mice provide valuable opportunities for the study of chondroprotection within an intact joint. Obtaining cartilage plugs from murine joints is currently not a feasible option. The CoF values computed with this approach were higher than those obtained with cartilage plug methods; however, they were within the range CoF values from studies investigating whole joints [4, 19-23].

The two methods for computing CoF of AC yielded significantly different results. Based on the calculated CV and ICC values, the Lin μ model had increased measurement precision and reliability, likely providing a more useful tool for detecting subtle differences among experimental groups. Additionally, a majority of studies that have investigated the frictional properties of articular cartilage with pendulums and whole joints have used the Stanton model, making it useful for drawing comparisons with other values in literature [3-4, 6, 13, 21-22, 24-25]. Conversely, Exp μ provided a better fit to the experimental data, based on RMSE and ASE, especially noting that the amplitude decay was curvilinear. Exp μ also accounts for viscous damping, and significantly lower CoF values.

2.6 Acknowledgements

The authors would like to acknowledge their funding sources: NIH AR050180, NIH P20-RRO24484, RIH Orthopaedic Foundation, Inc., and University Orthopedics, Inc. Thank you to VICON for use of cameras and software for motion capture. Thank you to Jason Machan, PhD for help with statistical analysis. The authors also thank: Michael Rainbow, Evan Leventhal, and Chung-Ja Cha, PhD for their assistance.

2.7 References

1. Crisco, J.J., J. Blume, E. Teeple, B.C. Fleming, and G.D. Jay, *Assuming exponential decay by incorporating viscous damping improves the prediction of the coefficient of friction in pendulum tests of whole articular joints*. Proc Inst Mech Eng [H], 2007. **221**(3): p. 325-33.
2. Teeple, E., B.C. Fleming, A.P. Mechrefe, J.J. Crisco, M.F. Brady, and G.D. Jay, *Frictional properties of Hartley guinea pig knees with and without proteolytic disruption of the articular surfaces*. Osteoarthritis and Cartilage, 2007. **15**(3): p. 309-15.
3. Stanton, T.E., *Boundary lubrication in engineering practice*. Engineer, 1923. **135**: p. 678-680.
4. Teeple, E., B.C. Fleming, A.P. Mechrefe, J.J. Crisco, M.F. Brady, and G.D. Jay, *Frictional properties of Hartley guinea pig knees with and without proteolytic disruption of the articular surfaces*. Osteoarthritis Cartilage, 2007. **15**(3): p. 309-15.
5. Jones, E.S., *Joint Lubrication*. The Lancet, 1936. **230**: p. 1043-1044.
6. Wright, V. and D. Dowson, *Lubrication and cartilage*. J Anat, 1976. **121**(Pt 1): p. 107-18.
7. Caligaris, M. and G.A. Ateshian, *Effects of sustained interstitial fluid pressurization under migrating contact area, and boundary lubrication by synovial fluid, on cartilage friction*. Osteoarthritis Cartilage, 2008. **16**(10): p. 1220-7.

8. Forster, H. and J. Fisher, *The influence of loading time and lubricant on the friction of articular cartilage*. Proc Inst Mech Eng [H], 1996. **210**(2): p. 109-19.
9. Gleghorn, J.P., A.R. Jones, C.R. Flannery, and L.J. Bonassar, *Boundary mode frictional properties of engineered cartilaginous tissues*. Eur Cell Mater, 2007. **14**: p. 20-8; discussion 28-9.
10. Krishnan, R., E.N. Mariner, and G.A. Ateshian, *Effect of dynamic loading on the frictional response of bovine articular cartilage*. J Biomech, 2005. **38**(8): p. 1665-73.
11. Linn, F.C., *Lubrication of animal joints. I. The arthrotripsometer*. J Bone Joint Surg Am, 1967. **49**(6): p. 1079-98.
12. Schmidt, T.A. and R.L. Sah, *Effect of synovial fluid on boundary lubrication of articular cartilage*. Osteoarthritis Cartilage, 2007. **15**(1): p. 35-47.
13. Tanaka, E., N. Kawai, M. Tanaka, M. Todoh, T. van Eijden, K. Hanaoka, D.A. Dalla-Bona, T. Takata, and K. Tanne, *The frictional coefficient of the temporomandibular joint and its dependency on the magnitude and duration of joint loading*. J Dent Res, 2004. **83**(5): p. 404-7.
14. Coles, J.M., J.J. Blum, G.D. Jay, E.M. Darling, F. Guilak, and S. Zauscher, *In situ friction measurement on murine cartilage by atomic force microscopy*. J Biomech, 2008. **41**(3): p. 541-8.
15. Park, S., K.D. Costa, and G.A. Ateshian, *Microscale frictional response of bovine articular cartilage from atomic force microscopy*. J Biomech, 2004. **37**(11): p. 1679-87.

16. Jay, G.D., J.R. Torres, D.K. Rhee, H.J. Helminen, M.M. Hytinen, C.J. Cha, K. Elsaid, K.S. Kim, Y. Cui, and M.L. Warman, *Association between friction and wear in diarthrodial joints lacking lubricin*. *Arthritis Rheum*, 2007. **56**(11): p. 3662-9.
17. Fischer, M.S. and R. Blickhan, *The tri-segmented limbs of therian mammals: kinematics, dynamics, and self-stabilization--a review*. *J Exp Zool A Comp Exp Biol*, 2006. **305**(11): p. 935-52.
18. Fischer, M.S., N. Schilling, M. Schmidt, D. Haarhaus, and H. Witte, *Basic limb kinematics of small therian mammals*. *J Exp Biol*, 2002. **205**(Pt 9): p. 1315-38.
19. Barnett, C.H. and A.F. Cobbold, *Lubrication within living joints*. *The Journal of Bone and Joint Surgery*, 1962. **44B**(3): p. 662-674.
20. Teeple, E., K.A. Elsaid, B.C. Fleming, G.D. Jay, K. Aslani, J.J. Crisco, and A.P. Mechrefe, *Coefficients of friction, lubricin, and cartilage damage in the anterior cruciate ligament-deficient guinea pig knee*. *J Orthop Res*, 2008. **26**(2): p. 231-7.
21. Unsworth, A., D. Dowson, and V. Wright, *Some new evidence on human joint lubrication*. *Ann Rheum Dis*, 1975. **34**(4): p. 277-85.
22. McCutchen, C.W., *The frictional properties of animal joints*. *Wear*, 1962. **5**: p. 1.
23. Roberts, B.J., A. Unsworth, and N. Mian, *Modes of lubrication in human hip joints*. *Ann Rheum Dis*, 1982. **41**(3): p. 217-24.
24. Charnley, J., *The lubrication of animal joints in relation to surgical reconstruction by arthroplasty*. *Ann Rheum Dis*, 1960. **19**: p. 10-9.
25. Tanaka, E., T. Iwabe, D.A. Dalla-Bona, N. Kawai, T. van Eijden, M. Tanaka, S. Kitagawa, T. Takata, and K. Tanne, *The effect of experimental cartilage damage*

and impairment and restoration of synovial lubrication on friction in the temporomandibular joint. J Orofac Pain, 2005. **19**(4): p. 331-6.

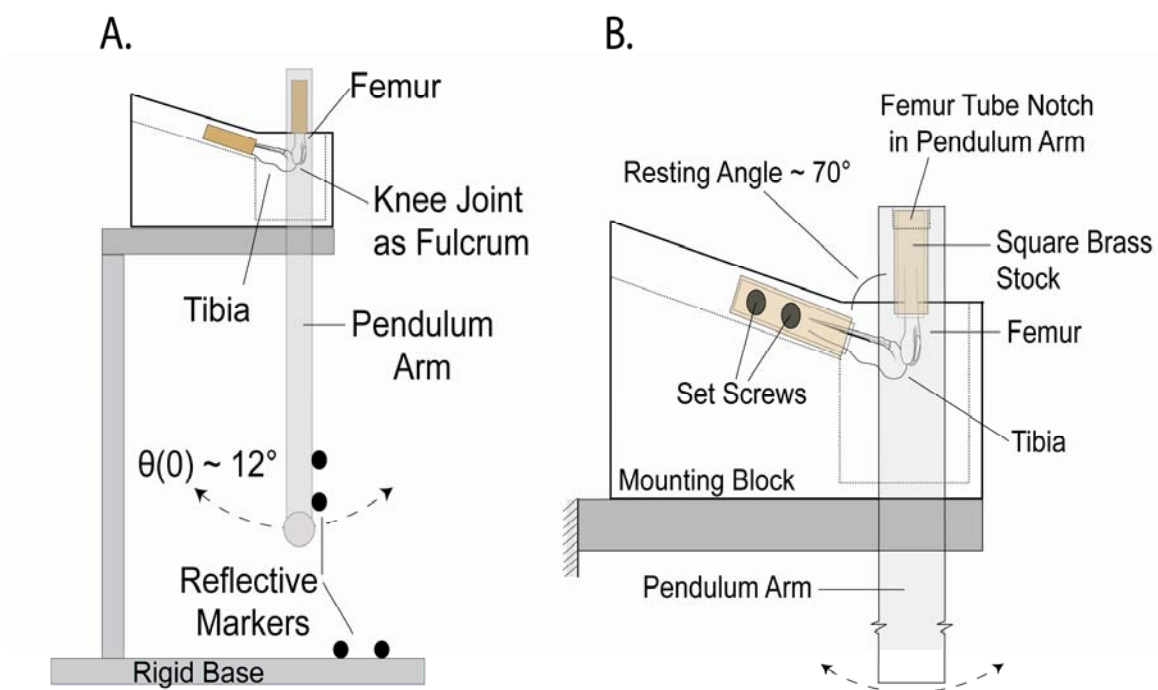


Figure 2.1: Schematic of simple pendulum system used for amplitude decay data collection (A). The pendulum arm was fixed to the proximal end of the femur and the tibia was rigidly mounted to a base platform. Four reflective markers were attached to both the pendulum arm and to the base (not all markers shown) for 3-D motion tracking. The arm was set to an initial angle of $\sim 12^\circ$, released, and allowed to oscillate freely until damping out completely. Close-up schematic of the knee joint mounting system (B). Both limbs were embedded in square 6.25 mm tubing with a urethane-potting compound and secured into the apparatus at a resting angle of 70° . The tibia was fixed to the base with four set screws (two on each side of the limb). The proximal end of the tube-fitted femur fit into a square notch cut into the pendulum arm.

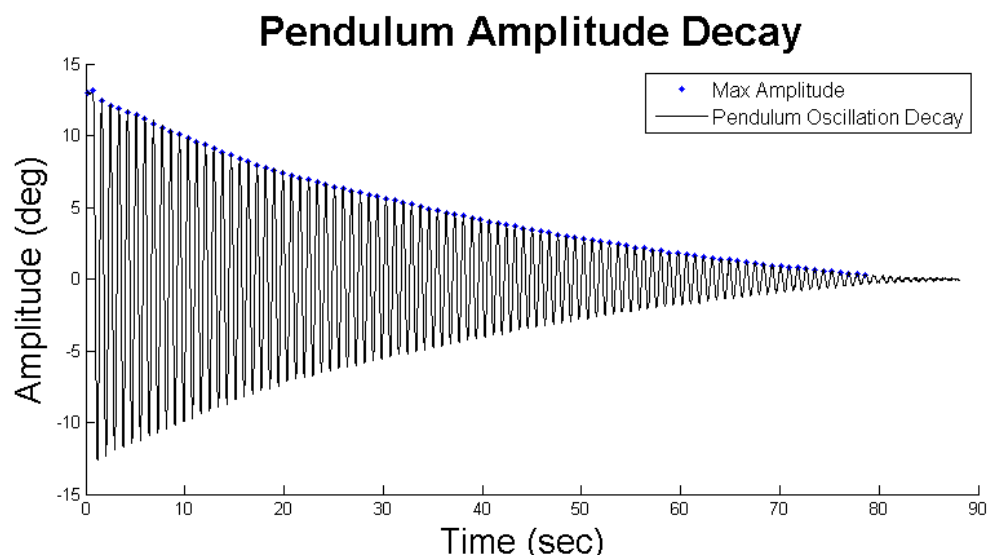


Figure 2.2: Representative plot of pendulum oscillation decay starting with initial release of the pendulum arm through damping out of the system. Points denote the maximum amplitude of each cycle.

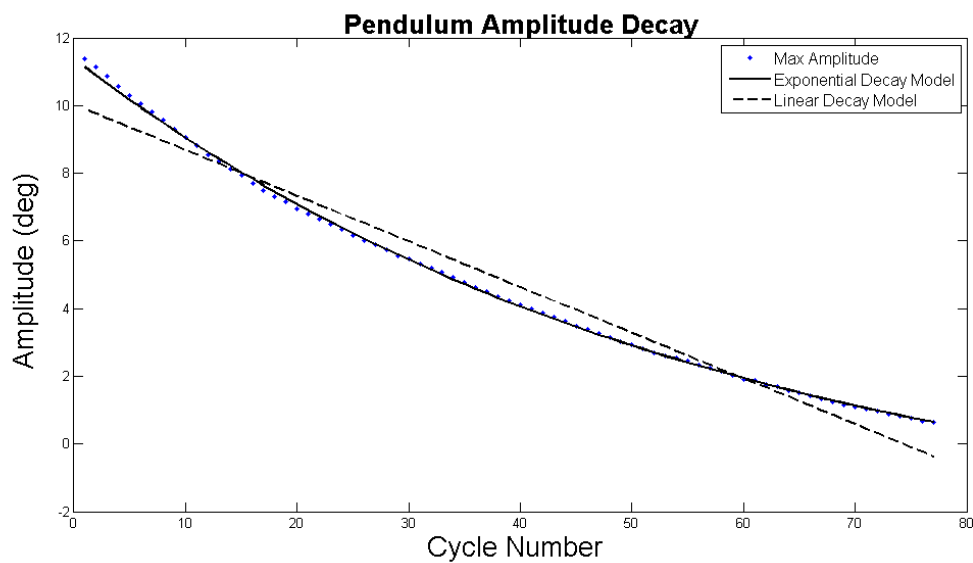


Figure 2.3: Representative plot of the Lin μ (dashed line) and Exp μ (solid line), which accounts for viscous damping fit to the maximum amplitudes points for each cycle. The Exp μ model provided a much closer fit to the experimental data with a RMSE of 0.078° and an ASE of 0.033° , versus the Lin μ RMSE of 0.55° and ASE of 0.185° .

Chapter 3

Cyclic Loading Increases the Coefficient of Friction of Frozen *Prg4*^{+/+} and *Prg4*^{+/-} Mouse Knee Joints but Not Fresh Knee Joints

Elizabeth I. Drewniak, Gregory D. Jay, Braden C. Fleming, Joseph J. Crisco,

The following chapter has been submitted to the *Journal of Biomechanics* for review.

3.1 Abstract

The initiation of osteoarthritis (OA) has been attributed to biological, mechanical, and structural factors; however, these causes are still not well understood. In attempts to ascertain more information about the mechanical factors that contribute to OA, researchers have taken a multitude of approaches to study articular cartilage (AC), including *ex vivo* tribological studies on a variety of joints across a range of species. Lubricin (encoded by the gene, *Prg4*) provides chondroprotection within synovial joints.

The primary goal of this study was to examine the effects of cyclic loading on the frictional properties (CoF) of intact *Prg4*^{+/+} and *Prg4*^{+/-} mouse knee joints undergoing cyclic loading. Additionally, this study investigated the effects of freezing on the CoF of cyclically loaded joints. Knees from *Prg4*^{+/+} and *Prg4*^{+/-} mice (n=18 pairs/genotype) were divided into “fresh” (n=12 pairs /genotype) and “frozen” (n=6 pairs /genotype) groups. Fresh joints were prepared for testing immediately following euthanasia; while frozen joints were flash frozen with liquid nitrogen. A passive pendulum was used to collect data to measure the CoF of intact mouse knees. Cyclic loading on the experimental joints was performed with an active pendulum. Friction measurements were taken at various time points during cyclic loading. One hundred twenty minutes of cyclic loading did not significantly increase the CoF of fresh joints. Frozen specimens, however, demonstrated a significant increase of CoF values following 120 minutes of cyclic loading. Studies evaluating the frictional properties of AC should be performed on fresh specimens, as our data suggests that freezing may be a confounding factor.

3.2 Introduction

Many studies have focused on the tribology of synovial joints to better understand osteoarthritis (OA). Various methods have been used to measure the coefficient of friction (CoF), such as the use of pendulums. While pendulums have been used with a variety of joints, CoF values ranged from 0.001 to 0.13 [1-3]; more work is needed to further investigate how CoF responds to biomechanical testing, such as cyclic loading, which simulates *in vivo* motion. Joint lubrication serves to reduce friction and wear within synovial joints. Lubricin, a glycoprotein encoded by the *Prg4* gene, provides chondroprotection, inhibits cellular adhesion, and acts as a boundary lubricant [4-5]. Our primary objective was to investigate the effects of freezing and cyclic loading on the CoF of knee joints from mice with two alleles of *Prg4* (*Prg4*^{+/+}) and one allele of *Prg4* (*Prg4*^{+/-}) using two custom-built pendulum systems.

3.3 Methods

Using procedures approved by the Rhode Island Hospital Animal Welfare Committee, hind limbs from *Prg4*^{+/+} and *Prg4*^{+/-} mice (n=18/genotype) were disarticulated at the hip joint following euthanasia. All specimens were 10-week-old (± 0.5 weeks) mice. Hind limbs from each *Prg4* genotype (n=6 “frozen” pairs) were flash frozen with liquid nitrogen and stored at -80°C . On the day of testing, they were thawed at room temperature and prepared as described below. The remaining hind limbs from both *Prg4* genotypes (n=12 “fresh” pairs) were prepared and tested on the day of euthanasia.

Skin, musculature, and connective tissues were removed, but the joint capsule was left whole. Each paw was disarticulated at the ankle, leaving the femur, knee joint, tibia, and fibula intact. In order to mount specimens in the pendulum systems, the proximal femur and the distal tibia were rigidly potted in square brass tubes (6.25 mm width and 25.4 mm long) with a urethane-potting compound (Smooth-On, Easton, PA).

Two custom-made pendulum systems were developed. CoF was measured using a passive pendulum system and previously described methods [6]. An active pendulum system was designed for cyclic loading (**Figure 3.1**). The specimen mounting system for the active system was identical to that of the passive system in which the knee joint served as the pendulum fulcrum; however, the joint was contained within a well filled with cell culture medium that served to hydrate and maintain viability of the tissue. The pendulum arm was attached to a DC motor by means of a series of linkages and bearings

in order to drive the active system. The joint was driven at a rate of $\sim 1.5\text{Hz}$ through $\pm 15^\circ$ of flexion and extension.

One knee joint from each pair was randomly selected as the experimental knee, while the contra-lateral knee was designated as the control. Once oscillation data were collected for each control knee ($t=0\text{min}$), it was placed unloaded in cultured media for the duration of testing. Following all testing of the experimental knee data, CoF oscillation data collection was repeated for the control joint to standardize the exposure time. Initial oscillation data were collected for the experimental knee. The specimen was then placed in the active pendulum system and cyclically loaded for 120 minutes. During this time, CoF data were collected at $t=2.5, 15, 30, 45, 60,$ and 120 minutes.

A two-way repeated measures ANOVA was used to assess differences in CoF values across time points and treatment groups (Fresh *Prg4*^{+/+}, Frozen *Prg4*^{+/+}, Fresh *Prg4*^{+/-}, Frozen *Prg4*^{+/-}). A significant p-value of less than 0.05 was set *a priori*. Percent change in CoF following cyclic was also calculated for each of the experimental groups.

3.4 Results

One hundred twenty minutes of cyclic loading did not significantly affect the CoF values of fresh specimens from either *Prg4* genotype ($p=0.872$ and $p=0.380$ for *Prg4*^{+/+} and *Prg4*^{+/-}, respectively). The same duration of cyclic loading did result in significant increases in the CoF values of *Prg4*^{+/+} and *Prg4*^{+/-} specimens that were flash frozen and thawed prior to specimen preparation and testing ($p=0.015$ and $p<0.001$, respectively). Cyclic loading of frozen *Prg4*^{+/+} knees resulted in a 94.8% increase in CoF value from 0.027 ± 0.004 (mean \pm SD) to 0.052 ± 0.031 , while the CoF of frozen *Prg4*^{+/-} joints demonstrated the greatest increase of 187.8% from 0.033 ± 0.007 to 0.095 ± 0.026 (**Figure 3.2**). Fresh specimens averaged only an 11.65% increase with one hundred twenty minutes of cyclic loading. CoF values of all control knees remained essentially constant and within 1.0% over the duration of the experiment.

3.5 Discussion

The goal of this work was to investigate the effects of cyclic loading and freezing on the CoF of intact *Prg4+/+* and *Prg4+/-* mouse knee joints. Unexpectedly, one hundred twenty minutes of cyclic loading resulted in significant increases of CoF in specimens that were frozen prior to preparation and CoF data collection, but cyclic loading did not affect CoF values of fresh *Prg4+/+* and *Prg4+/-* specimens prepared and tested immediately following euthanasia. These findings were unanticipated due to the fact that previous studies that utilized cyclic loading to assess the CoF of AC reported increases in both fresh and frozen tissue. Using a tribological simulation of freshly harvested medial compartmental bovine knees, McCann *et al.*, demonstrated that while cyclic loading values were higher in meniscectomized specimens, CoF increases were recorded in all joints following cyclic loading [7]. Additionally, Forster and Fisher reported significant CoF increases following two hours of continuous sliding of bovine cartilage plugs in their pin-on-disc system. The authors stated that the cartilage samples were frozen and stored at -20°C in Ringer's solution until testing, but mentioned that pilot data comparing friction measurements of fresh and frozen samples yielded no differences [8]. A third study, by Williams *et al.* investigated the effects of osteochondral plug storage over the course of one, seven, fourteen, and twenty-eight days. The AC was assessed for viability, chondrocyte metabolic activity, and biochemical and biomechanical properties. Tissue designated for biomechanical testing was frozen at -80°C until the day of testing. It was noted that while freezing killed chondrocytes, it should not significantly affect results

from biomechanical testing, including indentation stiffness measurements, equilibrium tensile properties, and response to static and dynamic compression testing [9].

Forster and Fisher and Williams *et al.* reported that freezing did not affect the results of their biomechanical testing [8-9]. Our data suggests that freezing samples may be a confounding factor, as it did have an effect on the frictional properties of intact mouse knee joints following cyclic loading. Hence, tissue storage could pose challenges when designing studies using biotribological and biomaterial testing on articular cartilage and synovial joints. The only joints that demonstrated significant increases over the course of the experiment were the specimens that were frozen prior to cyclic loading. This study must be taken into consideration when developing experimental protocols, particularly work that requires *prolonged* testing. Additionally, these results could have clinical implications for cartilage storage and repair techniques, due to the fact that osteochondral allograft transplantation is a well-established method for the treatment of cartilage defects of the knee, including OA [9].

Prg4^{+/+} and *Prg4*^{+/-} mouse knee joints were used for this investigation. As mentioned above, the *Prg4* gene codes for lubricin, a glycoprotein that provides lubrication in synovial joints. In addition to revealing that freezing effects the manner in which the CoF of mouse knee joints respond to cyclic loading, there also seems to be a lubricin dosing effect given the response of frozen joints at t=120min. While the CoF of frozen joints of both *Prg4*^{+/+} and *Prg4*^{+/-} mice demonstrated significant increases following cyclic loading, as compared to their initial CoF values (t=0min), frozen *Prg4*^{+/-} mouse joints, which contain only one allele of *Prg4*, were significantly higher than CoF values from frozen *Prg4*^{+/+} joints, with two alleles of *Prg4*, at t=120min.

These results show that freezing affects the frictional properties of the joints; additionally, the one *Prg4* allele in *Prg4*^{+/-} joints was not capable of providing sufficient chondroprotection, as compared to *Prg4*^{+/+} joints.

The findings from this study will contribute to protocol development of future investigations. The small size of the intact mouse knee joints posed design challenges. However, the final design of both pendulum systems allowed for a repeatable, reliable long-term biomechanical testing on joints from small species. The experimental protocol for this study only called for 120 minutes of testing; however, the well containing cell culture media allows for long-term whole joint tribological testing. Also, the design of the pendulums allows for unconstrained flexion-extension motion permitting simulation of *in vivo* motions. The advantages of this testing scheme exploits the availability of mouse strains with gene mutations related to cartilage development and homeostasis.

3.6 Acknowledgements

The authors would like to acknowledge their funding sources: NIH (AR050180, P20-RRO24484), Rhode Island Hospital Orthopaedic Foundation, Inc., and University Orthopaedics, Inc. Thank you to Ling Zhang, MD for assistance in maintaining the *Prg4* +/+, +/-, and -/- mouse colony.

3.7 References

1. Forster, H. and J. Fisher, *The influence of loading time and lubricant on the friction of articular cartilage*. Proceedings of the Institution of Mechanical Engineers, Part H, 1996. **210**(2): p. 109-19.
2. Mow, V.C., Huiskes, R., ed. *Basic Orthopaedic Biomechanics & Mechano-Biology*. Third ed. 2005, Lippincott, Williams & Wilkins: Philadelphia. 720.
3. Teeple, E., B.C. Fleming, A.P. Mechrefe, J.J. Crisco, M.F. Brady, and G.D. Jay, *Frictional properties of Hartley guinea pig knees with and without proteolytic disruption of the articular surfaces*. Osteoarthritis and Cartilage, 2007. **15**(3): p. 309-15.
4. Jay, G.D., K.A. Elsaid, J. Zack, K. Robinson, F. Trespalacios, C.J. Cha, and C.O. Chichester, *Lubricating ability of aspirated synovial fluid from emergency department patients with knee joint synovitis*. Journal of Rheumatology, 2004. **31**(3): p. 557-64.
5. Rhee, D.K., J. Marcelino, M. Baker, Y. Gong, P. Smits, V. Lefebvre, G.D. Jay, M. Stewart, H. Wang, M.L. Warman, and J.D. Carpten, *The secreted glycoprotein lubricin protects cartilage surfaces and inhibits synovial cell overgrowth*. J Clin Invest, 2005. **115**(3): p. 622-31.
6. Drewniak, E.I., G.D. Jay, B.C. Fleming, and J.J. Crisco, *Comparison of two methods for calculating the frictional properties of articular cartilage using a simple pendulum and intact mouse knee joints*. Journal of Biomechanics, 2009. **42**(12): p. 1996-9.

7. McCann, L., E. Ingham, Z. Jin, and J. Fisher, *Influence of the meniscus on friction and degradation of cartilage in the natural knee joint*. *Osteoarthritis and Cartilage*, 2009. **17**(8): p. 995-1000.
8. Forster, H. and J. Fisher, *The influence of continuous sliding and subsequent surface wear on the friction of articular cartilage*. *Proceedings of the Institution of Mechanical Engineers, Part H*, 1999. **213**(4): p. 329-45.
9. Williams, S.K., D. Amiel, S.T. Ball, R.T. Allen, V.W. Wong, A.C. Chen, R.L. Sah, and W.D. Bugbee, *Prolonged storage effects on the articular cartilage of fresh human osteochondral allografts*. *Journal of Bone and Joint Surgery Am*, 2003. **85-A**(11): p. 2111-20.

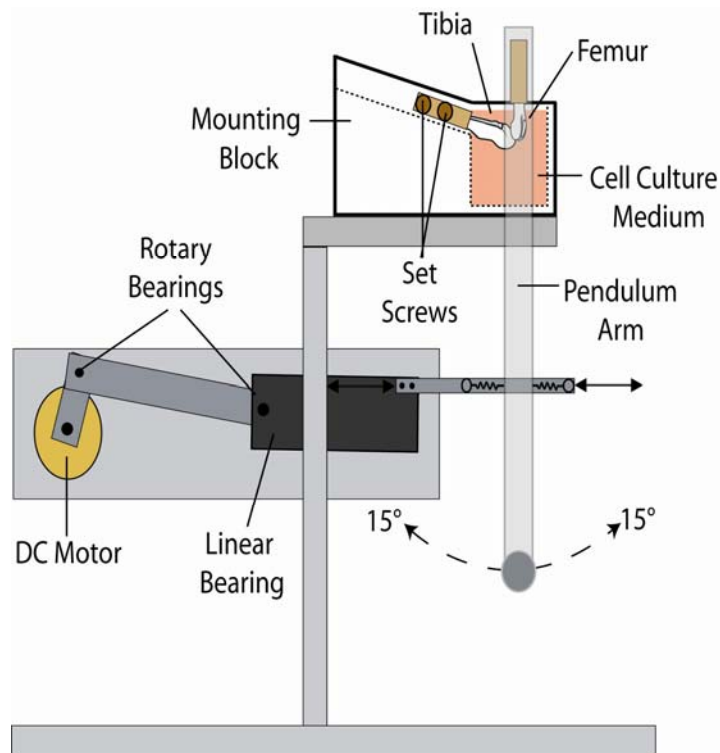


Figure 3.1: A custom-built, active pendulum was used to perform unconstrained cyclic loading with intact *Prg4*^{+/+} and *Prg4*^{+/-} mouse knee joints serving as the fulcrum of the system. The DC motor drives the specimen through $\pm 15^\circ$ of flexion-extension via a series of linkages, rotary bearings, and a linear bearing. A well containing cell culture medium hydrates the joint and helps to maintain viability.

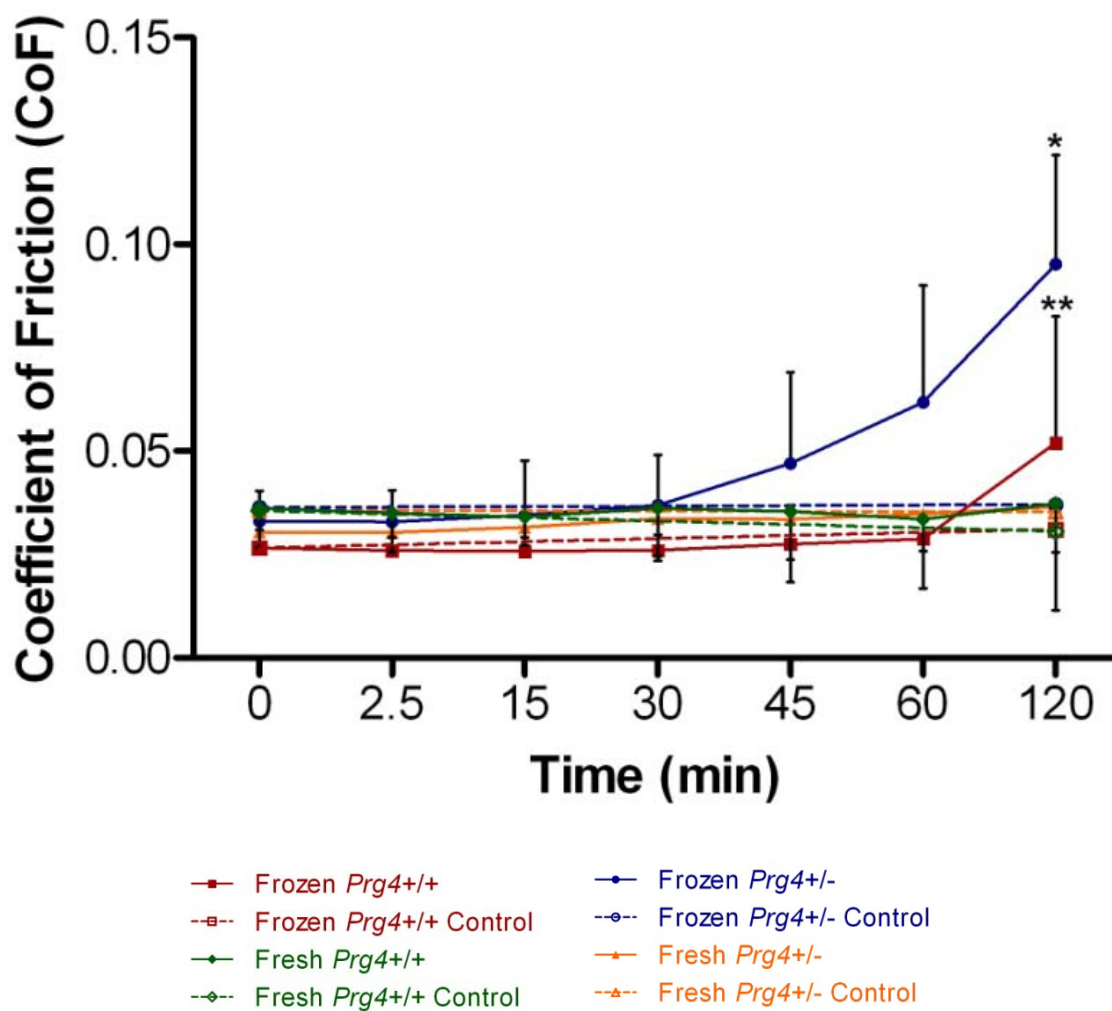


Figure 3.2: Mean values of experimental and contra-lateral control CoF values of Fresh and Frozen joints from *Prg4*^{+/+} and *Prg4*^{+/-} mice (n=12 fresh pairs per genotype; n=6 frozen pairs per genotype) over the course of testing. Standard deviation error bars provided for cyclically loaded groups. CoF values of unloaded joints remained constant between their initial and final CoF measurements. Experimental Frozen and Fresh CoF values started approximately equal; however, the Frozen CoF values of both *Prg4* genotypes significantly (* denotes $p < 0.001$; ** denotes $p = 0.015$) increased following 120 minutes of cyclic loading, as compared to their initial (t=0min) CoF measurements.

Chapter 4

Cyclic Loading Increases Friction and Changes Cartilage Surface Integrity in Lubricin Mutant Mouse Knees

Elizabeth I. Drewniak, Gregory D. Jay, Braden C. Fleming, Ling Zhang, Matthew L. Warman, Joseph J. Crisco

The following chapter has been submitted to *Arthritis & Rheumatism* for review.

4.1 Abstract

4.1.1 Objective

To investigate the effects of lubricin gene dosage and cyclic loading on whole joint coefficient of friction (CoF) and articular cartilage surface integrity in mouse knee joints.

4.1.2 Methods

Two custom-built pendulums were designed for cyclic loading and CoF testing. Joints from mice with two alleles of lubricin (*Prg4*^{+/+}), one allele of lubricin (*Prg4*^{+/-}), and no working copies of lubricin (*Prg4*^{-/-}) were subjected to 26 hours of loading; CoF values were measured at multiple time points. Contra-lateral control joints were kept unloaded. Following testing, all joints were examined for histologic evidence of damage and viability.

4.1.3 Results

At baseline, *Prg4*^{-/-} CoF values were significantly higher than *Prg4*^{+/+} and *Prg4*^{+/-} values ($p < 0.001$). Cyclic loading continuously increased CoF in *Prg4*^{-/-} joints. In contrast, *Prg4*^{+/-} and *Prg4*^{+/+} joints had no CoF increases during the first 4 hours of loading. After 26 hours of loading, joints from all genotypes had increased CoF values compared to baseline and controls. However, significantly greater increases occurred in *Prg4*^{-/-} and *Prg4*^{+/-} joints. CoF increases were not associated with histologic changes or cell viability.

4.1.4 Conclusion

A reliable method for cyclically loading joints and measuring CoF was developed. Mice lacking lubricin have increased baseline CoF values and are not protected from further increases caused by loading. *Prg4*^{+/-} mice are indistinguishable from *Prg4*^{+/+} mice at baseline, but have significantly greater CoF values following 26 hours of loading. Lubricin dosage affects joint properties during loading, and may have clinical implications in patients for whom injury or illness alters lubricin abundance.

4.2 Introduction

Lubricin, a major component of synovial fluid and the articular cartilage surface, is a mucinous glycoprotein encoded by the gene *Prg4* [1]. To understand the *in vivo* function of lubricin, lubricin-null mice (*Prg4*^{-/-}) were generated. *Prg4*^{-/-} mice appear normal at birth, but develop precocious clinical, radiological, and histological signs of joint disease as they age [2]. These features recapitulate findings in patients with the camptodactyly-arthropathy-coxa vara-pericarditis syndrome (CACP), due to hereditary lubricin deficiency. Based on *in vivo* studies in *Prg4*^{-/-} mice, lubricin was postulated to provide chondroprotection by acting as a boundary lubricant, a cell adhesion inhibitor, and a synoviocyte growth regulator (2, 3). While the precocious cartilage failure observed in patients with CACP and in *Prg4*^{-/-} mice indicates that lubricin is essential for chondroprotection, it is not known whether lubricin levels that are below *Prg4*^{+/+} levels, but not completely absent, can also impair chondroprotection. *In vitro* studies that measured boundary lubrication at different concentrations of lubricin, and clinical studies showing that lubricin levels fall in humans and other mammals following traumatic joint injury, suggest that a correlation may exist between lubricin concentration and chondroprotection [3-19]. This work seeks to directly test this hypothesis by comparing changes in the knee articular cartilage of mice with two alleles for *Prg4* (*Prg4*^{+/+}), one allele of *Prg4* (*Prg4*^{+/-}) no working copy of *Prg4* (*Prg4*^{-/-}) by measuring the coefficient of friction (CoF) following a sustained period of cyclic joint loading.

Cyclic loading has been used in many studies to better understand the mechanical and material properties of articular cartilage [14, 19-22]. Pin-on-disc systems rub

cartilage samples against apposing cartilage plugs or man-made surfaces. Such systems have been used to collect information on friction, deformation, and wear, among other properties [19-21, 23-24]. *In vitro* pin-on-disc testing methods allow for a tissue-specific investigation of articular cartilage; however, these methods do not account for menisci, ligaments, synovial fluid, or joint capsules, which must all be considered when studying joint function and health. For this study, an active pendulum system was developed to apply cyclic loading to intact mouse knee joints in order to assess lubricin's role in preventing cartilage wear.

The objective of this study was to determine whether lubricin abundance affects whole joint friction properties and articular cartilage surface integrity of intact mouse knees when subjected to cyclic loading. It was hypothesized that mice lacking both copies of *Prg4* (i.e. *Prg4*^{-/-}) would have higher CoF values and more extensive surface damage than mice with two alleles of *Prg4* (i.e. *Prg4*^{+/+}).

4.3 Materials and Methods

4.3.1 Specimens

In accordance with procedures approved by the institution's Animal Welfare Committee, hind limbs from 10-week-old (± 0.5 weeks) male *Prg4*^{+/+}, *Prg4*^{+/-}, and *Prg4*^{-/-} mice (n=12 for each genotype) were disarticulated at the hip joint following euthanasia. The generation of these mice has been previously described and they have been backcrossed onto a C57BL6/J background [1]. Following disarticulation, skin, musculature, and connective tissue were dissected free, but joint capsules were left intact. Each paw was removed at the ankle joint, leaving just the femur, knee joint, tibia, and fibula. In order to mount specimens in the testing systems, the proximal femur and the distal tibia were rigidly potted with a urethane-potting compound (Smooth-On, Easton, PA) in square brass tubes (6.25 mm width and 25.4 mm long).

4.3.2 Pendulum Systems

Two custom-made pendulum systems were used in this study: a passive pendulum system for determining joint CoF (**Figure 4.1A**) and an active system for applying unconstrained cyclic loading (**Figure 4.1B**). Both systems included a platform with a specimen-mounting block (**Figure 4.1C**). The tube encasing the tibia was set in the mounting block and fixed with two set screws. The pendulum arm was fit to the proximal femur and weighed approximately two times that of the mice used in this study (~50g). The femoral tube was attached to the pendulum arm by a square notch located in the top

portion of the pendulum. The knee joint served as the fulcrum of the pendulum and had an equilibrium knee flexion angle of $\sim 70^\circ$, which is the mean flexion angle mice and other small rodents experience during normal ambulation [25-26]. A total of eight reflective markers were placed on the pendulum system for motion tracking; four were fixed to the pendulum arm, and an additional four were attached to the base of the system. To determine the CoF using the passive system, the limb was rotated from its vertical equilibrium position to a starting angle of $\sim 12 \pm 2^\circ$ (Fig 1B), released and allowed to oscillate freely, until returning to its equilibrium state. Motion was tracked with a Qualisys AB system (Gothenburg, Sweden) at a rate of 60Hz. Custom MATLAB (Mathworks, Inc., Natick, MA) code calculated the CoF using a Stanton linear decay model [27-28]. Three trials were recorded for each joint at each time point. These values were then averaged together and used for statistical analysis.

The active pendulum was used for cyclic loading. The specimen mounting system was identical to the passive pendulum system, however the joint was placed within a well filled with cell culture medium [29] to hydrate and prolong the viability of the tissue. The well contained approximately 35 ml of medium, so that the joint was completely submerged. Testing took place at room temperature and the well was replenished as necessary. The pendulum arm was attached to a DC motor via a series of linkages, rotary bearings, and a linear bearing to drive the active pendulum. The joint was driven through $\pm 15^\circ$ of flexion and extension at a rate of ~ 1.5 Hz.

4.3.3 Cyclic Loading Protocol

One hind limb from each pair was randomly selected as the experimental knee that would undergo cyclic loading, while the contra-lateral knee joint served as the control (**Figure 4.2**). Oscillation data were collected with the passive pendulum for each knee (t=0 min time point) to obtain baseline CoF values. The control joint was then placed unloaded in culture medium, while the experimental limb was mounted in the active pendulum system for cyclic loading. The experimental joint was cyclically loaded for a period of two hours. At specific time points, the specimen was briefly returned to the passive pendulum to measure the CoF. Following the 2 hours of cyclic loading, the experimental joint was placed unloaded in cell culture medium for 12 hours, after which the CoF was again measured before the joint was subjected to an additional 24 hours of cyclic loading. During this second session of cyclic loading, the specimen was again briefly returned to the passive pendulum to measure the CoF (**Figure 4.2**). In addition to control knees having baseline CoF values measured, control knee CoF values were also measured after 38 hours in culture medium (**Figure 4.2**).

4.3.4 Histological Processing and Analysis

Following collection of the final CoF measurements, experimental and control specimens were placed in 10% buffered formalin for fixation. Specimens were decalcified, embedded in paraffin wax, and cut into 5 μm coronal sections. Sections were then deparaffinized and dehydrated with xylenes and serial ethanols. Finally, sections were stained with Safranin-O and fast green and counter-stained and mounted with permount (Fisher Scientific). Five observers, blinded to genotype (*Prg4* +/+, +/- and -/-),

as well as treatment group (cyclically loaded vs. unloaded), evaluated the articular cartilage integrity using a scoring system that has been developed and validated specifically for mouse cartilage [30]. This system focused on the following categories: articular cartilage structure (0-4), surface layer morphology (0-3), and pericellular loss of Safranin-O staining (0-4). Each observer independently scored each tibial plateau, and then the final score was determined following group adjudication. Next, scores for each plateau were averaged to obtain one score for each category per joint. Scores from each category were combined to determine a total for each joint.

4.3.5 Chondrocyte Viability

Because this study involved prolonged *ex vivo* testing of murine knee joints, chondrocyte viability was assessed using fluorescein diacetate (FDA) and propidium iodide (PI) paravital staining. Additional *Prg4*^{+/+}, *+/+*, and *-/-* specimens (n=2 pairs per genotype; two experimental and two control knee joints per genotype) were used to confirm chondrocyte viability. Specimens underwent preparation and testing protocols as described above. Following testing, the capsules from both cyclically loaded and control specimens were dissected away and joints were disarticulated. Using a scalpel, cartilage surfaces were separated from each long bone to ensure that the FDA/PI dye penetrated through the tissue. FDA stock solution was prepared by dissolving 40.1 mg of FDA (Sigma) in 10 ml of acetone. 100 mg of PI was dissolved in 10 ml of distilled water to create a stock solution of PI. A working solution of FDA was prepared by combining 5 μ l of stock solution with 15 ml of PBS; 10 μ l of PI stock solution were combined with 10 ml of PBS and 2.5% EDTA to make a working PI solution. Equal volumes of each

working solution were mixed to create the final stain. Cartilage samples were incubated in the final stain in the dark at room temperature for five minutes. Following incubation, samples underwent five successive washes with PBS. Lastly, the cartilage sections were mounted on glass slides with Vectashield mounting medium (Vector Laboratories).

Confocal images were acquired with a Nikon C1si confocal (Nikon Inc., Mellville, NY) using diode lasers 488 and 561. Serial optical sections were performed with EZ-C1 computer software (Nikon Inc., Mellville, NY). Z-series sections were collected at 1.5 μm with a 20x PlanApo lens and a scan zoom of 1x. Each wavelength was acquired separately by invoking frame lambda. Projections were performed in Elements (Nikon, Inc., Mellville, NY) computer software.

4.3.6 Statistical Analysis

A three-way ANOVA on log-adjusted CoF values was used to assess the effects of time, genotype, and limb (experimental vs. control) on the CoF values. A log-normal mixed model was used to assess the CoF values across all time points. A significant p-value of less than 0.05 was set *a priori*.

A two-way ANOVA was used to test for statistically significant differences among *Prg4* genotypes (+/+, +/- vs. -/-) and treatment groups (experimental vs. control) within each histological scoring category and for the overall total score (SigmaStat, Systat Software, Inc., Chicago, IL). A significant p-value of less than 0.05 was set *a priori*.

4.4 Results

Baseline (t=0hr) CoF values in *Prg4*^{+/+} joints (0.036 ± 0.0096 ; mean \pm SD) and *Prg4*^{+/-} joints (0.030 ± 0.0044) did not significantly differ from each other (**Figure 4.3A and B**). In contrast, the baseline CoF of *Prg4*^{-/-} mouse knees (0.077 ± 0.0095) was significantly higher than *Prg4*^{+/+} and *Prg4*^{+/-} joints ($p<0.001$). After 38 hours in culture medium, the CoF values of unloaded joints did not differ significantly from the CoF values obtained at baseline for mice with the same *Prg4* genotype (**Figure 4.3A**).

Prg4^{-/-} joints exhibited a progressive increase in CoF values during the first two hours of cyclic loading, while no increases in CoF were observed in *Prg4*^{+/+} and *Prg4*^{+/-} joints (**Figure 4.3A**). CoF changes did not occur when the *Prg4*^{+/+}, ^{+/-}, or ^{-/-} joints were then unloaded for 12 hours (**Figure 4.3A**). However, CoF continued to increase in *Prg4*^{-/-} joints when cyclic loading was resumed, reading a final CoF value of 0.13 ± 0.014 (**Figure 4.3A and B**). In contrast, there was no change in CoF in *Prg4*^{+/+} joints during the first six hours of cyclic loading, but, by the end of the experiment, CoF had risen to 0.061 ± 0.034 . *Prg4*^{+/-} joints exhibited no change in CoF during the first four hours of cyclic loading, a mild increase (0.053 ± 0.034) after six hours of cyclic loading, rising to 0.12 ± 0.049 at the end of the experiment (**Figure 4.3A and B**). Therefore, although mean CoF values of all *Prg4* genotypes rose following 26 total hours of cyclic loading, the increases were much greater for *Prg4*^{+/-} and ^{-/-} joints compared to *Prg4*^{+/+} joints (**Figure 4.3B**).

As anticipated, based on previous studies [13], *Prg4*^{-/-} knee joints differed histologically from *Prg4*^{+/+} joints. Unloaded *Prg4*^{-/-} joints had significantly ($p < 0.001$) higher scores for articular cartilage surface structure and for surface layer morphology compared to unloaded *Prg4*^{+/+}, and *Prg4*^{+/-} joints, the latter two being indistinguishable. Significant ($p < 0.001$) differences in these measures were also found between the loaded *Prg4*^{-/-} joints compared with *Prg4*^{+/+} and *Prg4*^{+/-} joints (**Table 4.1 and Figure 4.4**). Interestingly, within a genotype, joints that had been cyclically loaded for 26 hours did not appear grossly different from their contra-lateral unloaded controls. However, following loading *Prg4*^{-/-} joints, but neither *Prg4*^{+/-} nor *Prg4*^{+/+} joints, had a significantly ($p = 0.013$) higher surface layer morphology scores compared to their non-loaded control.

Although the cyclically loaded and control knee joints were kept in cell culture medium for the entire 38 hours of the experiment, the lack of endogenous blood circulation and the retention of the synovial capsule surrounding the joint could have limited oxygen and nutrient availability within the joint and caused chondrocyte death. All cartilage samples contained living chondrocytes, as assessed by FDA/PI staining, independent of genotype and loading protocol (**Figure 4.5**).

4.5 Discussion

The objectives of this study were to investigate the effects of cyclic loading on the surface integrity of articular cartilage and on whole joint frictional properties in mice, and to contrast the effects of cyclic loading in mice that are wild-type (*Prg4*^{+/+}), heterozygous (*Prg4*^{+/-}), or homozygous (*Prg4*^{-/-}) for inactivating mutations in *Prg4*, the gene that encodes lubricin.

In contrast to other studies, which observed significant increases in CoF within two hours of cyclic loading, in this study, CoF increases were not observed until at least 4 hours of cyclic loading in *Prg4*^{+/+} and *Prg4*^{+/-} joints. This difference in the timing of CoF change may be due to the testing modality, which allowed the articular cartilage to remain undisturbed within an intact synovial capsule. Other studies employed articular cartilage that was excised from bovine knees [21-22, 31]. Excision from the intact knee joint could have made these specimens more prone to rapid changes in CoF due to weeping of water and glycosaminoglycans from the lateral surfaces or from the loss of water at the cartilage surface due to evaporation. Using medial compartmental bovine knees with and without meniscectomies and a tribological simulator to apply physiologically relevant (cyclic) loading for two hours, McCann *et al.* reported CoF increases, which were larger in meniscectomized specimens [22]. Forster and Fisher investigated the influence of continuous sliding on bovine articular cartilage plugs using a custom-built friction apparatus. They also demonstrated increases in CoF over the course of 120 minutes of testing [21]. Park *et al.* used bovine cartilage plugs to examine the effect of a sliding motion on the CoF, as measured by a custom-made friction device and

by atomic force microscopy (AFM). Both methods yielded friction increases during the course of the 2 hour experiment [31].

Although the use of intact knees did not directly measure cartilage friction, in theory, it more accurately measured the friction within a joint as it functions *in vivo*. Tribological testing with cartilage plugs has the advantage of directly isolating and observing articular cartilage behavior, and cartilage's response to mechanical load and treatments [23]. Hence, when a cartilage plug is loaded for testing, plowing friction is theoretically eliminated, resulting in only a surface friction measurement [24]. CoF values obtained through the use of AFM are generally higher, oftentimes by an order of magnitude, than values obtained with whole joint methods or cartilage plugs [3, 32]. AFM allows for a characterization of the effects of boundary lubrication on the frictional properties of AC, independent of the interstitial fluid pressurization that is found within diarthrodial joints [3, 24, 32]. While whole-joint pendulum system described within this study provides a robust *ex vivo* methodology that is capable of simulating *in vivo* knee conditions, it must be noted that the CoF values measured were not purely indicative of the frictional properties at the AC surface. These whole joint measurements take all components of the joint into account, including the menisci, cruciate ligaments, opposing joint surfaces, and joint capsule. Thus, the lubrication mechanisms differ in whole joints, as compared to those found in cartilage plug and AFM specimens. One method for avoiding these potential effects would be to statically load each joint for a period of time prior to collecting oscillation decay data. A large range of CoF values exist for AC; however, at this point in time, there is no "gold-standard" CoF value [24]. Until such a

value can be determined, it is more valuable to investigate the effects of a specific treatment (chemical, biomechanical, etc.) on CoF values.

Cyclic loading appears to be the sole cause for the increase of CoF values in this experiment, due to the fact that unloaded (contra-lateral control) knees had no change in CoF after 38 hours in cell culture medium. In contrast, CoF values of cyclically loaded joints increased during the same 38-hour period. The fact that the CoF increased following cyclic loading is consistent with findings from previous studies [21-22]. Interestingly, only *Prg4*^{-/-} joints demonstrated a clear increase in CoF following 2 hours of cyclic loading. This increase in CoF remained unchanged even when the joints were then stored unloaded in culture medium for 12 hours, but continued to increase when the cyclic loading resumed.

Lubricin, also referred to as proteoglycan 4 and superficial zone protein, is produced by synoviocytes that line the joint capsule and by chondrocytes within the superficial zone of articular cartilage. Previous work has demonstrated that the absence of lubricin results in protein deposition on cartilage surfaces, the disappearance of superficial zone chondrocytes, and synoviocyte overgrowth [1]. Additionally, *Prg4*^{-/-} mouse knee joints have been shown to develop evidence of cartilage wear by two weeks of age [33]. The results presented here confirm the important role of lubricin for protection against load-induced wear. The assays employed in this study demonstrated that cyclic loading had no effect on the CoF in *Prg4*^{+/+} mouse knee joints loaded for at least 6 hours, whereas a continual increase in CoF occurred in *Prg4*^{-/-} joints over that same period. Intriguingly, the CoF in *Prg4*^{+/-} knees at baseline and during the first 4 hours of cyclic loading was indistinguishable from *Prg4*^{+/+} joints. However, by 6 hours

of cyclic loading a difference between *Prg4*^{+/-} and *Prg4*^{+/+} knee joints began to emerge. After 26 hours of cyclic loading *Prg4*^{+/-} joints had developed CoF values that were closer to those of *Prg4*^{-/-} joints rather than *Prg4*^{+/+} joints. These results suggest that the ability of lubricin to provide long-term protection to joints is dose (i.e. concentration) dependent, which could have important clinical implications.

It is reasonable to question whether an increased CoF occurring only after 6 hours of cyclic loading in the *Prg4*^{+/-} joints will be clinically relevant, particularly since there was no difference between *Prg4*^{+/-} and *Prg4*^{+/+} joints at baseline or following 4 hours of cyclic loading. It can be speculated that mice and humans who are genetically deficient for one allele of *Prg4* may synthesize sufficient quantities of lubricin during normal use, but be unable to do so during periods of excessive use. Cyclic loading may denude areas of lubricin from the cartilage surface that must either be re-filled by newly synthesized lubricin from underlying superficial zone chondrocytes or by the deposition of lubricin from synovial fluid. Continuous passive motion of joints has previously been reported to induce lubricin expression by superficial zone chondrocytes [14], so genetic or acquired diseases that decrease lubricin synthesis and delay lubricin replacement on denuded surfaces could contribute to precocious cartilage wear. Too few heterozygous carriers of CACP mutations have been studied to know whether carriers have increased rates of joint failure compared to non-carriers. However, if insufficient lubricin production is responsible for the rise in CoF that occurs following cyclic loading, then therapies aimed at supplementing lubricin or increasing its production may improve long term outcomes in patients who have a significant reduction in lubricin abundance as a result of injury or illness.

Friction is defined as the resistance of motion between two joint surfaces in contact with one another [24]. As the CoF values presented in this study have demonstrated, cyclic loading alters the frictional properties of articular cartilage. Because this assay utilized excised limbs and occurred over 38 hours, it was important to confirm that the chondrocytes in the tested joints remained alive throughout the study. Viable cells were observed in all specimens with fluorescein diacetate (FDA) and propidium iodide (PI) paravital stains; therefore, cell death did not account for the CoF increases that were observed after 26 hours of cyclic loading for all *Prg4* genotypes. This result was not surprising due to the fact that studies have shown that cartilage can maintain between 91% and 97% chondrocyte viability after 14 days and 70% to 83% viability after 28 days when stored in culture medium at 4°C [34-35]. However, one cannot preclude the possibility that this protocol reduced the biosynthetic activity of chondrocytes and synoviocytes in the absence of cell death.

Because the friction measurements were performed using a pendulum system on whole joints, there is a possibility that tissues other than the AC contributed to this increase in CoF. Twenty-six hours of cyclic loading in the active pendulum system could have altered the other components of the knee joints. As we reported, viable AC was found; however, cyclic loading could have also affected the viability of the synovium, which provides nutrients for the joint. Future studies should investigate the effects of cyclic loading on the integrity of the synovium, in addition to AC viability. Testing in the active pendulum could have also weakened or altered the biomechanical properties of the menisci and intra-capsular ligaments. Lastly, it is worth noting that both the *Prg4*^{+/-} and *Prg4*^{-/-} joints exhibited high CoF values following testing, in comparison to wild type

joints. The lack of one or both *Prg4* alleles could have affected tissues other than AC. Sun *et al.* identified lubricin within the canine anterior cruciate ligament, lateral collateral ligament, meniscus, muscle, skin, and flexor digitorum profundus tendon, in addition to AC [36-37]. Shine and Spector also reported on the presence and distribution of lubricin within the caprine intervertebral disc, noting that there was lubricin-positive staining in the outer annulus fibrosus [38]. More recently, Kohrs *et al.* investigated fascicle gliding in the tendons of the three *Prg4* mouse genotypes, finding that an absence of lubricin was associated with increased interfascicular friction [39]. Hence, the lack of one or both *Prg4* alleles found in heterozygous and knockout mice could result in deleterious effects on many of the tissues within the knee joint following cyclic loading.

Finally, the use of mice in this biomechanical study posed design challenges due to the small size of the specimens. However, achieving a reliable and reproducible *ex vivo* cyclic loading apparatus for mouse knee joints could be useful given the accessibility of mouse strains with gene mutations related to cartilage development and homeostasis.

4.6 Acknowledgements

The authors would like to acknowledge their funding sources: NIH (AR050180, P20-RRO24484), Rhode Island Hospital Orthopaedic Foundation, Inc., and University Orthopaedics, Inc. Thanks to Jason Machan, PhD for assistance with the statistical analyses and Virginia Hovanesian for help with confocal microscopy imaging.

4.7 References

1. Rhee, D.K., J. Marcelino, M. Baker, Y. Gong, P. Smits, V. Lefebvre, G.D. Jay, M. Stewart, H. Wang, M.L. Warman, and J.D. Carpten, *The secreted glycoprotein lubricin protects cartilage surfaces and inhibits synovial cell overgrowth*. J Clin Invest, 2005. **115**(3): p. 622-31.
2. Bao, J.P., W.P. Chen, and L.D. Wu, *Lubricin: a novel potential biotherapeutic approaches for the treatment of osteoarthritis*. Mol Biol Rep, 2010.
3. Coles, J.M., L. Zhang, J.J. Blum, M.L. Warman, G.D. Jay, F. Guilak, and S. Zauscher, *Loss of cartilage structure, stiffness, and frictional properties in mice lacking PRG4*. Arthritis Rheum, 2010. **62**(6): p. 1666-74.
4. Elsaid, K.A., B.C. Fleming, H.L. Oksendahl, J.T. Machan, P.D. Fadale, M.J. Hulstyn, R. Shalvoy, and G.D. Jay, *Decreased lubricin concentrations and markers of joint inflammation in the synovial fluid of patients with anterior cruciate ligament injury*. Arthritis Rheum, 2008. **58**(6): p. 1707-15.
5. Elsaid, K.A., G.D. Jay, M.L. Warman, D.K. Rhee, and C.O. Chichester, *Association of articular cartilage degradation and loss of boundary-lubricating ability of synovial fluid following injury and inflammatory arthritis*. Arthritis Rheum, 2005. **52**(6): p. 1746-55.
6. Elsaid, K.A., J.T. Machan, K. Waller, B.C. Fleming, and G.D. Jay, *The impact of anterior cruciate ligament injury on lubricin metabolism and the effect of inhibiting tumor necrosis factor alpha on chondroprotection in an animal model*. Arthritis Rheum, 2009. **60**(10): p. 2997-3006.

7. Jay, G.D., *Characterization of a bovine synovial fluid lubricating factor. I. Chemical, surface activity and lubricating properties.* Connect Tissue Res, 1992. **28**(1-2): p. 71-88.
8. Jay, G.D., D.E. Britt, and C.J. Cha, *Lubricin is a product of megakaryocyte stimulating factor gene expression by human synovial fibroblasts.* J Rheumatol, 2000. **27**(3): p. 594-600.
9. Jay, G.D., B.C. Fleming, B.A. Watkins, K.A. McHugh, S.C. Anderson, L.X. Zhang, E. Teeple, K.A. Waller, and K.A. Elsaid, *Prevention of cartilage degeneration and restoration of chondroprotection by lubricin tribosupplementation in the rat following anterior cruciate ligament transection.* Arthritis Rheum, 2010. **62**(8): p. 2382-91.
10. Jay, G.D., K. Haberstroh, and C.J. Cha, *Comparison of the boundary-lubricating ability of bovine synovial fluid, lubricin, and Healon.* J Biomed Mater Res, 1998. **40**(3): p. 414-8.
11. Jay, G.D. and B.S. Hong, *Characterization of a bovine synovial fluid lubricating factor. II. Comparison with purified ocular and salivary mucin.* Connect Tissue Res, 1992. **28**(1-2): p. 89-98.
12. Jay, G.D., B.P. Lane, and L. Sokoloff, *Characterization of a bovine synovial fluid lubricating factor. III. The interaction with hyaluronic acid.* Connect Tissue Res, 1992. **28**(4): p. 245-55.
13. Jay, G.D., J.R. Torres, D.K. Rhee, H.J. Helminen, M.M. Hytinen, C.J. Cha, K. Elsaid, K.S. Kim, Y. Cui, and M.L. Warman, *Association between friction and*

- wear in diarthrodial joints lacking lubricin*. Arthritis Rheum, 2007. **56**(11): p. 3662-9.
14. Nugent-Derfus, G.E., T. Takara, K. O'Neill J, S.B. Cahill, S. Gortz, T. Pong, H. Inoue, N.M. Aneloski, W.W. Wang, K.I. Vega, T.J. Klein, N.D. Hsieh-Bonassera, W.C. Bae, J.D. Burke, W.D. Bugbee, and R.L. Sah, *Continuous passive motion applied to whole joints stimulates chondrocyte biosynthesis of PRG4*. Osteoarthritis Cartilage, 2007. **15**(5): p. 566-74.
 15. Schaefer, D.B., D. Wendt, M. Moretti, M. Jakob, G.D. Jay, M. Heberer, and I. Martin, *Lubricin reduces cartilage--cartilage integration*. Biorheology, 2004. **41**(3-4): p. 503-8.
 16. Taguchi, M., Y.L. Sun, C. Zhao, M.E. Zobitz, C.J. Cha, G.D. Jay, K.N. An, and P.C. Amadio, *Lubricin surface modification improves extrasynovial tendon gliding in a canine model in vitro*. J Bone Joint Surg Am, 2008. **90**(1): p. 129-35.
 17. Zappone, B., M. Ruths, G.W. Greene, G.D. Jay, and J.N. Israelachvili, *Adsorption, lubrication, and wear of lubricin on model surfaces: polymer brush-like behavior of a glycoprotein*. Biophys J, 2007. **92**(5): p. 1693-708.
 18. Zhao, C., Y.L. Sun, R.L. Kirk, A.R. Thoreson, G.D. Jay, S.L. Moran, K.N. An, and P.C. Amadio, *Effects of a lubricin-containing compound on the results of flexor tendon repair in a canine model in vivo*. J Bone Joint Surg Am, 2010. **92**(6): p. 1453-61.
 19. Graindorge, S., W. Ferrandez, E. Ingham, Z. Jin, P. Twigg, and J. Fisher, *The role of the surface amorphous layer of articular cartilage in joint lubrication*. Proc Inst Mech Eng H, 2006. **220**(5): p. 597-607.

20. Forster, H. and J. Fisher, *The influence of loading time and lubricant on the friction of articular cartilage*. Proc Inst Mech Eng [H], 1996. **210**(2): p. 109-19.
21. Forster, H. and J. Fisher, *The influence of continuous sliding and subsequent surface wear on the friction of articular cartilage*. Proc Inst Mech Eng H, 1999. **213**(4): p. 329-45.
22. McCann, L., E. Ingham, Z. Jin, and J. Fisher, *Influence of the meniscus on friction and degradation of cartilage in the natural knee joint*. Osteoarthritis Cartilage, 2009. **17**(8): p. 995-1000.
23. Katta, J., Z. Jin, E. Ingham, and J. Fisher, *Biotribology of articular cartilage--a review of the recent advances*. Med Eng Phys, 2008. **30**(10): p. 1349-63.
24. Mow, V.C., Huiskes, R., ed. *Basic Orthopaedic Biomechanics & Mechano-Biology*. Third ed. 2005, Lippincott, Williams & Wilkins: Philadelphia. 720.
25. Fischer, M.S. and R. Blickhan, *The tri-segmented limbs of therian mammals: kinematics, dynamics, and self-stabilization--a review*. J Exp Zoolog A Comp Exp Biol, 2006. **305**(11): p. 935-52.
26. Fischer, M.S., N. Schilling, M. Schmidt, D. Haarhaus, and H. Witte, *Basic limb kinematics of small therian mammals*. J Exp Biol, 2002. **205**(Pt 9): p. 1315-38.
27. Crisco, J.J., J. Blume, E. Teeple, B.C. Fleming, and G.D. Jay, *Assuming exponential decay by incorporating viscous damping improves the prediction of the coefficient of friction in pendulum tests of whole articular joints*. Proc Inst Mech Eng [H], 2007. **221**(3): p. 325-33.
28. Stanton, T.E., *Boundary lubrication in engineering practice*. Engineer, 1923. **135**: p. 678-680.

29. Huser, C.A., M. Peacock, and M.E. Davies, *Inhibition of caspase-9 reduces chondrocyte apoptosis and proteoglycan loss following mechanical trauma*. Osteoarthritis Cartilage, 2006. **14**(10): p. 1002-10.
30. Coles, J.M., L. Zhang, J.J. Blum, M.L. Warman, G.D. Jay, F. Guilak, and S. Zauscher, *Loss of cartilage structure, stiffness, and frictional properties in mice lacking Prg4*. Arthritis Rheum, 2010.
31. Park, S., K.D. Costa, and G.A. Ateshian, *Microscale frictional response of bovine articular cartilage from atomic force microscopy*. J Biomech, 2004. **37**(11): p. 1679-87.
32. Park, S., K.D. Costa, and G.A. Ateshian, *Microscale frictional response of bovine articular cartilage from atomic force microscopy*. Journal of Biomechanics, 2004. **37**(11): p. 1679-87.
33. Jay, G.D., J.R. Torres, D.K. Rhee, H.J. Helminen, M.M. Hytinen, C.J. Cha, K.A. Elsaid, K.S. Kim, Y. Cui, and M.L. Warman, *Association between friction and wear in diarthrodial joints lacking lubricin*. Arthritis & Rheumatism, 2007. **56**(11): p. 3662-3669.
34. Ball, S.T., D. Amiel, S.K. Williams, W. Tontz, A.C. Chen, R.L. Sah, and W.D. Bugbee, *The effects of storage on fresh human osteochondral allografts*. Clin Orthop Relat Res, 2004(418): p. 246-52.
35. Williams, S.K., D. Amiel, S.T. Ball, R.T. Allen, V.W. Wong, A.C. Chen, R.L. Sah, and W.D. Bugbee, *Prolonged storage effects on the articular cartilage of fresh human osteochondral allografts*. J Bone Joint Surg Am, 2003. **85-A**(11): p. 2111-20.

36. Sun, Y., E.J. Berger, C. Zhao, K.N. An, P.C. Amadio, and G. Jay, *Mapping lubricin in canine musculoskeletal tissues*. Connect Tissue Res, 2006. **47**(4): p. 215-21.
37. Sun, Y., E.J. Berger, C. Zhao, G.D. Jay, K.N. An, and P.C. Amadio, *Expression and mapping of lubricin in canine flexor tendon*. Journal of Orthopaedic Research, 2006. **24**(9): p. 1861-8.
38. Shine, K.M. and M. Spector, *The presence and distribution of lubricin in the caprine intervertebral disc*. J Orthop Res, 2008. **26**(10): p. 1398-406.
39. Kohrs, R.T., C. Zhao, Y.L. Sun, G.D. Jay, L. Zhang, M.L. Warman, K.N. An, and P.C. Amadio, *Tendon fascicle gliding in wild type, heterozygous, and lubricin knockout mice*. J Orthop Res, 2010.

Table 4.1: Means and standard deviations of histological scores for all categories and overall totals for cyclically loaded (Exp) and unloaded (Ctl) *Prg4* mouse knee cartilage. * denotes significantly higher AC Surface Structure and Surface Layer Morphology scores compared to *Prg4*^{+/+} and +/- (p<0.001). + denotes significantly higher Surface Layer Morphology score compared to unloaded *Prg4*^{-/-} scores.

Scoring Category	<i>Prg4</i> ^{+/+}		<i>Prg4</i> +/-		<i>Prg4</i> ^{-/-}	
	Exp	Ctl	Exp	Ctl	Exp	Ctl
	Mean±SD	Mean±SD	Mean±SD	Mean±SD	Mean±SD	Mean±SD
AC Surface Structure	0.21 ± 0.33	0.21 ± 0.40	0.40 ± 0.52	0.20 ± 0.26	2.05 ± 0.52*	1.91 ± 0.77*
Surface Layer Morphology	0.38 ± 0.43	0.30 ± 0.33	0.65 ± 0.47	0.25 ± 0.26	2.09 ± 0.20*+	1.59 ± 0.86*
Pericellular SafO Loss	0.88 ± 0.74	0.83 ± 0.65	1.55 ± 0.99	1.40 ± 1.17	1.14 ± 0.60	1.18 ± 0.98
TOTAL	1.46 ± 1.14	1.33 ± 0.96	2.60 ± 1.61	1.85 ± 1.33	5.27 ± 1.06	4.68 ± 2.14

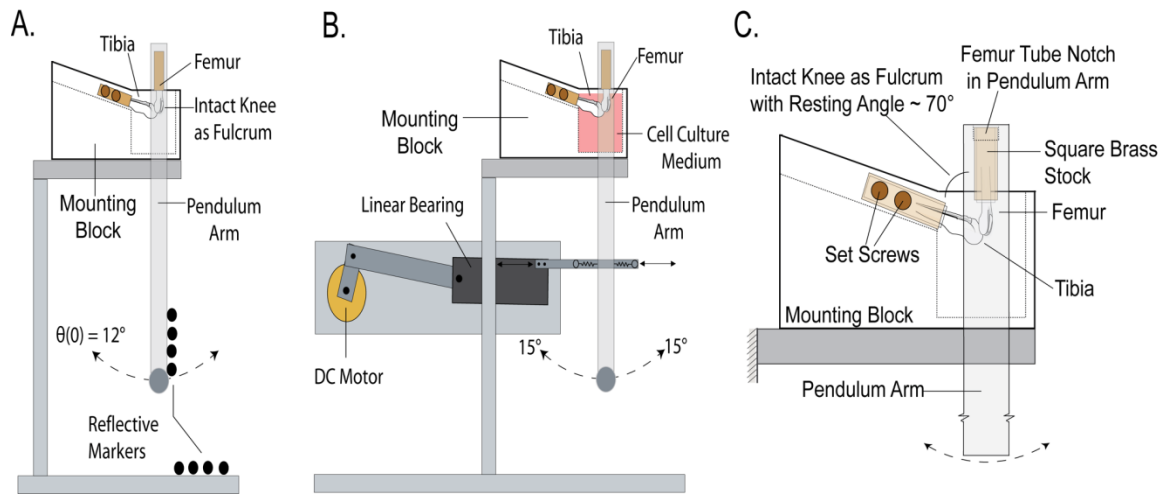


Figure 4.1: Two pendulum systems were used to complete the experiments. A passive pendulum system was used to measure the CoF (A). Experimental joints were loaded into an active pendulum system for cyclic loading (B). Specimens were loaded into the mounting block (C).

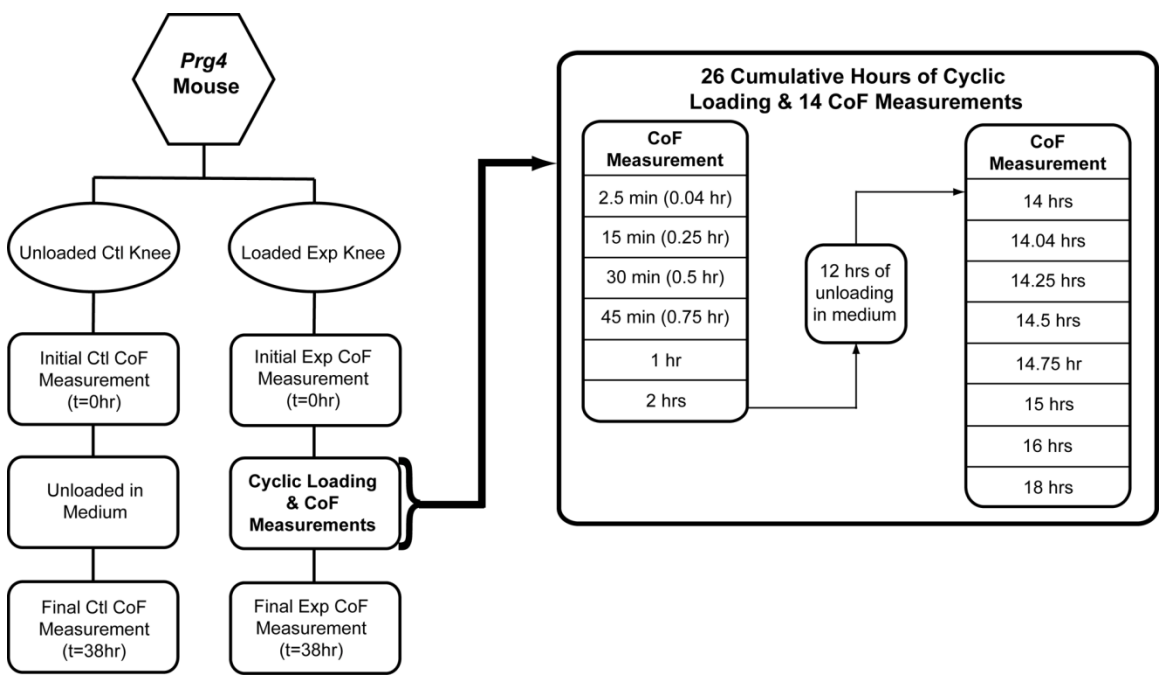


Figure 4.2: A flowchart of the experimental protocol starting with a pair of *Prg4* mouse hind limbs. Each experimental limb underwent 26 cumulative hours of cyclic loading, twelve hours of unloading in cell culture medium, and oscillation data collection at sixteen time points while control limbs remained in an unloaded state in culture medium for the duration of testing.

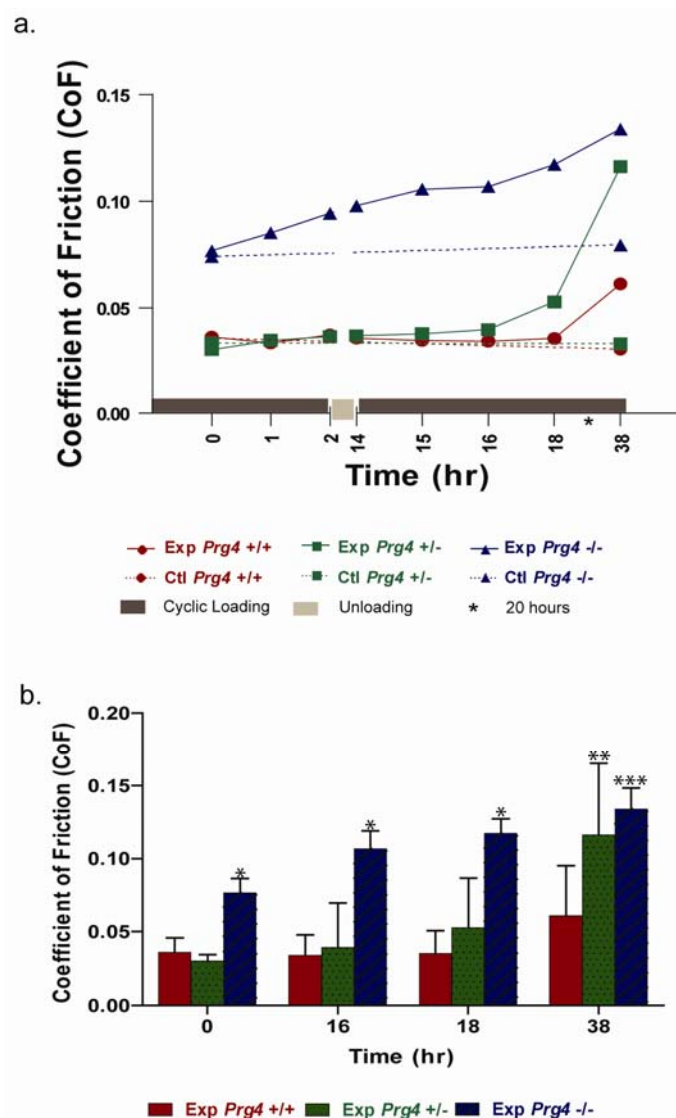


Figure 4.3: A.) Mean values of experimental and contra-lateral control CoF data over the course of testing with the coefficient of friction values on the y-axis and time (hr) on the x-axis. The shaded bars at the bottom represent the time during which the experimental joint is cyclically loaded and unloaded. All control CoF values remained constant; however, the *Prg4*^{-/-} control CoF values were significantly higher than the CoF values of the other two genotypes ($p < 0.0001$). Experimental *Prg4*^{-/-} CoF values started significantly higher and rose steadily during the twenty-six hours of cyclic loading. Experimental *Prg4*^{+/+} and +/- CoF values started approximately equal; however, by the final time point, *Prg4*^{+/-} CoF values were closer to those of *Prg4*^{-/-} joints than to *Prg4*^{+/+} joints. B.) Mean CoF values for each genotype at t = 0, 16, 18, 38hrs. At t = 0, 16 and 18 hrs, *Prg4*^{-/-} CoF values were significantly higher than the wild type and heterozygous values, as denoted with * ($p < 0.0001$). However, at t = 38hrs, both *Prg4*^{-/-} and +/- CoF values were significantly higher than *Prg4*^{+/+} values. ** denotes $p = 0.0028$, while *** denotes $p < 0.0001$.

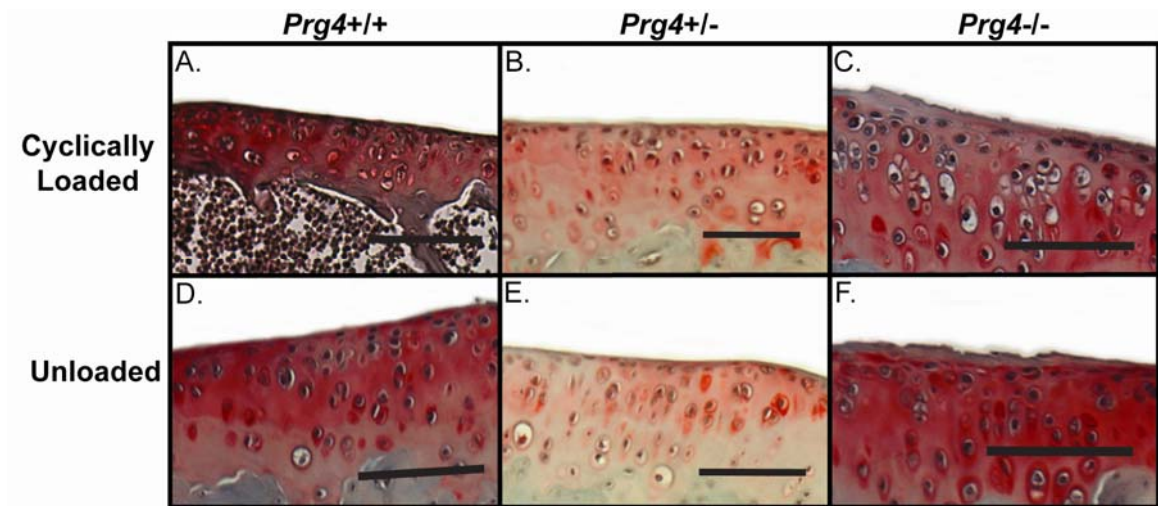


Figure 4.4: The images displayed within this figure represent the median total histological score for each *Prg4* genotype and treatment group. Cyclically loaded *Prg4* $+/+$ with a score of 1.0 (A), unloaded *Prg4* $+/+$ with a score of 1.0 (D), cyclically loaded *Prg4* $+/-$ with a score of 2.5 (B), unloaded *Prg4* $+/-$ with a score of 2.0 (E), cyclically loaded *Prg4* $-/-$ with a score of 5.0 (C), unloaded *Prg4* $-/-$ with a score of 5.0 (F) specimens captured at 10x magnification. Scale bar denotes 100 μm .

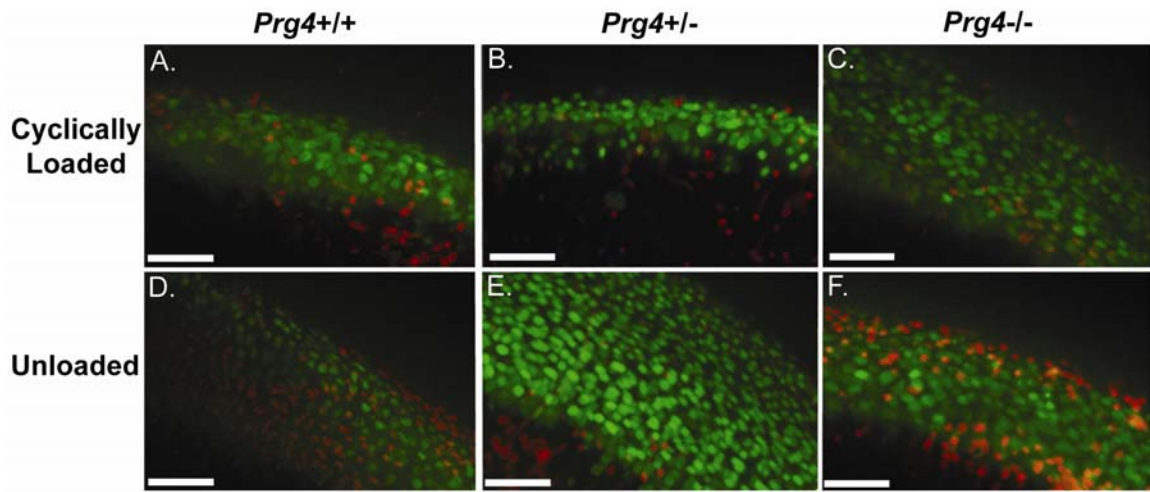


Figure 4.5: Representative FDA/PI viability images of femoral chondylar cartilage from cyclically loaded *Prg4* +/+ (A), unloaded *Prg4* +/+ (D), cyclically loaded *Prg4* +/- (B), unloaded *Prg4* +/- (E), cyclically loaded *Prg4* -/- (C), unloaded *Prg4* -/- (F) specimens which were loaded or unloaded for 38 hours. Images were captured at 20x magnification with the scale bar denoting 50 μ m.

Chapter 5

Discussion and Conclusions

5.1 Discussion

The major findings from this line of work have been presented in Chapters 2-4. However, over the course of this study, a number of additional observations have been made, and will be discussed in the following sections. While some of the work described below did not produce the expected outcomes, we feel that it is still worth presenting, as it could lay groundwork for future tribological studies of articular cartilage (AC).

5.1.1 Friction Modeling: Linear versus Exponential

Chapter 2 discusses the differences between two methods of modeling the coefficient of friction (CoF) of intact mouse knee joints, including a Stanton linear decay model and an exponential decay model that accounts for viscous damping. Briefly, this study highlighted the benefits of each model. The Stanton linear decay model demonstrated increased precision and reliability, as determined with coefficient of variation calculations (CV) and the intra-class correlation coefficient (ICC), respectively. Additionally, at this point in time, most whole joint friction studies rely upon the Stanton

model to calculate their CoF values [1-6]. Conversely, the exponential decay model delivered a better fit for the experimental data as determined by root mean square error (RMSE) and asymptomatic standard error (ASE) calculations. Also, as reported, the exponential decay model yielded CoF values that were significantly lower than the CoF values generated with the Stanton linear model.

Given the fact that a majority of studies use the Stanton model to calculate the CoF of intact joints [1-6], this method was used in Chapters 3 and 4. The work conducted for Chapter 2 required a sample size of ten. Over the course of testing of these ten specimens, no issues or problems were detected. However, when these models were used for the increased sample sizes in Chapters 3 and 4, the robustness of the exponential decay model was put to the test and found to be insufficient to handle all oscillation decay patterns.

Clearly, the Stanton linear model was most accurate with specimens that displayed a perfectly linear oscillation decay from which the CoF value was calculated. The exponential model that accounts for damping is capable of successfully modeling the CoF of specimens with slightly curvilinear oscillation decay. In a small number of cases, the specimen or the manner in which it was prepared caused biomechanical discontinuities. More specifically, in a handful of cases, there was a rapid decrease in oscillation amplitude followed by a smooth, gradual decay (**Figure 5.1a**). This pattern of oscillation decay was most likely the result of soft tissue within the capsule impeding movement at the larger oscillation angles. When this occurred, convergence of the exponential decay model failed, outputting a CoF value that was approximately equal to 0 ($\text{CoF} \approx 1 \times 10^{-14}$). By removing the initial oscillation cycles from the data that was used to

model the CoF, an improved fit (**Figure 5.1b**) was achieved. By excluding the first several points, the exponential decay model was able to output a CoF value of 0.0193 ± 0.0017 (mean \pm SD), with an RMSE of 0.499° . These modifications resulted in small decreases of the Stanton CoF values from 0.0337 ± 0.002 (mean \pm SD) to 0.0302 ± 0.0012 .

Another specimen displayed extremely curvilinear oscillation decay (**Figure 5.2a.**). In this particular instance, the complex decay pattern in the x-direction (flexion-extension) appears to correspond with increased rotation in the y-direction (varus-valgus) (**Figure 5.2b.**). While the trials discussed above could achieve a better-fitting model by excluding the first few cycles of oscillation data, in this case, there was no way to improve the fit of the model to the pendulum motion. This coupled decay pattern was an example of a biomechanical discontinuity, and was most likely a result of the manner in which the specimen was loaded into the pendulum system for that particular CoF time point. Despite these anomalies, the combination of the passive pendulum for collection of CoF data and the active system for cyclic loading allowed for a repeatable, reliable, and cost-effective system for investigating the biotribological properties of small rodent knee joints in an unconstrained manner.

5.1.2 Effect of Gender and Cyclic Loading on CoF

The goal of Aim 2 of this dissertation was to investigate the effects of cyclic loading on the CoF of intact lubricin mutant mouse knee joints. While Chapter 4 demonstrates the major findings that support Aim 2, an additional observation was made

during this investigation. We found that the gender of the mouse had an effect on the response to cyclic loading.

As mentioned in Chapter 1, researchers have focused on tribology in attempts to better understand osteoarthritis (OA). Various techniques have been used to examine the biotribological properties of AC, including the measurement of the coefficient of friction (CoF). Investigators have measured the CoF in a variety of species across several joints. The goal of this work was to determine whether gender affects the frictional response of intact murine joints to cyclic loading. It was hypothesized that cyclic loading would have the same effect on the coefficient of friction of intact knee joints from male and female mice. This work was accomplished using intact knee joints from 10-week-old C57BL6/J (*Prg4*^{+/+}) mice as the fulcrum of two pendulum systems.

Hind limbs from C57BL6/J (*Prg4*^{+/+}) 10-week-old mice (n=6 male pairs, n=6 female pairs) were excised post-euthanasia. Specimens were prepared and tested using the same methods described in Chapter 4. Briefly, once the intact knee joints were prepared, experimental limbs were subjected to 26 cumulative hours of cyclic loading with the active pendulum system. The CoF was measured using the passive pendulum at 16 separate time points. The contra-lateral joint from each pair was used as a control for the cyclically loaded joint, and was placed unloaded in cell culture medium for the duration of testing. In addition to calculating the CoF values, custom MATLAB code was used to examine the path lengths of the pendulum arm in the x- (flexion-extension) and y- directions (varus-valgus) during oscillation. Mean (\pm SD) CoF values were calculated for all joints at each time point. Differences between initial and final CoF were evaluated with a paired t-test. Differences between males and females at the final time point were

compared with a t-test (SigmaStat3.5, Systat Software, Inc., San Jose, CA). A significant value of $p < 0.05$ was set *a priori*.

Twenty-six cumulative hours of cyclic loading significantly increased CoF values of the female mouse knee AC ($p < 0.009$), while cyclic loading did not significantly increase CoF values of male mouse knee AC ($p = 0.560$) (**Table 5.1**). Contra lateral control CoF values remained constant over the course of the experiment. Pendulum path length showed no correlation with CoF values, time, or gender.

The purpose of this study was to determine whether gender plays a role in the frictional response of intact mouse knee joints to cyclic loading. Two previous studies used varying techniques to assess the frictional properties of cartilage plugs under cyclic loading [7-8]. Both studies showed the same general trend of increasing CoF values over the course of testing; however, neither study noted the gender of the specimens used for testing. While the CoF of the female knee joints rose, it took much more time to finally increase compared to the previous studies. The CoF of the male AC did not experience a similar increase. An unexpected finding from this work was that gender of the mouse had an effect on the response to cyclic loading; the CoF of joints from female mice increased significantly in comparison to the CoF of joints from male mice. We expected low variability across the genders due to the fact that the mice were from generated from the same colony.

5.1.3 Imaging of Murine Articular Cartilage

One of the major aims of this dissertation was to investigate the effects of cyclic loading on the articulating surfaces of lubricin mutant mouse knee joints (Aim 3). Chapter 4 addressed Specific Aim 3 by assessing the effects of cyclic loading on *Prg4*^{+/+}, *Prg4*^{+/-}, and *Prg4*^{-/-} mouse knee joints. In this chapter, light microscopy was used to view tissue stained with with safranin-o with fast green counter-stained tissue. Confocal microscopy was used to image tissue dyed with fluorescein diacetate with propidium iodide to study chondrocyte viability. In addition to these imaging techniques, several other types of microscopy were employed to examine the articulating surfaces following cyclic loading. These included scanning electron microscopy (SEM), white light interferometry (WLI), and atomic force microscopy (AFM). Unfortunately, due to a variety of reasons described below, these methods were not successful for imaging the articulating surfaces of mouse knee joints.

5.1.3.1 Scanning Electron Microscopy (SEM)

Scanning electron microscopy provides high-resolution images of articular cartilage. Electron microscopy, first developed in the 1930's, has improved to the point where SEM can resolve images to 3.5nm with magnifications of 200,000x. Unlike light microscopy and transmission electron microscopy, which create images from optical properties, SEM uses lenses to generate a focused, demagnified spot of electrons that are scanned over a surface [9]. In order for this technique to work, the surface must be conductive. In the case of non-conductive materials, such as biological specimens like articular cartilage, a coating of palladium-gold alloy can be applied with a sputter coater

[9]. Once in the vacuum chamber of the SEM, a gun shoots a beam of electrons at the sample. As the electrons strike the specimen and rebound back, a layer of secondary electrons is generated. These secondary electrons are collected, processed, and translated into a series of pixels on a monitor. The secondary electrons collected result in black and white topographical maps of the surfaces of specimens [9].

Due to the small scale of mouse knee joints, the use of SEM was investigated as potential method for imaging their articulating surfaces. In order to accomplish this imaging, hind limbs were harvested post-euthanasia from *Prg4*^{+/+}, *+/*-, and *-/-* mice (n=1 per genotype). Soft tissue was removed and the joint capsule was opened. Each joint was disarticulated, separating the distal femur and the proximal tibia. The menisci were dissected away, exposing the articulating surfaces. Specimens were placed in 10% formalin for four days. Following fixation, limbs were rinsed with saline and then dehydrated with ascending dilutions of ethanol (25, 50, 75, 100, and 100%) for a period of 1.5 hours each. Following ethanol dehydration, each sample was placed in the critical point drier and exposed to three flushes of CO₂, which removed all water by applying high pressures and varying temperatures forcing phase transitions from liquid to vapor. Next specimens were mounted on aluminum stubs using double-sided sticky carbon disks. Each stub contained the femur and tibia of a given genotype. Prior to imaging, samples were sputter-coated with Gold-Palladium (2 cycles of 3 minutes at 20 mA). Specimens were then placed in the SEM chamber (Hitachi, Ltd., Tokyo, Japan). Once the SEM had warmed up for a period of at least 15 minutes, the “Gun Tilt,” “Gun Horizon,” “Aperture,” and “Stigmation” were optimized. Images were captured at 8.0 kV, with a

beam current of 10, a working distance of 17 mm, and “L” pixel size (1024x797). Magnifications ranged from as low as 50.0x to as high as 4.50Kx.

When collecting images to be used for surface damage assessments, specimens must be mounted on aluminum posts with uniform orientation and imaged at the same magnifications to ensure that images can be examined for comparison. Because the SEM images presented herein were taken during a pilot study, specimen orientations were not completely uniform and images were taken at a variety of magnifications. Hence, they can only be assessed qualitatively (**Figures 5.3-5.5**).

SEM has limitations particularly when dealing with biological samples. Due to the fact that SEM requires a vacuum, samples must be completely dry. Biological samples can be dried following preparation with a critical point dryer, which applies high pressures under both low and high temperatures creating transitions from liquids to gases. Unfortunately, this has the potential to have deleterious effects on cellular samples. Articular cartilage is comprised of chondrocytes, collagen, proteoglycans, water, inorganic salts, and small amounts of matrix proteins such as glycoproteins and lipids. Water accounts for 60-85% of the wet weight of AC. Hence, when viewing samples with SEM, the properties of the AC may be altered by the dehydration and critical point drying processes, which may result in artifact and be detrimental to the accuracy of the images produced with SEM [8, 10]. A newer imaging method, “Environmental SEM” (ESEM), is a more attractive method for biological specimens. Instead of a high-pressure vacuum, ESEM allows for the viewing of biological tissues in a low-pressure gaseous environment with high humidity. This process was made possible with the creation of a secondary-

electron detector that is able to withstand the presence of water vapor [9, 11]. Unfortunately, at the time of testing, this technology was not available at our institution.

Figures 5.3-5.5 display images of the articulating surfaces of untested (specimens that did not undergo cyclic loading) *Prg4*^{+/+}, *Prg4*^{+/-}, and *Prg4*^{-/-} mouse knees. The *Prg4*^{-/-} AC (**Figure 5.5**) showed greater amounts of surface damage when assessed qualitatively and compared to the surfaces of *Prg4*^{+/+} and *Prg4*^{+/-} mouse AC. These findings were not surprising given the fact that *Prg4*^{-/-} mice do not have the benefits of lubricin's chondroprotective capabilities. Both SEM and ESEM have been used to characterize the effects of wear testing or continuous sliding on AC surfaces [8, 11]. One study investigated surface and particle morphology following wear testing. More specifically, intact ovine knee joints were tested in a custom joint simulator for various periods of time at varying rates. Cartilage was then imaged with SEM and ESEM. The images obtained demonstrated that AC surface damage increased with the duration of testing. Additionally, wear particles changed shape and size as testing progressed [11]. In another study, wear tests were carried out with bovine cartilage-on-metal contacts under a constant load. Cartilage and metal were rubbed against each other creating reciprocating motion friction tests for varying amounts of time. SEM and ESEM were used for surface roughness analysis. This work demonstrated that while surface wear was consistent with a slight increase in friction, the period of loading more closely related to the coefficient of friction [8]. While both of these studies made conclusions regarding the effects of testing on AC surfaces, they also noted that ESEM is a much more useful imaging tool for tissues, such as AC, due to the fact that it allows the specimen to be imaged in its natural state. The harsh fixation and dehydration techniques may alter the characteristics of AC

given the high water content of this tissue [8, 11]. Additionally, ESEM was capable of imaging the “surface lamina,” which was not seen with conventional SEM [8].

Clearly, ESEM has several advantages over SEM. Given the shortcomings of SEM when imaging biological tissues, this technique was not pursued any further than this pilot study. Unfortunately, ESEM was not available at our institution at the time of testing. Hence, additional imaging techniques were investigated.

5.1.3.2 White Light Interferometry (WLI)

SEM has been widely used by the orthopaedic research community to assess the surface topography of articular cartilage; however, it is only capable of qualitative outcome measures. WLI, on the other hand, is one of only a few imaging techniques that provides quantitative topographical data [12]. Interferometry utilizes a reflection microscope which compares a waveform reflected from a flat reference mirror with a waveform from the surface of a sample being imaged. Using a Mirau interference objective, interference fringes are superimposed on the image of the surface of the sample and they are acquired with a CCD camera. A virtual probe plane is then established from the intensity profile of the white light fringes along the vertical optical axis of the microscope. In other words, the output from WLI is made up of the superposition of fringes from a number of wavelengths. Using specialized algorithms capable of detecting the peak of the envelope of each pixel within an image, a complete measurement can be made [13]. With the proper equipment and software, this reliable, non-contact optical profiling system can obtain nanometric axial resolution of 1-80nm [13]. WLI has been used for many years to characterize the topography of a variety of materials, including

biological surfaces, such as cell adhesion on composite films in cell culture and biomimetic hydroxyapatite layers. However, there have been limited studies investigating the topography of articular cartilage using WLI [12-14].

We conducted a pilot study to investigate the feasibility of using WLI to analyze the articulating surfaces of *Prg4* mouse knees. Using methods approved by our institution's IACUC, hind limbs were disarticulated from 10 week-old *Prg4*^{+/-} mice (n=4 pairs). All soft tissue was removed and knee joints were disarticulated, revealing the articular cartilage. Using a scalpel, the distal femur and proximal tibia were removed from their long bones, creating a flat surface. In order for WLI to obtain data, surfaces must be completely dry; reflections from liquids on the surface of samples can interfere with imaging. These AC surfaces were patted dry with kim wipes. Specimens were then mounted on a slide. A Zygo NewViewTM 6000 Interferometer (Zygo[®], Middlefield, CT) was combined with MetroPro[®] Software (Zygo[®], Middlefield, CT) to image the topography of the *Prg4*^{+/-} knee AC.

Despite the ability for WLI to provide quantitative 3D topography data, there have been only a small number of studies that have investigated this technique for the characterization of articular cartilage. One study used full thickness cylindrical bovine explants and human talar AC samples. The goal of this study was to assess the feasibility of measuring the AC surface topography prior to staining the tissue for chondrocyte viability [12]. Shekhawat *et al.* were able to develop and optimized surface preparation protocols that allowed them to detect differences in surface roughness (Ra). Additionally, they found statistically significant correlations between Ra scores and histological degeneration scores using the human talar AC samples. They concluded that WLI allows

surface topography measurements of AC without compromising chondrocyte viability [12].

A second study moved beyond the optimization of preparation techniques and used WLI to investigate the role of the surface amorphous layer (SAL) of AC in joint lubrication [14]. Using bovine cartilage plugs, the authors imaged healthy samples, AC tissue treated with SDS to remove the SAL, and samples with a regenerated SAL to compare the features of the surfaces following the various treatments. Images of healthy AC were smooth and featureless, whereas the SDS treated surfaces contained pits and humps. It was determined that the characteristics of the treated surfaces were significantly rougher than the healthy AC. Additionally, the surface with the regenerated SAL was quite smooth, but not entirely featureless. The SAL-regenerated surfaces exhibited numerous small-scale features and larger-scale undulations [14].

These studies demonstrate the capabilities of quantitatively assessing bovine AC; however, WLI was not as successful when used to investigate the articulating surfaces of *Prg4* mouse knees. The bovine samples were orders of magnitude larger than the murine samples. Hence, the small portions of the bovine plugs that were examined were extremely flat, in comparison to the mouse AC. When using WLI to assess the mouse topography, the curvature of the tibial plateaus and femoral chondyles prevented the system from collecting complete data. **Figure 5.6** displays typical output from the MetroPro[®] software, including a profile surface map, oblique plot, and intensity map. The intensity map gives a qualitative topographical view of the cartilage surface; however, due to the curvature of the specimen, the interferometer was not able to capture all of the data needed to obtain accurate quantitative data. Missing data was indicated in the top left

portion of **Figure 5.6** with black space. In the case of an ideal specimen, this screen would not contain any black space. Each and every *Prg4* specimen had a substantial amount of missing data (black space).

5.1.3.3 Atomic Force Microscopy (AFM)

While WLI has the potential to serve as an effective topographical imaging tool for AC specimens from joints with little to no curvature, it falls short with the articulating surfaces of mouse knees, as demonstrated by **Figure 5.6**. Like WLI, AFM is also capable of providing quantitative topographical data and imaging on the micro-scale. AFM has been used more and more frequently for tribological studies on both the micro- and nano-scale. In addition to measuring topographical properties such as surface roughness and wear, AFM can be used to obtain mechanical properties such as friction and elastic modulus [7].

AFM was developed by Binnig *et al.* in 1986 [15] by modifying and combining a scanning tunnel microscope (STM) and a stylus profilometer (SP). STM and SP use a tip or stylus to scan the surface of a sample, detect variations in the topography, and finally generate three dimensional renderings. Binnig *et al.*, modified these systems so that the STM could be utilized to record the motion of a cantilever beam with an ultra-small mass [15]. The contact between the cantilever tip and the specimen surface produces deflection or torsion, which can be measured with a photodetector resulting in surface interaction forces that can be used to extract friction or adhesion data.

We conducted a pilot study investigating the feasibility of using AFM to image *Prg4* mouse knee AC and obtain micro-scale surface roughness measurements. *Prg4*^{+/+},

Prg4^{+/-} and *Prg4*^{-/-} mouse knees (n=2 pairs per genotype) were prepared in the same manner as described in Chapters 2-4. Experimentally designated specimens underwent 26 cumulative hours of cyclic loading and 12 hours of unloading in cell culture medium. Contra-lateral control joints were placed unloaded in cell culture medium. Once testing was complete, joints were disarticulated and the AC was cleared of any soft tissue including intra-capsular ligaments and menisci. Specimens were then wrapped in saline soaked gauze and frozen at -20°C. On the day of imaging, specimens were thawed at room temperature. The distal portion of each femur was cut from the rest of the bone, creating a flat surface for mounting. Tibial plateaus could not be imaged because of their concavity. Each specimen was secured to a petri dish with super glue and hydrated with PBS. Specimens were then mounted in an MFP-3D-BIO AFM (Asylum Research, Santa Barbara, CA) with a sharp tip attached to a cantilever, $k \sim 1.3$ N/m (Novascan Technologies, Ames, IA) positioned over the medial femoral chondyle. 20x20 μm images were collected for specimens from *Prg4*^{+/+}, *Prg4*^{+/-}, and *Prg4*^{-/-} mice with Igor Pro software (WaveMetrics, Portland, OR). Images were assessed for surface roughness data including RMS values, maximum and minimum heights, and volume, among other measures.

As mentioned above, AFM has been used in several studies to examine the topographical properties of articular cartilage [10, 16-17]. Additionally, AFM has been used specifically to characterize the properties of AC of *Prg4*^{+/+} and *Prg4*^{-/-} mouse femoral heads at a variety of ages [18-19]. Previous studies investigating the micro-scale topographical properties of bovine and porcine AC plugs demonstrated that untreated specimens were consistently nonfibrous, featureless, and smooth. Specimens digested

with alkaline protease revealed fibrous surfaces. Images captured for this pilot study of cyclically loaded *Prg4* mouse knee AC and their contra-lateral controls were quite inconsistent. There were no discernable differences between cyclically loaded experimental AC and unloaded control AC. While a few images displayed seemingly normal surface characteristics (**Figure 5.7**), most exhibited highly irregular surfaces (**Figure 5.8**). The irregular images had pillow-like particulates on the articulating surfaces as seen in **Figure 5.8**. The only noticeable difference across the three *Prg4* genotypes was that the *Prg4*^{-/-} had larger particulates, in comparison to *Prg4*^{+/+} and *Prg4*^{+/-} surfaces. These differences were accounted for in the surface roughness data in **Tables 5.2-5.3**. While data was collected for each specimen, these measurements cannot be considered accurate due to the surface abnormalities. The results of this pilot study were inconclusive. No findings could be made regarding the micro-scale damage caused by cyclic loading.

We are confident that improved specimen preparation protocols and optimized AFM settings could yield more accurate images and surface roughness data due to the fact that Coles *et al.* [18-19] have characterized the mechanical and frictional properties of lubricin mutant femoral head AC using AFM. They demonstrated that the lack of the *Prg4* gene results in significant biomechanical and structural modifications. These AC differences became amplified with increasing age. Hence, they concluded, like this dissertation, that lubricin is vital to joint structure and function. Unlike our testing, Coles *et al.*, did not perform cyclic loading on any of their specimens. Additionally, they conducted their investigations on the femoral heads of *Prg4*^{+/+} and *Prg4*^{-/-} mice. The use of femoral heads as specimens was more optimal than AC surfaces from knee joints.

This is due to the fact that AFM requires that specimen surfaces be flat or convex. The tibial plateaus could not be assessed with AFM because their articulating surfaces were concave. Additionally, some of the images of femoral chondyles collected for this pilot study were blurry, most likely a result of the tip slipping across the specimen as a result of the extremely convex curvature. While the results presented here did not provide the desired information regarding the micro-scale topographical characteristics and surface roughness, a more in depth study optimizing the specimen preparation and imaging settings would most likely generate useful data regarding lubricin's ability to provide chondroprotection during *ex vivo* cyclic loading.

5.1.4 Future Applications of the Pendulum Systems

The work presented within this dissertation focused primarily on a murine whole knee joint model; and, as discussed in Chapter 4, these reliable and reproducible *ex vivo* cyclic loading methods could be used to investigate any mouse strains with genetic mutations related to cartilage development and homeostasis. However, the pendulum systems were also designed so that with slight modifications, both systems could be used to test specimens from larger animals, including rats. While rats cannot be genetically modified, their larger size, in comparison to mice, makes them an attractive experimental model. Because rats are an order of magnitude larger than mice, various aspects of the knee joints can be modified and examined for changes in whole joint frictional properties as a result of just surgical intervention as well as the effects of the surgery combined with cyclic loading. Anterior cruciate ligament transection (ACLT) is just one of the many potential surgical models that could be investigated with the pendulum systems.

The anterior cruciate ligament (ACL) is one of the four major ligaments within a knee joint. Its primary function is to control anterior displacement of the tibia. The ACL also provides rotational stability. Rupture of the ACL is one of the most common sports injuries suffered by athletes in the United States. There are a variety of options for treatment of an ACL tear or rupture, which range from nonsurgical interventions such as physical therapy to ACL reconstruction. No matter the treatment option, ACL rupture places patients at a higher risk of developing OA, which is most likely due to altered biomechanics.

In this pilot study, rat hind limbs were used to investigate the effects of ACLT on whole joint friction properties of intact rat knees. Prior to specimen preparation and data collection, a new pendulum, scaled to the size of the rat, was designed and constructed. Using procedures approved by the Rhode Island Hospital Animal Welfare Committee (IACUC), hind limbs were harvested post-euthanasia. Specimens were then wrapped with saline soaked gauze and frozen at -20°C until the day of testing. Freezing was not a concern in this study due to the fact that the specimens would not be subjected to cyclic loading. On the day of testing, specimens were thawed at room temperature and prepared using the methods described in Chapters 2-4. Briefly, skin and musculature were removed, but the joint capsule was left intact. The distal tibia and proximal femur of each hind limb were potted in ~ 1 cm-square brass tubes using a urethane potting compound. Each specimen was then mounted in the passive pendulum and oscillation data were collected as described in Chapters 2-4 with the exception of the initial oscillation angle. In this study, specimens were brought to $17 \pm 2.5^{\circ}$, as opposed to $12 \pm 2^{\circ}$, before being released. Five trials were collected for each specimen with an intact capsule.

Following intact data collection, the ACL of each specimen was surgically transected. More specifically, once the five oscillation trials were completed and the specimen was removed from the passive pendulum system, a scalpel was used to make an incision lateral to the patella. The knee was placed in extension so that the patella could be dislocated and moved out of the field of view. Next, the knee was flexed and a scalpel was inserted into the capsule. The ACL was transected with a lateral cut. The PCL was left intact. Two to three sutures were used to close the capsule. The specimen was then remounted in the passive pendulum system and five trials of oscillation were collected.

Custom MATLAB code was used to calculate CoF values using both the Stanton linear decay model and the exponential model that accounts for viscous damping. Root mean square error (RMSE) was calculated for each model. While the dominant motion of the pendulum was flexion-extension (x-axis of the coordinate system), motion was tracked in all three-dimensions. Varus-valgus motion was tracked along the y-axis and internal-external rotation was tracked along the z-axis. The maximum difference in amplitude ($^{\circ}$) was calculated for the y- axis, represented with Max_y. Means and standard deviations were calculated and reported for CoF values using both models (Stanton and Exponential). Pair t-tests were used to compare intact versus ACLT CoF values (SigmaStat3.5, Systat Software, Inc., San Jose, CA). A significant value of $p < 0.05$ was set *a priori*.

As expected, based on results from Chapter 2 [2], the Stanton linear decay model resulted in higher mean CoF values than CoF values calculated with the exponential decay model that accounted for viscous damping (**Table 5.4**). Despite the low sample size, both models yielded significant increases in CoF values following the ACLT

($p=0.008$ for Stanton; $p=0.02$ for exponential). While there was no correlation between the magnitude of Max_y, and CoF values using either model, there was an apparent correlation between RMSE and Max_y (**Figure 5.9**); the greater the RMSE, the larger the Max_y, a logical relationship. The CoF models base their calculations upon flexion-extension; so, in the case that the knee joint has an increased amount of varus-valgus motion (Max_y), the models will not fit as closely to the data, resulting in larger RMSE values.

Clearly the work presented here requires further investigation, including a larger sample size. Also, the addition of an intermediate test condition, in which the capsule has been opened, prior to transaction, would add further value to this line of work. However, it demonstrates the ability to examine knee joints from larger animals. As stated in Chapter 4, the combination of the passive and active pendulum systems allow for a reliable and reproducible *ex vivo* testing method for mouse joints. These results demonstrate that, with minor modifications, these systems can accommodate larger specimens, hence augmenting their usefulness as a biomechanical testing method.

5.2 Conclusions

The findings presented within this dissertation reveal the effects of *ex vivo* tribological testing on intact lubricin mutant mouse knee joints, and demonstrate the importance of lubricin's chondroprotective role within mammalian synovial joints. This work lays the groundwork for additional studies investigating the relationship between the bulk frictional properties and surface integrity of the articular cartilage within knee joints. It also provides motivation for more in depth studies of carriers of camptodactyly-arthropathy-coxa vara-pericarditis syndrome (CACP). The specific aims of the work described within Chapters 2-4 were to: (1) design two pendulum systems for testing intact mouse knee joints; (2) investigate the effects of cyclic loading on the coefficient of friction of intact lubricin mutant mouse knee joints; and (3) characterize the effects of cyclic loading on the surface integrity of lubricin mutant mouse knee cartilage. Chapter 1 of this dissertation described the motivation for pursuing this line of research; it also explained these specific aims in greater detail.

5.2.1 Specific Aim 1: Design two pendulum systems for testing intact mouse knee joints – a passive system to measure the coefficient of friction and an active system to perform cyclic loading.

The main objective of Chapter 2 was to complete Aim 1 by developing a testing apparatus and protocols capable of measuring the frictional properties of whole mouse knee joints. Additionally, Chapter 2 compared two models that could be used to calculate

the CoF of intact mouse knees. A passive pendulum was designed in which the mouse knee joint served as the fulcrum of the system. The mounting system, in conjunction with the pendulum arm, allowed for unconstrained motion. In this study, two mathematical models were used to measure the frictional properties of the intact knee joints based upon oscillation decay of a freely swinging joint. These models included: a Stanton linear decay model and an exponential decay model that accounted for viscous damping. Both generated frictional data for the intact mouse knees; however, the findings varied by model. While the linear model had reduced variability, it yielded higher CoF values. The exponential model provided a better fit; however, it generated lower CoF values. Both models should be considered when assessing the frictional properties of intact joints.

Chapters 3 and 4 demonstrated the successful application of Aim 1. In each of these chapters, two pendulum systems were used to assess the biomechanical properties of intact mouse knee joints. As in Chapter 2, the passive pendulum was used to measure the CoF. Additionally, Chapters 3 and 4 highlighted the use of an active pendulum system, which applied cyclic loading to the joints. In both studies, experimental joints were cyclically loaded for designated amounts of time while contra-lateral control specimens remained unloaded. Cyclically loaded joints were then compared to the unloaded joints for parameters described below in Sections 5.2.2 and 5.2.3.

5.2.2 **Specific Aim 2:** Investigate the effects of cyclic loading on the coefficient of friction of intact lubricin mutant mouse knee joints.

The second aim of this dissertation was addressed in Chapters 3 and 4, in which *Prg4* mouse knee joints were subjected to cyclic loading carried out with an active

pendulum system that was developed in Aim 1. In Chapter 3, *Prg4*^{+/+} and *Prg4*^{+/-} mouse knees were subjected to one hundred twenty minutes of cyclic loading, and the CoF was measured at several time points. Within each genotype, specimens were divided into two groups: “frozen” and “fresh,” that referred to the manner in which the joints were stored and prepared. As discussed, frozen knees were flash frozen with liquid nitrogen prior to preparation and testing, while fresh joints were prepared and tested immediately following euthanasia. The data revealed that cyclically loading did not affect the CoF of freshly prepared specimens from either *Prg4* genotype. However, cyclically loaded frozen specimens had significantly higher CoF values. More specifically, the frozen *Prg4*^{+/-} joints demonstrated significantly higher CoF values following testing when compared to frozen *Prg4*^{+/+} cyclically loaded knees.

Chapter 4 further investigated the objective of Aim 2 by subjecting experimental *Prg4*^{+/+}, *Prg4*^{+/-}, and *Prg4*^{-/-} mouse knee joints to twenty-six cumulative hours of cyclical loading, while contra-lateral control limbs remained unloaded. CoF measurements were collected across several time points. The data demonstrated that lubricin plays a significant role in the protection of articular cartilage undergoing *ex vivo* cyclic loading. *Prg4*^{-/-} specimens had significantly higher CoF values than *Prg4*^{+/+} and *Prg4*^{+/-} knees, which had approximately equal CoF values, prior to cyclic loading. The final CoF values of all *Prg4* genotypes were higher than the initial values, however, these values increased by varying amounts following cyclic loading. The CoF values of contra-lateral control joints remained constant over the course of testing; further demonstrating that cyclic loading affects the frictional properties of *Prg4* mouse knees.

The data and results presented in Chapters 3 and 4 satisfied the objective of Aim 2 by demonstrating the effects of cyclic loading on the frictional properties of intact *Prg4*^{+/+}, *Prg4*^{+/-}, and *Prg4*^{-/-} mouse knees.

5.2.3 Specific Aim 3: Characterize the effects of cyclic loading on the surface integrity of lubricin mutant mouse knee cartilage.

Chapter 4 addresses Aim 3 of this dissertation. Cyclic loading was successfully carried out using the active pendulum system designed to fulfill Aim 1. As described earlier in Section 5.1.3, three forms of microscopy were investigated as possible methods with which the effects of cyclic loading could be characterized. These forms of microscopy included: scanning electron microscopy (SEM), white light interferometry (WLI), and atomic force microscopy (AFM). Due to limitations of these imaging technologies and their required preparation methods, they were not pursued beyond pilot studies. Instead, the effects of cyclic loading upon the surface integrity of lubricin mutant mouse knee cartilage were assessed in Chapter 4.

In this study, experimental specimens were cyclically loaded for twenty-six hours, while contra-lateral control joints remained unloaded. Following testing, joints were processed for histological staining with safranin O with fast green counterstain. These slides were then assessed and scored by a group of double-blinded reviewers. Although the differences between cyclically loaded and unloaded joints were not statistically significant for most categories, the experimental joints were increased. Additionally, joints from *Prg4*^{-/-} mice were significantly higher than *Prg4*^{+/+} and *Prg4*^{+/-} knees. These results demonstrate that cyclically loading does have a slight effect on the integrity

of articulating surfaces of *Prg4* mouse knee joints. A more in depth examination of AC with environmental SEM or AFM may reveal micro-scale articular damage. Lastly, chondrocyte viability was investigated via staining with fluorescein diacetate and propidium iodide. Images captured with confocal microscopy demonstrated that cyclically loaded and unloaded specimens from each *Prg4* genotype contained viable chondrocytes; hence demonstrating that the prolonged *ex vivo* biomechanical testing affected the viability of all specimens in the same manner.

Using the data obtained in Chapter 4, we were able to examine the effects of cyclic loading across *Prg4*^{+/+}, *Prg4*^{+/-}, and *Prg4*^{-/-} specimens. While statistical significance was not achieved, histological staining and scoring provided a better understanding of the articulating surfaces following cyclic loading.

5.3 Summary

The work presented within this dissertation served to establish methods for assessing the effects of cyclic loading on the bulk frictional properties and cartilage surface integrity of lubricin mutant mouse knee joints. These findings support and complement the existing data pertaining to the vital role that lubricin plays within mammalian synovial joints. While the end goal of this line of research would ultimately be the development of a tribological supplement, these results demonstrate that long-term whole joint tribological testing is possible and should be pursued further. Additionally, this work revealed a lubricin-dosing response within *Prg4* mouse joints, which could have clinically relevant implications for carriers of CACP: Lack of a functional *Prg4* allele may place these individuals at a potentially greater risk for developing OA, or other synovial joint disorders. Lastly, the pendulum systems developed for this research will allow for future long-term *ex vivo* biomechanical studies of intact knee joints.

5.4 References

1. Crisco, J.J., J. Blume, E. Teeple, B.C. Fleming, and G.D. Jay, *Assuming exponential decay by incorporating viscous damping improves the prediction of the coefficient of friction in pendulum tests of whole articular joints*. Proceedings of the Institution of Mechanical Engineers, Part H, 2007. **221**(3): p. 325-33.
2. Drewniak, E.I., G.D. Jay, B.C. Fleming, and J.J. Crisco, *Comparison of two methods for calculating the frictional properties of articular cartilage using a simple pendulum and intact mouse knee joints*. Journal of Biomechanics, 2009. **42**(12): p. 1996-9.
3. Jones, E.S., *Joint Lubrication*. The Lancet, 1936. **230**: p. 1043-1044.
4. Stanton, T.E., *Boundary lubrication in engineering practice*. Engineer, 1923. **135**: p. 678-680.
5. Teeple, E., B.C. Fleming, A.P. Mechrefe, J.J. Crisco, M.F. Brady, and G.D. Jay, *Frictional properties of Hartley guinea pig knees with and without proteolytic disruption of the articular surfaces*. Osteoarthritis and Cartilage, 2007. **15**(3): p. 309-15.
6. Wright, V. and D. Dowson, *Lubrication and cartilage*. J Anat, 1976. **121**(Pt 1): p. 107-18.
7. Park, S., K.D. Costa, and G.A. Ateshian, *Microscale frictional response of bovine articular cartilage from atomic force microscopy*. Journal of Biomechanics, 2004. **37**(11): p. 1679-87.

8. Forster, H. and J. Fisher, *The influence of continuous sliding and subsequent surface wear on the friction of articular cartilage*. Proceedings of the Institution of Mechanical Engineers, Part H, 1999. **213**(4): p. 329-45.
9. Bozzola, J.J. and L.D. Russell, *Electron Microscopy: principles and techniques for biologists*. Second ed. 1992, Sudbury, MA: Jones and Bartlett Publishers.
10. Kumar, P., M. Oka, J. Toguchida, M. Kobayashi, E. Uchida, T. Nakamura, and K. Tanaka, *Role of uppermost superficial surface layer of articular cartilage in the lubrication mechanism of joints*. J Anat, 2001. **199**(Pt 3): p. 241-50.
11. Graindorge, S. and G. Stachowiak, *Changes occurring in the surface morphology of articular cartilage during wear*. Wear, 2000. **241**: p. 143-150.
12. Shekhawat, V.K., M.P. Laurent, C. Muehleman, and M.A. Wimmer, *Surface topography of viable articular cartilage measured with scanning white light interferometry*. Osteoarthritis Cartilage, 2009. **17**(9): p. 1197-203.
13. Pecheva, E., P. Montgomery, D. Montaner, and L. Pramatarova, *White light scanning interferometry adapted for large-area optical analysis of thick and rough hydroxyapatite layers*. Langmuir, 2007. **23**(7): p. 3912-8.
14. Graindorge, S., W. Ferrandez, E. Ingham, Z. Jin, P. Twigg, and J. Fisher, *The role of the surface amorphous layer of articular cartilage in joint lubrication*. Proceedings of the Institution of Mechanical Engineers, Part H, 2006. **220**(5): p. 597-607.
15. Binnig, G., C.F. Quate, and C. Gerber, *Atomic Force Microscope*. Physical Review Letters, 1986. **56**(9): p. 930-933.

16. Jurvelin, J.S., D.J. Muller, M. Wong, D. Studer, A. Engel, and E.B. Hunziker, *Surface and subsurface morphology of bovine humeral articular cartilage as assessed by atomic force and transmission electron microscopy*. J Struct Biol, 1996. **117**(1): p. 45-54.
17. Moa-Anderson, B.J., K.D. Costa, C.T. Hung, and G.A. Ateshian. *Bovine articular cartilage surface topography and roughness in fresh versus frozen tissue samples using atomic force microscopy*. in *Summer Bioengineering Conference*. 2003. Sonesta Beach Resort, Key Biscayne, FL.
18. Coles, J.M., J.J. Blum, G.D. Jay, E.M. Darling, F. Guilak, and S. Zauscher, *In situ friction measurement on murine cartilage by atomic force microscopy*. Journal of Biomechanics, 2008. **41**(3): p. 541-8.
19. Coles, J.M., L. Zhang, J.J. Blum, M.L. Warman, G.D. Jay, F. Guilak, and S. Zauscher, *Loss of cartilage structure, stiffness, and frictional properties in mice lacking PRG4*. Arthritis Rheum, 2010. **62**(6): p. 1666-74.

Table 5.1: Mean (\pm SD) coefficient of friction (CoF) values for articular cartilage of both males and females prior to cyclic loading (Initial) and immediately following all testing (Final). * denotes that final female CoF values were significantly higher than initial female CoF values ($p < 0.009$).

Gender	CoF (mean\pmSD)	
	Initial CoF	Final CoF
Male	0.0387 \pm 0.0129	0.0417 \pm 0.0204
Female	0.0329 \pm 0.0087	0.118 \pm 0.0476*

Table 5.2: Mean and standard deviation values (n=5 scans per specimen; n=2 pairs per *Prg4* genotype) for *Prg4*^{+/+}, *Prg4*^{+/-}, and *Prg4*^{-/-} femoral chondyle articular cartilage surface roughness parameters measured with atomic force microscopy. As anticipated, *Prg4*^{-/-} RMS values were higher than *Prg4*^{+/+} and *Prg4*^{+/-} RMS values.

Surface Roughness	<i>Prg4</i>^{+/+}		<i>Prg4</i>^{+/-}		<i>Prg4</i>^{-/-}	
	Mean	St. Dev.	Mean	St. Dev.	Mean	St. Dev.
Max (nm):	274.67	164.69	229.11	14.70	327.26	134.73
Min (nm):	-160.86	144.54	-148.39	127.73	-289.45	163.05
RMS (nm):	88.60	42.37	61.46	25.55	150.21	57.07
Average Deviation (nm):	58.13	36.56	41.84	20.65	94.20	51.05
Volume (μm³):	0.81	0.64	-0.10	0.16	0.35	1.16

Table 5.3: Surface roughness data obtained with atomic force microscopy comparing cyclically loaded (experimental; n=5 scans per specimen; n=2 specimens per *Prg4* genotype) and unloaded (contra-lateral control; n=5 scans per specimen; n=2 specimens per *Prg4* genotype) joints from *Prg4*^{+/+}, *Prg4*^{+/-}, and *Prg4*^{-/-} femoral chondyle articular cartilage. We expected that cyclically loaded surfaces would have increased RMS values compared to their unloaded control joints. However, unloaded joints had higher RMS values for each genotype.

	<i>Prg4</i> ^{+/+}		<i>Prg4</i> ^{+/-}		<i>Prg4</i> ^{-/-}	
Surface Roughness	Cyclically Loaded	Unloaded	Cyclically Loaded	Unloaded	Cyclically Loaded	Unloaded
Max (nm):	185.68	363.67	166.86	260.24	317.77	336.74
Min (nm):	-86.58	-235.13	-75.09	-185.03	-201.82	-377.07
RMS (nm):	71.18	106.02	39.82	72.27	135.71	164.72
Average Deviation (nm):	38.88	77.37	24.26	50.64	80.01	108.39
Volume (μm³):	1.22	0.39	0.16	-0.24	0.64	0.05

Table 5.4: Mean CoF values, standard deviations, and root mean square error calculations for intact rat knee joints and the same measures for the joints following transection of the anterior cruciate ligament (ACLT). CoF values determined with the Stanton linear decay model and the exponential model that accounts for viscous damping.

CoF Model	Intact			ACLT		
	CoF	St. Dev.	RMSE (°)	CoF	St. Dev.	RMSE (°)
Stanton	0.0232	0.0023	0.5870	0.0364	0.0048	0.5313
Exponential	0.0144	0.0034	0.2492	0.0267	0.0046	0.2545

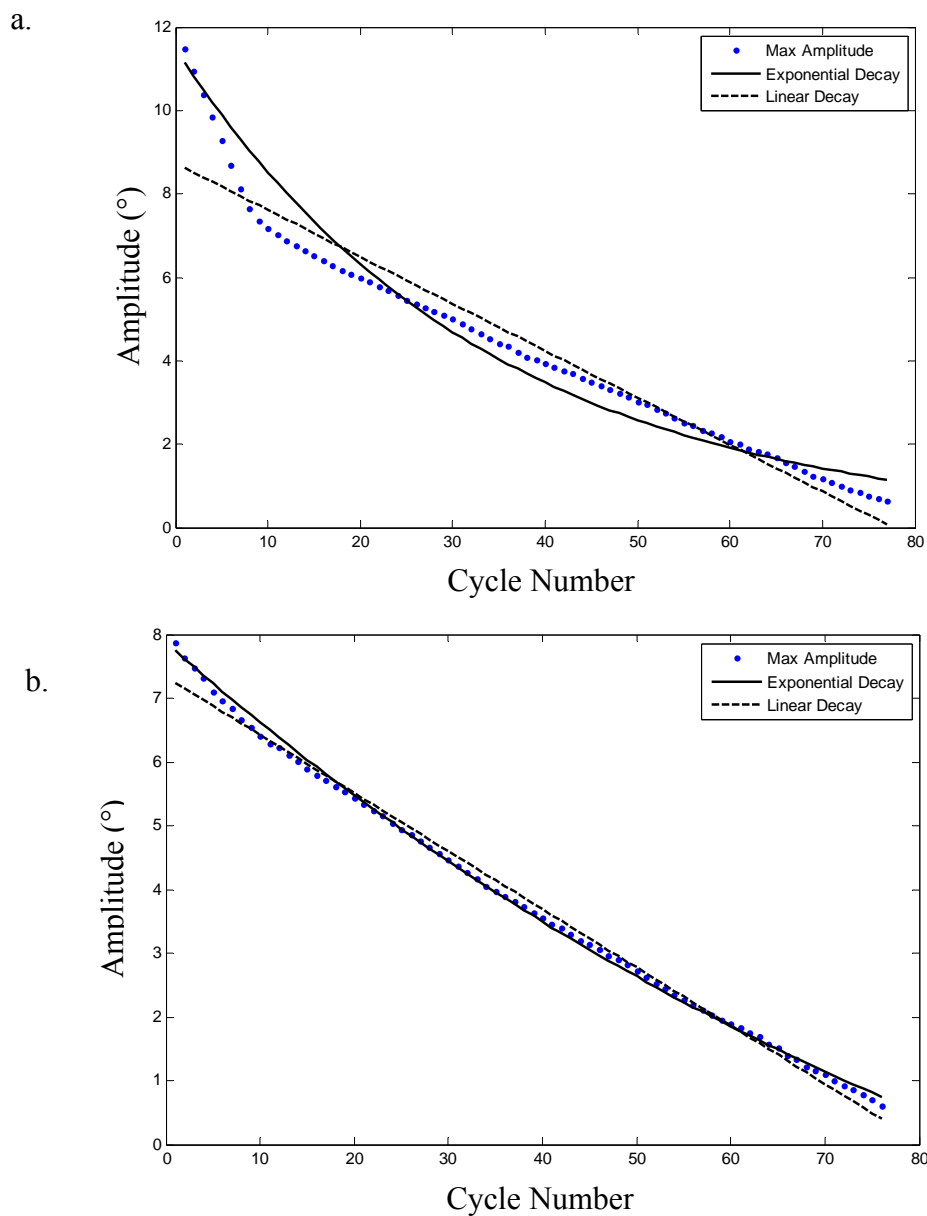


Figure 5.1: An example of a trial of oscillation decay with a rapid decrease in oscillation amplitude followed by a smooth, gradual decay (a), which most likely resulted from soft tissue within the capsule impeding upon the movement at the larger oscillation angles. By excluding the first few oscillation maximums, both models were able to more closely fit the data (b). Doing so reduced the Stanton CoF from 0.0337 ± 0.002 (mean \pm SD) to 0.0302 ± 0.0012 , and allowed the exponential model to fit to the data and calculate a CoF value of 0.0193 ± 0.0017 .

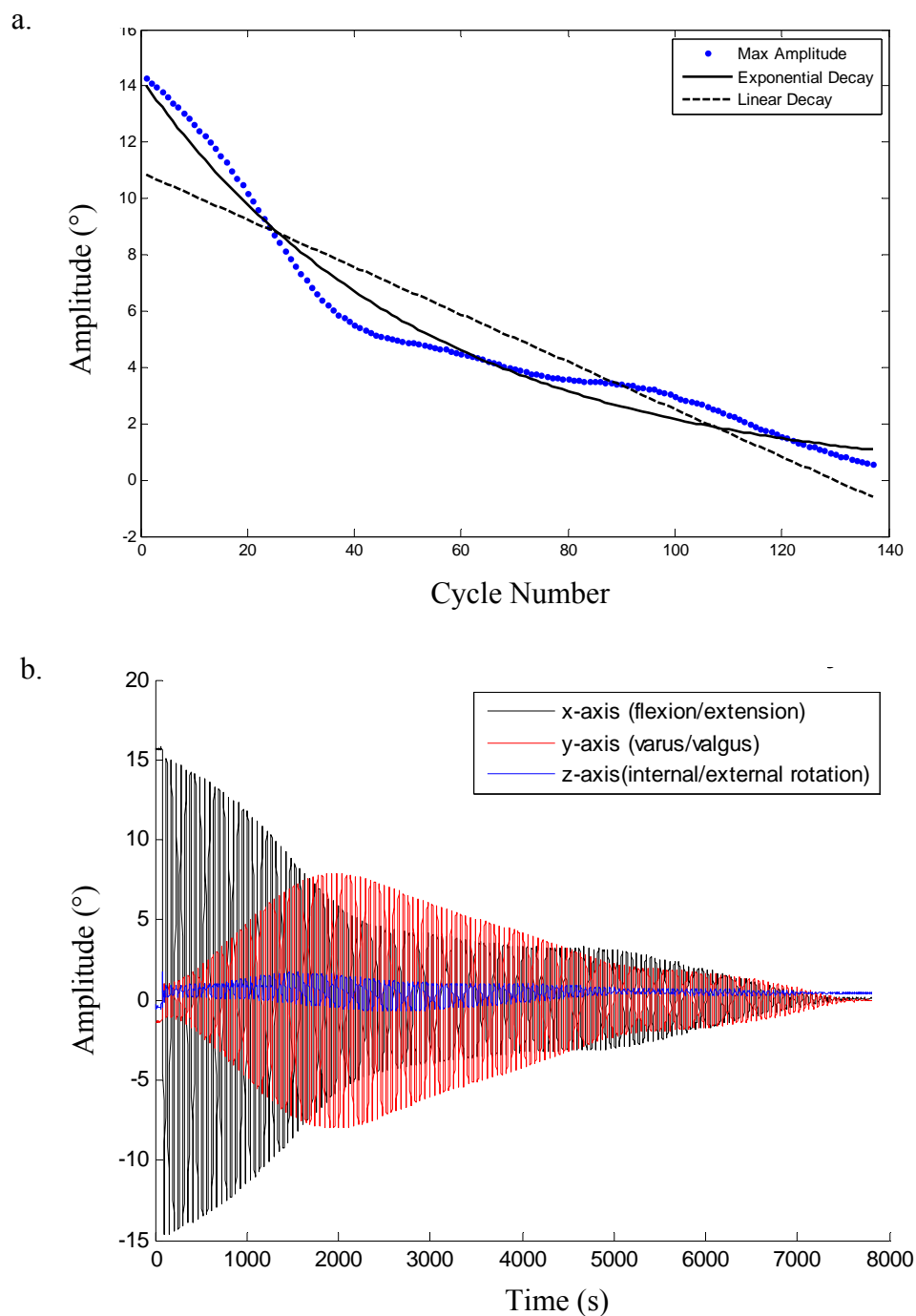


Figure 5.2: An example of a highly complex oscillation decay pattern. Neither model could obtain a close fit to the experimental data (a), even resulting in the failure of the exponential model (CoF value of ~ 0 for this trial). In this example, the highly complex pattern was affected by the extreme varus-valgus motion of the joint (b).

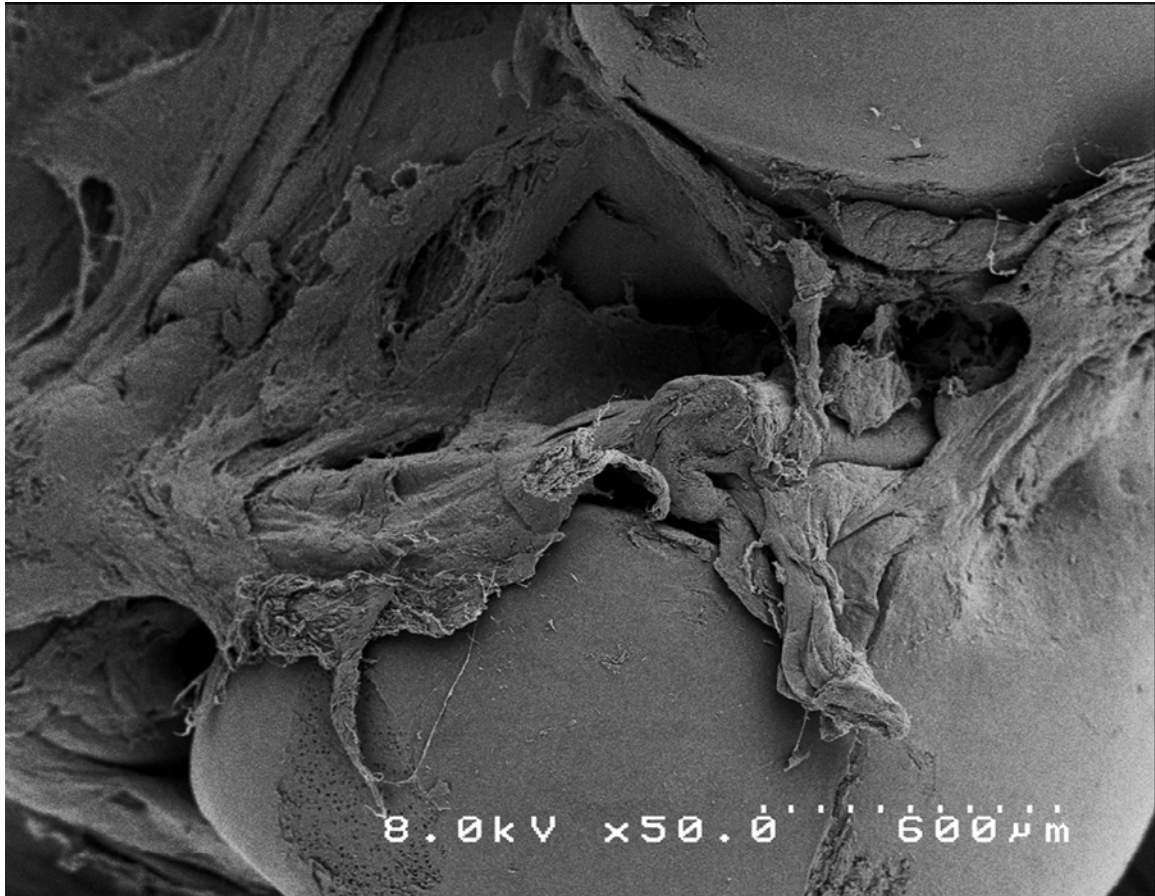


Figure 5.3: SEM image of the tibial plateau of a 12-week-old *Prg4*^{+/+} mouse. The majority of the articular cartilage appeared smooth and featureless. The visual surface damage was most likely artifact from the specimen dissection and preparation.

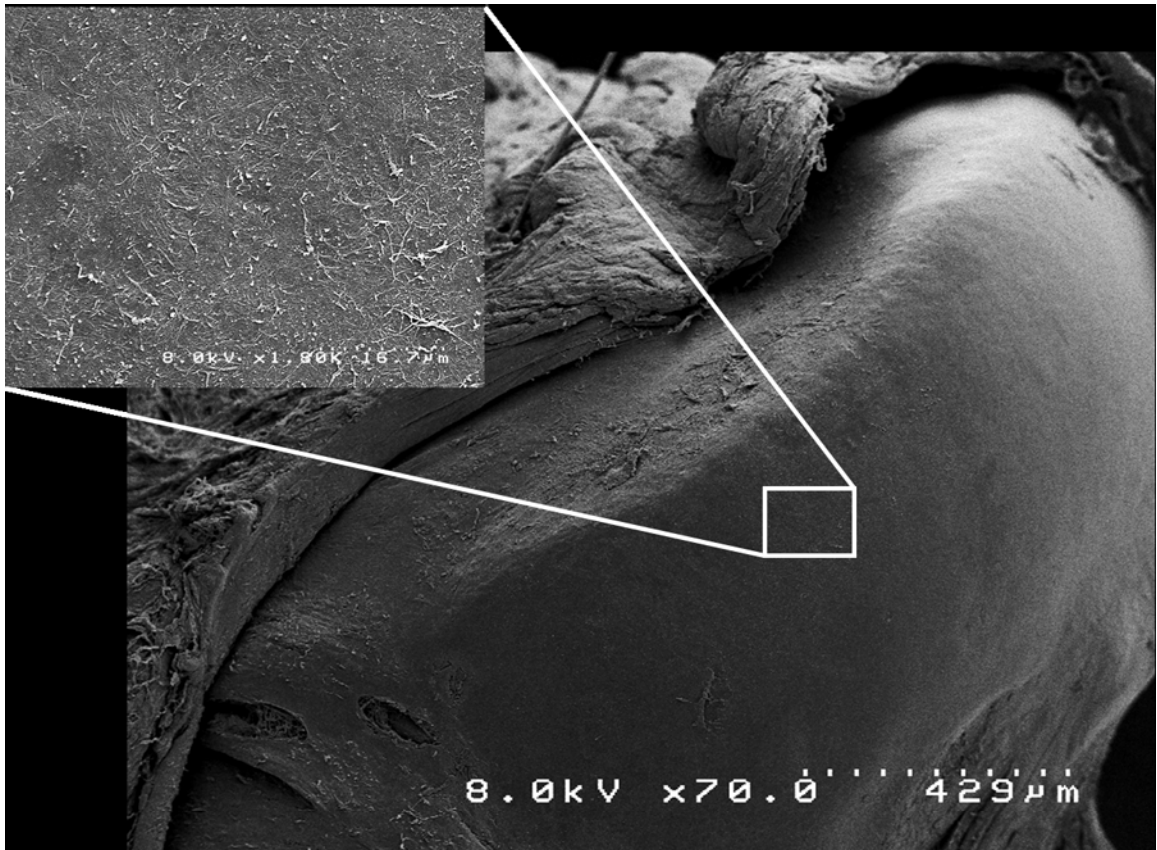


Figure 5.4: SEM image of the medial femoral chondyle of a 12-week-old *Prg4*^{+/-} mouse. The surface was smooth and featureless. The magnified image (scale bar = 16.7 μm) of the articulating surface was displayed a small degree of roughness.

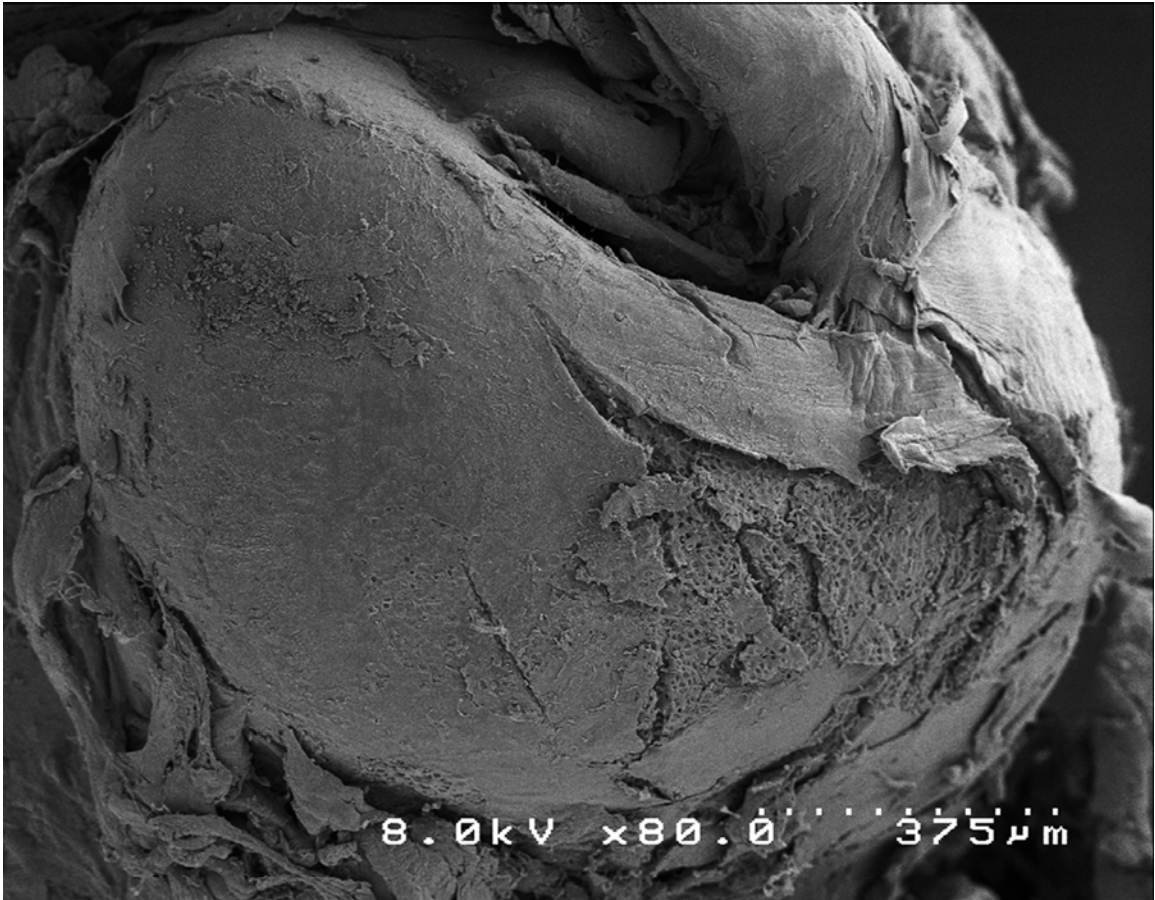


Figure 5.5: SEM image of the lateral femoral chondyle of a 12-week-old *Prg4*^{-/-} mouse. In comparison to SEM images of *Prg4*^{+/+} and *Prg4*^{+/-} AC, *Prg4*^{-/-} AC (**Figures 5.3 and 5.4**) shows a greater degree of damage.

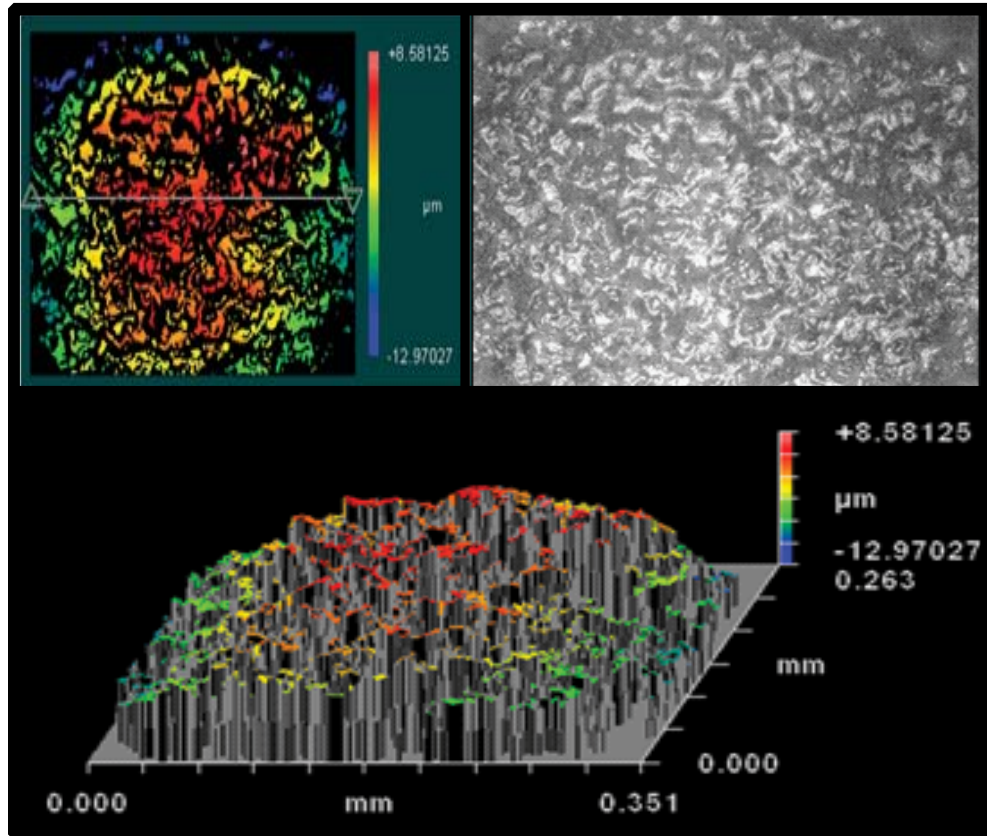


Figure 5.6: WLI output of a 10-week-old *Prg4*^{+/-} femoral chondyle imaged with a 20x mirau objective. Image output includes a surface profile (top left), intensity map (top right), and oblique plot (bottom). Ideally, the surface profile would include no black space, which represents missing data.

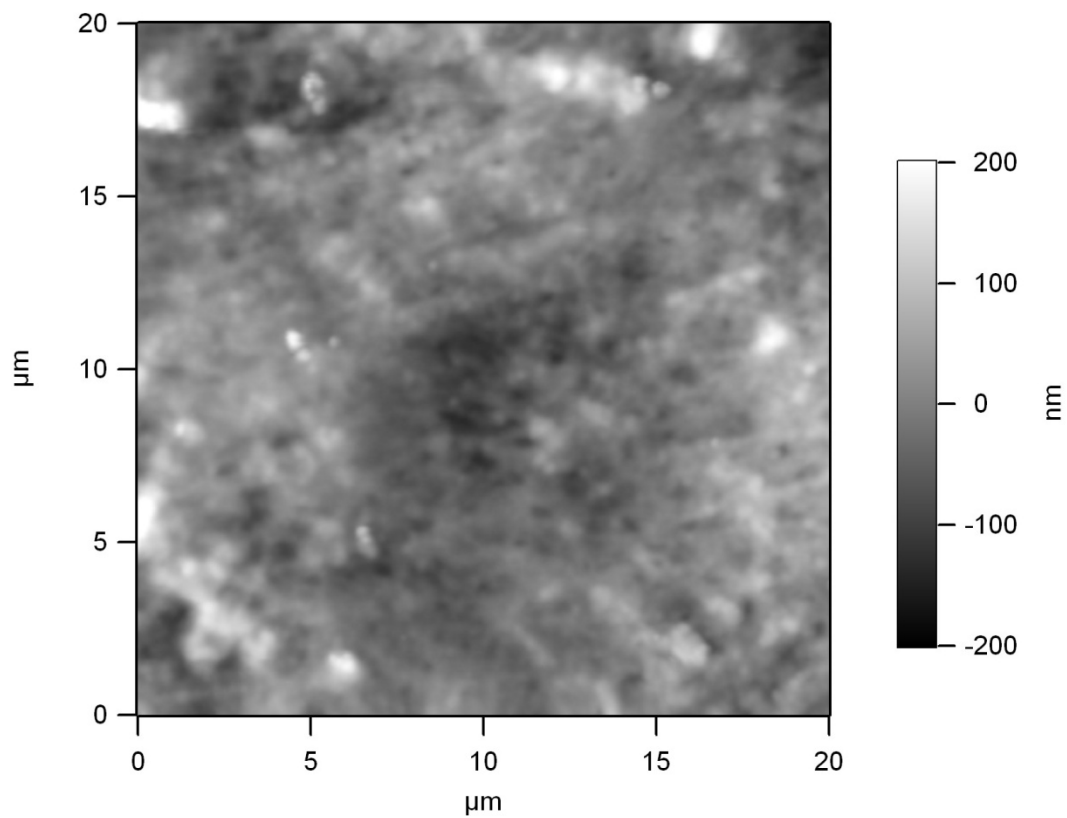


Figure 5.7: Image of a 10 week old *Prg4*^{+/+} femoral chondyle captured with atomic force microscopy. This image demonstrates what we would expect; the surface is clear, and the image does not contain blurred lines denoting the slipping of the tip across the sample.

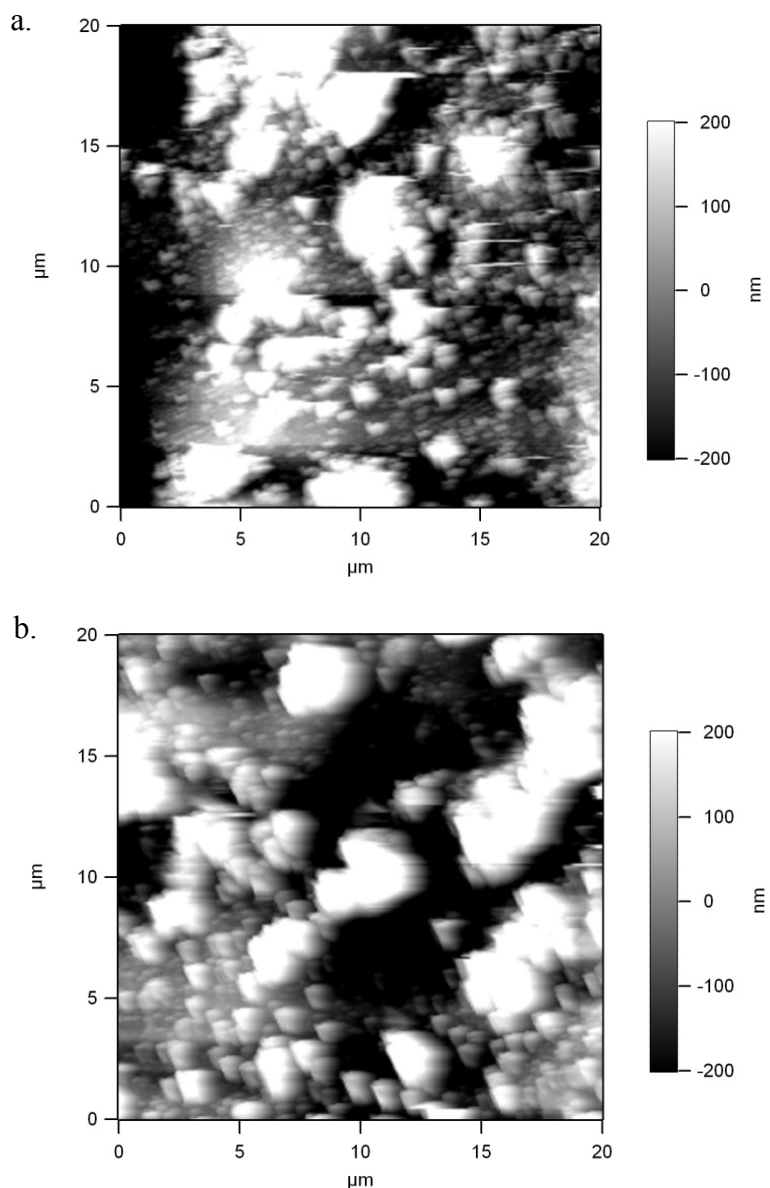


Figure 5.8: Examples of 10-week-old *Prg4*^{+/+} (a) and *Prg4*^{-/-} (b) femoral chondyles imaged with atomic force microscopy in which the surfaces were covered with large pillow-like particles. While surface asperities would be expected on *Prg4*^{-/-} specimens, *Prg4*^{+/+} should be featureless like the **Figure 5.7**. However, most of the collected images displayed irregular surfaces. More work is required to optimize the preparation and data collecting settings in order to obtain better results, but this task will be hindered by the curvature of the tibial plateaus and femoral chondyles.

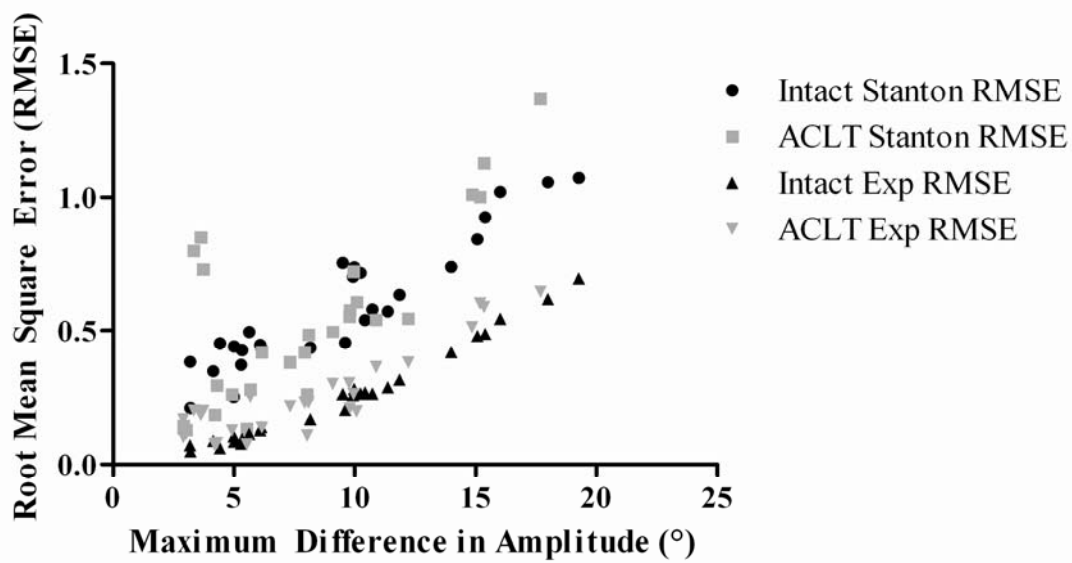


Figure 5.9: There was a correlation between RMSE of the CoF models and Max_y (Maximum Difference in Amplitude). Increases in RMSE correlated with larger Max_y values. The CoF models base their calculations upon flexion-extension; so, in the case that the knee joint has an abnormally large amount of varus-valgus motion (Max_y), the models will not fit as closely to the data, resulting in larger RMSE values.